I: DELIVERY OF CARBOHYDRATE ANTIGENS BY GLYCOPOLYMERS AS POTENTIAL ANTI-CANCER VACCINES; II: A STUDY OF THE IMPACTS OF VALENCY AND DENSITY ON IMMUNE RESPONSE AGAINST A TUMOR ASSOCIATED CARBOHYDRATE ANTIGEN

By

Qian Qin

A DISSERTATION

Submitted to
Michigan State University
in partial fulfillment of the requirements
for the degree of

Chemistry—Doctor of Philosophy

2019

ABSTRACT

I: DELIVERY OF CARBOHYDRATE ANTIGENS BY GLYCOPOLYMERS AS POTENTIAL ANTI-CANCER VACCINES; II: A STUDY OF THE IMPACTS OF VALENCY AND DENSITY ON IMMUNE RESPONSE AGAINST A TUMOR ASSOCIATED CARBOHYDRATE ANTIGEN

By

Qian Qin

Tumor associated carbohydrate antigens (TACAs) are overexpressed on tumor cells, which renders them attractive targets for anti-cancer vaccines. To overcome the poor immunogenecity of TACAs, a polymer platform was designed for antigen presentation by taking advantage of the polymeric backbone to deliver TACA and helper T (Th) cell epitope on the same chain. The block copolymer was synthesized by cyanoxyl-mediated free radical polymerization followed by conjugation with a TACA Tn antigen and a mouse Th-cell peptide epitope derived from poliovirus (PV) to afford the vaccine construct. The glycopolymer vaccine elicited a robust immune response with significant titers of IgG antibodies and the antibodies generated recognized Tn antigens on tumor cell surface.

For successful carbohydrate based anti-cancer vaccines, it is critical that B cells are activated to secret antibodies targeting TACAs. Despite the availability of many TACA based constructs, systematic understanding of the effects of structural features on antiglycan antibody responses is lacking. In this study, a series of defined synthetic glycopolymers bearing a representative TACA, i.e., the Thomsen-nouveau (Tn) antigen, have been prepared to probe the induction of early B cell activation and antibody production via a T cell independent mechanism. Valency and density of the antigen in the polymers turned out to be critical. An average of greater than 6 Tn per chain was needed to induce antibody production. Glycopolymers with 40 antigens per chain and backbone molecular

weight of 450 kDa gave the strongest stimulation to B cells *in vitro*, which correlated well with its *in vivo* activity. Deviations from the desired valency and density led to decreased antibody production or even antigen specific B cell non-responsiveness. These findings provide important insights on how to modulate anti-TACA immune responses facilitating the development of TACA based anti-cancer vaccines using glycopolymers.

ACKNOWLEDGEMENTS

First of all, I would like to thank my advisor Professor Xuefei Huang without whose guidance and support throughout the years, it would not have been possible for me to accomplish this journey. His dedication, wisdom and patience inspired and encouraged me to learn to bravely embrace and overcome all the difficulties I have encountered. I feel so lucky that I was given this great opportunity to work on such exciting and challenging projects, which covered a wide range of science from carbohydrate chemistry to polymer chemistry, protein chemistry, and immunology, and helped me develop and improve my learning abilities and problem solving skills, which I find later in my career as a scientist to be truly valuable.

I would like to express my gratitude to Professor Kevin Walker, Professor Gary Blanchard and Professor Tim Whitehead for kindly serving as my guidance committee and their efforts and time devoted to reading my dissertation and providing great feedback. And many thanks to my former committee members Professor Gregory Baker, who very sadly has left us a few years ago but will be greatly missed by all of us, and Professor Sungjin Kim from MMG who moved to UC Davis for their helpful discussion and advice during my early years of research. I am also thankful for Dr. Dan Holmes from the NMR facility and Professor Dan Jones and Lijun Chen from the Mass Spectrometry core facility for the time they spent on training me on the instruments and helping me with troubleshooting, method development and data analysis.

People in the Huang group have always been of tremendous help to me both in work and in life. I would like to thank Berm, Bo, Herbert, Hovig, Moe, Philip, Steve,

Vivian and Zhaojun for teaching me all kinds of lab techniques, sharing tips and tricks and offering helpful suggestions especially when I was new to the field. Also thank all the past and current members of the group for your help and support.

I could not be more grateful for having my dearest friends during perhaps one of the toughest times of my life. I would never forget your calls early in the morning from different time zones to wake me up either to cram for exams or to head out early for my experiments. I would never forget you were there for me trying to keep me awake and make me smile the very first night I had to run experiments till 2 am in the morning. I would never forget we cheered each other up when we both had to pull all nighters. Thank you all for your presence in my life, and for all the happiness and sorrow we shared together when we went through our own ups and downs in our life. I could not imagine how I would make it without all of you.

Finally, I deeply appreciate my family's continuous support and understanding when I chose chemistry as my major in college, when I made up my mind to pursue my degree here far away from home, and when I could not make it home for family gettogethers during the Chinese New Year or any other important moments. Thank you my parents from the bottom of my heart for being there for me all the time, for building me up when it seemed like everything was falling apart, for loving and enduring me with all my pathetic flaws, for encouraging and guiding me to live my life to the fullest, and for making me who I am today.

TABLE OF CONTENTS

LIST OF TABLES	viii
LIST OF FIGURES	ix
LIST OF SCHEMES	XV
KEY TO ABBREVIATION	xvii
CHAPTER 1: Synthetic linear glycopolymers and their biological application	ıs 1
1.1: Introduction of glycopolymers and multivalent interactions	
1.2: Synthesis of linear glycopolymers	
1.2.1: Direct polymerization of glycomonomers	
1.2.2: Post-glycosylation of pre-formed polymers	
1.3: Glycopolymers as probes to study biological processes	
1.3.1: Interaction with plant derived lectins	
1.3.2: Glycoarray	
1.3.3: Mimics of cell-associated glycans	
1.3.4: Interaction with the immune system	
1.3.4.1: Glycopolymers for immune activation	
1.3.4.2: Glycopolymers for immune down-regulation	
1.3.5: Interaction with viral and bacterial proteins	
1.4: Other biological applications of glycopolymers	
1.5: Summary	
REFERENCES	
CHAPTER 2: Carbohydrate antigen delivery by water soluble copolymers as	3
potential anti-cancer vaccines	64
2.1: Introduction	
2.1.1: Tumor associated carbohydrate antigens (TACAs)	64
2.1.2: Challenges in TACA delivery and overview of different carrier pl	atforms
2.2: Results and discussion	
2.2.1: Synthesis of Tn antigen (Scheme 2.1)	71
2.2.2: Design, synthesis and characterization of glycopolymers	
2.2.3: Immunological studies to evaluate vaccine efficacy	
2.3: Conclusions	
2.4: Experimental section	
2.4.1: General experimental procedures and methods for synthesis	
2.4.2: Synthesis of Tn antigen	
2.4.3: Synthesis of block copolymer	89
2.4.4: Synthesis of peptidic glycopolymer	90
2.4.5: Synthesis of the control polymer	92

2.4.6: Mouse immunization	92
2.4.7: ELISA assays	
2.4.8: Fluorescence-activated cell sorting (FACS)	93
APPENDIX	
REFERENCES	
CHAPTER 3: Valency and density matter: deciphering impacts of immunogen	
structures on immune responses against a tumor associated carbohydrate antig	en
using synthetic glycopolymers	
3.1: Introduction	
3.2: Results and discussion	
3.2.1: Design, synthesis and characterization of glycopolymers	
3.2.2: The specific B cell detection by enzyme-linked immunospot	
(ELISPOT) and flow cytometry	•
3.2.3: Early B cell activation events induced by different glycopolymers	
3.2.4: In vivo studies	
3.2.5: B cell tolerance	
3.3: Conclusions	
3.4: Experimental section	
3.4.1: General experimental procedures and methods for synthesis	
3.4.2: Synthesis of glycopolymers	
3.4.3: Cell viability	
3.4.4: Cell isolation and culture	
3.4.5: ELISOPT assays	142
3.4.6: Flow cytometry for Tn specific B cells	
3.4.7: Measurement of apoptosis	
3.4.8: BCR clustering and colocalization with GM1	
3.4.9: Calcium flux assay	
3.4.10: Flow cytometry for cell surface markers	
3.4.11: Mouse immunization	
3.4.12: ELISA assays	
APPENDIX.	
REFERENCES	

LIST OF TABLES

Table 2.1: Major TACAs identified in cancer tissues 64
Table 2.2: Reaction yields for polymers 22, 24, 26 and 28. 77
Table 3.1: Polymers and glycopolymers synthesized for the current study. 118
Table 3.2: Summary of ELISPOT and flow cytometry results of 450kDa glycopolymer treated spleen cells. Flow cytometry data are the average of a minimum of three independent experiments (n≥3). The statistical analysis results are presented in Figure 3.2
Table 3.3: a) Summary of hydrodynamic diameters and zeta potential of glycopolymers bearing 450kDa backbones in cell culture media as measured by dynamic light scattering (DLS). b) Hydrodynamic diameters of 450k-80 and 450k-115 glycopolymers at various concentrations. These similar hydrodynamic diameter and zeta potential values suggested that these glycopolymers had similar physical properties and there were no aggregations under the experimental conditions.

LIST OF FIGURES

Figure 1.1: (a) monovalent ligand binds to monovalent receptor (b) multivalent ligands bind to multivalent receptors
Figure 1.2: Structures of (a) unsaturated neoglycopolymer and (b) saturated neoglycopolymer
Figure 1.3: Models for cell aggregation by Con A. (A) Two hypothetical cell surfaces bearing multiple mannose-terminated glycans (red circles) can be aggregated by Con A. (B) The observed enhancements in cell aggregation in the presence of multivalent ligands is highly likely due to the increased avidity of the Con A-scaffold complex for the cell surface. Reproduced with permission from reference ⁵⁷ Copyright 2002, Elsevier
Figure 1.4: Mucin mimetic glycopolymer arrays. (A) Conventional glycan arrays with poor control over glycan spatial presentation. (B) New glycan arrays using polymeric scaffolds are able to mimic native mucins more closely. Reproduced with permission from reference ⁶¹ Copyright 2012, American Chemical Society
Figure 1.5: Determination of cross-linking by lectins in mucin mimic glycopolymer microarrays. (A) When cross-linking does not occur, the observed dissociation constant should be independent of glycopolymer surface density. (B) When cross-linking happens, weaker binding should be observed with increasing spacing between neighboring glycopolymers (K _{d,high} and K _{d,low} denote dissociation constants for a lectin in a high and a low glycopolymer surface density array, respectively). Reproduced with permission from reference ⁶¹ Copyright 2012, American Chemical Society
Figure 1.6: Models for different cross-linking activities of SBA and HPA. (A) More weakly associating SBA engages in a reversible "bind-and-slide" mechanism with the glycopolymers which maximizes binding interactions through cross-linking. (B) High avidity HPA interacts with the glycopolymers in a strong "face-to-face" mode, possibly leading to the formation of kinetically trapped species with not enough unbound GalNAc residues available for cross-linking. Reproduced with permission from reference Copyright 2012, American Chemical Society
Figure 1.7: Preparation of glycoarray by immobilization of the <i>O</i> -cyanate chain-end functionalized glycopolymer with amine functionalized glass slides <i>via</i> isourea bond formation.
Figure 1.8: Orientation and density controlled glycopolymer microarray. Reaction conditions: (a) polyacrylamide-BA, NaHCO ₃ buffer (pH 10.3), (b) lysozyme-BA, NaHCO ₃ buffer (pH 10.3), (c) BSA-BA, NaHCO ₃ buffer (pH 10.3), (d) NaHCO ₃ buffer (pH 10.3), (e) 1 mM glucose, phosphate-buffered saline (PBS) buffer (pH 7.4)

Figure 1.9: (A) Structures of representative GAGs. $R = SO_3^-$ or H; $R_1 = SO_3^-$, H, or Ac; $R_1 = SO_3^-$, H, or Ac; $R_2 = SO_3^-$ or H; $R_3 = SO_3^-$, H, or Ac; $R_4 = SO_3^-$, H, or Ac; $R_5 = SO_5^-$ or H; $R_1 = SO_3^-$, H, or Ac; $R_2 = SO_5^-$ or H; $R_3 = SO_3^-$ or H; $R_4 = SO_3^-$, H, or Ac; $R_5 = SO_5^-$ or H; $R_5 = SO_5$
Figure 1.10: Structures of first generation glycopolymers with low lipophilicity of the end groups.
Figure 1.11: Structures of second generation glycopolymers
Figure 1.12: Structures of two types of phospholipid-terminated mucin mimetics: (a) "body-labeled" glycopolymers with a small number (2-3) of fluorophores distributed along the glycopolymer backbone (n \sim 240), and (b) "end-labeled" glycopolymers with only one terminal fluorescent dye per polymer chain (green = AF488, red = TR)
Figure 1.13: A schematic model for probing galectin-mediated ligand cross-linking or live cell surfaces. Synthetic glycopolymers bearing galectin-binding glycans (blue hexagons) with a lipid anchor on one end and either a FRET donor or acceptor dye on the other end were inserted into live cell membranes, and their τ_{FL}) and τ_{D} were monitored Reproduced with permission from reference ⁷⁸ Copyright 2012, American Chemical Society.
Figure 1.14: Overview of approach to develop gold nanoparticle-based synthetic glycopolymer anticancer vaccines. Breast cancer cells express aberrant mucins displaying Core 1 glycans such as Tn-antigen. The glycopolymers bearing Tn-antigens conjugated to gold nanoparticles can mimic the 'multicopy-multivalent' presentation. Reproduced with permission from reference ⁸³ Copyright 2013, American Chemical Society
Figure 1.15: Structures of polymer glycopeptide conjugate vaccines bearing tumor associated MUC1 glycopeptide and the T-helper-cell epitope P2 peptide
Figure 1.16: Schematic representation of the sequence-controlled multi-block copolymerization of ManA (M) and GluA (G)
Figure 1.17: Structures of polymers used to investigate CD22 recognition. Polymers with a DP of 250 (n \approx 250) were used. The substituents include the DNP group (R ₁ , blue), the CD22 ligand Neu5Ac α 2,6Gal β 1,4Glc (CD22L, R ₂ , red), or the spacer unit derived from ethanolamine coupling. The level of substitution of each group (mole fraction χ) is labeled for each polymer.
Figure 1.18: CD22 can interact with B cell surface glycoproteins that have terminal α 2,6-linked sialic acid residues (<i>cis</i> interactions), which can mask CD22's interactions with exogenous ligands (<i>trans</i> interactions).
Figure 1.19: DNP polymer can initiate activation of early B cell signaling events Copolymers bearing DNP and a ligand for CD22 result in the attenuation of B cell activation

Figure 1.20: A glycocalyx engineering approach to study sialoside-mediated immunoevsion from NK cells. (a) NK cells can be activated after binding to activating ligands when there are no inhibitory ligands on the target cell. When sialylated glycopolymers are inserted onto cancer cell membrane, they can bind to the Siglec family of inhibitory receptors and localize Siglecs to the site of activation, which results in Src homology region 2 domain-containing phosphatase (SHP)-1 and SHP-2 recruitment to prevent cellular activation. (b) Structure of phospholipid oxime glycopolymer. Reproduced with permission from reference 99 Copyright 2013, Springer Nature
Figure 1.21: Model of receptor clustering by synthetic ligands. (a) Chemoreceptors form dimers in the plasma membrane of E . $coli$ and each dimer appears to interact with a single ligand. (b) Multivalent ligands that cannot span the distance needed to cluster the receptors can only bind to individual dimers, as in (a). (c) Multivalent ligands of sufficient lengths are able to cluster the chemoreceptors. (d) Increasing the valency of a multivalent ligand can engage more receptor clustering, thus enhancing the bacterial response. Reproduced with permission from reference 106 Copyright 2000, Elsevier 48
Figure 1.22: CholA-anchored glycopolymers are recycled and return back to the cell surface. Reproduced with permission from reference Copyright 2015, John Wiley and Sons.
Figure 1.23: CholA-anchored glycopolymers are excluded from sites of adhesion formation and drive integrin clustering by a kinetic funnel effect. Reproduced with permission from reference ¹⁰⁸ Copyright 2015, John Wiley and Sons
Figure 1.24: Schematic presentation of trehalose glycopolymers synthesized by RAFT.52
Figure 1.25: Structure of the trehalose polymers.
Figure 1.26: Steps for generating multiple protein patterns. (I), spin coating with polystyrenyl ether trehalose (poly(SET))-protein-1 solution and writing of the first layer. (II), rinsing of the unexposed poly(SET)-protein-1 followed by spin coating poly(SET)-protein-2, alignment to the first layer and writing of the second layer. (III-IV), multiple protein patterns can be obtained by repeated spin coating, alignment, writing and rinsing steps. All of the above steps including EBL do not require cleanroom conditions. Reproduced with permission from reference ¹¹¹ Copyright 2015, Springer Nature
Figure 2.1: Representative structures of TACAs. 65
Figure 2.2: Tn(c)-KLH vaccine
Figure 2.3: Unimolecular trivalent antigen constructs

polymer 28 and the anti-Tn IgG titers on days 0, 35 and 89 from mice immunized with glycopolymer 28 and the anti-Tn IgG titers on days 0 and 35 from mice immunized with glycopolymer 28 and anti-polymer backbone IgG titers on days 35 from mice receiving control polymer 29. (c) Flow cytometry analysis of Jurkat cell binding by IgG antibodies in sera from representative mice immunized with glycopolymer 28 (orange curve) and control polymer 29 (blue curve). The shaded curve was from pre-immune serum binding with Jurkat cells. (d) Anti-Tn IgM titers on days 0, and 35 from mice immunized with glycopolymer 28 and the anti-Tn IgM titers on day 35 from mice receiving control polymer 29.
Figure 2.5: HPLC-UV spectrum of 10 μg PV peptide. Peak appears at ~24 min 96
Figure 2.6: GPC of the phenyl acetic acid derivative of copolymer 22 (eluent: DMF) 97
Figure 2.7: 500 MHz (D ₂ O), ¹ H NMR of 15
Figure 2.8: 600 MHz (D ₂ O), ¹³ C NMR of 15
Figure 2.9: 600 MHz (D ₂ O), ¹³ C NMR of 15
Figure 2.10: 500 MHz (D ₂ O), ¹ H NMR of copolymer 20
Figure 2.11: 500 MHz (D ₂ O), ¹ H NMR of copolymer 22
Figure 2.12: 500 MHz (D ₂ O), ¹ H NMR of glycopolymer 24
Figure 2.13: 500 MHz (D ₂ O), ¹ H NMR of glycopolymer 26
Figure 2.14: 500 MHz (D ₂ O), ¹ H NMR of peptidic glycopolymer 28
Figure 3.1: ELISPOT results of anti-Tn B cells treated with the following glycopolymers with 450kDa backbones: a) 450k-4; b) 450k-6; c) 450k-10; d) 450k-40; e) 450k-60; f) 450k-80; and g) 450k-115
Figure 3.2: Percentage of Tn-specific splenic B cells upon incubation with 450k, 450k-6 (Tn 2.1 μM), 450k-10 (Tn 1.05 μM, 2.1 μM), 450k-40 (Tn 6.3 μM, 8.4 μM), 450k-60 (Tn 8.4 μM), 450k-80 (Tn 4.2 μM), 450k-115 (Tn 6.3 μM) as determined by FACS analysis. Statistical analysis was performed using Student's t test. *** $p = 0.0002$ 450k-10 Tn 1.05 μM vs. 450k; **** $p < 0.0001$ 450k-10 Tn 1.05 μM, 450k-10 Tn 2.1 μM, 450k-40 Tn 6.3 μM, 450k-40 Tn 8.4 μM vs. 450k; *** $p < 0.005$ 450k-60, 450k-80 vs. 450k

Figure 3.3: a) Percentages of Tn specific apoptotic B cells upon incubation with 450k-40, 450k-80 or 450k-115 glycopolymers. The percentages were calculated by dividing the numbers of Tn-specific apoptotic B cells by the total number of Tn specific B cells as determined by flow cytometry. Statistical analysis was performed using Student's t test with <i>p</i> values obtained by comparing with cells incubated with the 450k-40 glycopolymer. Glycopolymers with valency higher than 40 induced more apoptosis of Tn specific B cells. b) Percentages of apoptotic cells in the overall B cell pools upon incubation with 450k-40, 450k-80 or 450k-115 glycopolymers showing no significant differences in overall B cell apoptosis. This suggests the apoptosis induction by higher valency glycopolymers was specific to Tn
Figure 3.4: ELISPOT of B cells incubated with a) 250k-40, b) 100k-40, c) 46k-40; d) 13k-4; e) 13k-10; and f) 100k-10 at varying Tn concentrations
Figure 3.5: Viability of EA.hy 926 cells upon incubation with various concentrations of 450k-40 polymer and 450k polymer (the same polymer concentration as 450k-40) for 48 hours. The cell viability was determined by the CytoTox 96 Non-radioactive cytotoxicity assay.
Figure 3.6: Confocal microscopy images of (a) untreated B cells; B cells incubated with (b) the control polymer 450k; (c) 450k-40 (Tn 8.4 μM); and (d) 450k-80 (Tn 4.2 μM). BCRs were stained red with rhodamine-anti-IgM μ chain specific F (ab') and GM1 was stained green with FITC-cholera toxin B subunit. Yellow color in the overlay images suggests the colocalization of BCR with GM1
Figure 3.7: Calcium flux of no cells; naïve B cells incubated with 450k polymer; naïve B cells incubated with 450k-40 glycopolymer, and B cells pre-activated with 450k-40 (Tn 8.4 μM) glycopolymer incubated subsequently with 450k-40 as detected by the fluo-4 NW dye.
Figure 3.8: Percentages of (a) CD69 ⁺ or (b) CD86 ⁺ B cells incubated with either control polymer 450k or 450k-40 as determined by flow cytometry. Higher percentages of cells treated with 450k-40 are CD69 and CD86 positive. Statistical analysis was performed using Student's t test

Figure 3.9: (a) Anti-Tn IgM titers of mice vaccinated with 450k-40 glycopolymer (Tn 4 μg), prior to immunization (day 0), 2, 4 and 8 days post immunization (Statistical analysis was performed using Student's t test. ns = nonsignificant; ** $p < 0.01$). The average IgM titers were highest at day 4; (b) Anti-Tn IgM titers of mice vaccinated with 450k-40 glycopolymer at doses of 1, 4 and 7 μg of Tn (Statistical analysis was performed using Student's t test. ** < 0.01). Blood was collected on day 4 after immunization. 4 μg Tn dose gave the highest average IgM titers; (c) Anti-Tn IgM titers of mice vaccinated with 450k polymer and various glycopolymers (Tn 4 μg) at day 4 after immunization. Consistent with <i>in vitro</i> results, 100k-40 and 450k-40 gave the highest average titers (Statistical analysis was performed using Student's t test. The p value for 450k-40 vs day 0 is *** $p = 0.0002$, vs 450k-80 is ** 0.002; The p value for 100k-40 vs 13k-4 is *** $p = 0.0002$). (d) ELISPOT of spleen cells (8 x 10 ⁵ cells per well) from non-immunized and 450k-40 immunized mice upon incubation with 450k-40 (Tn 8.4 μM) glycopolymer. Statistical analysis was performed using Student's t test (* $p = 0.02$)
Figure 3.10: (a) Addition of increasing concentrations of 13k-4 to B cells incubated with 450k-40 glycopolymer (8.4 μ M Tn concentration) suppressed the generation of Tn specific ASCs; (b) Addition of 13k-4 to B cells incubated with wheat germ agglutinin (1 μ g/mL) did not have any significant effects on wheat germ agglutinin specific ASCs. (c) Co-administration of 450k-40 (Tn 4 μ g) and 13k-4 (Tn 1 μ g) to mice significantly reduced IgM titers compared to mice receiving 450k-40 (Tn 4 μ g) only. Blood was collected on day 4 and day 8 following immunization. Statistical analysis was performed using Student's t test (** p < 0.01). These results suggest 13k-4 glycopolymer selectively induced non-responsiveness of Tn specific ASCs
Figure 3.11: GPC traces of methylated polymer 4, 8, 100k, 250k and 450k. (eluent : DMF)
Figure 3.12: 500 MHz (D ₂ O), ¹ H-NMR of polymer 4
Figure 3.13: 500 MHz (CDCl ₃), ¹ H-NMR of ^t Bu protected polymer 8
Figure 3.14: 500 MHz (D ₂ O), ¹ H-NMR of polymer 8

LIST OF SCHEMES

Scheme 1.1: Synthesis of glycopolymers by ROMP
Scheme 1.2: Homopolymerization of acrylic glycomonomers. 4
Scheme 1.3: Synthesis of monomer GAMA. 5
Scheme 1.4: ATRP of GAMA in protic media under mild conditions
Scheme 1.5: Synthesis of glycopolymers from biotinylated initiator by ATRP 6
Scheme 1.6: Synthesis of a lipo-glycopolymer
Scheme 1.7: The aqueous RAFT polymerization of MAGlu without protecting group. (V-501 = 4,4'-azobis(4-cyanovaleric acid).)
Scheme 1.8: Synthesis of glycopolymers by living radical polymerization and click chemistry. Reagents and conditions: (a) <i>N</i> -(n-ethyl)-2-pyridylmethanimine/CuBr, toluene, 70 °C; (b) <i>N</i> -(ethyl)-2-pyridylmethanimine/CuBr, methyl methacrylate (MMA) or methoxy(poly(ethylene glycol)) ₃₀₀ methacrylate (mPEG ₃₀₀ MA), toluene, 70 °C; (c) Tetra- <i>n</i> -butylammonium fluoride (TBAF), acetic acid, THF, -20 to +25 °C; (d) R ¹ N ₃ , (PPh ₃) ₃ CuBr, diisopropylethylamine (DIPEA).
Scheme 1.9: Synthesis of glycopolymers by one-pot CuAAC/LRP process with three possible pathways (benzyl 2-bromoisobutyrate was employed as the polymerization initiator)
Scheme 1.10: Polymer synthesis. Reagents and conditions: (a), NaOCH ₃ [cat.], dry CH ₃ OH, room temperature (RT), under N ₂ ; (b), AIBN, CHCl ₃ , 65 °C, 48 h; (c), K ₂ S ₂ O ₈ , H ₂ O: CH ₃ OH (4: 1), 65 °C, 48 h; (d), NaOCH ₃ [cat.], CH ₃ OH: CHCl ₃ (1: 1), RT, under N ₂ .
Scheme 1.11: Synthesis of dual-end-functionalized glycopolymers as mucin mimics by RAFT (ACVA = 4,4'-Azobis(4-cyanovaleric acid))
Scheme 1.12: Preparation of mucin mimic glycan array by covalent microcontact printing (μ-CP) of glycopolymer on azide-functionalized silicon oxide wafers
Scheme 1.13: Synthesis of biotinylated glycopolymers by RAFT followed by ligation of reducing sugars to hydrazide groups on the polymers
Scheme 1.14: Synthesis of glycopolymer and its conjugation to chicken serum albumin.
Scheme 2.1: Synthesis of azido-Tn analog

Scheme 2.2: Synthesis of polymer 22.	75
Scheme 2.3: Synthesis of glycopolymer 28.	77
Scheme 3.1: Synthesis of glycopolymers	116

KEY TO ABBREVIATION

μ-CP Microcontact printing

AAL Aleuria aurantea lectin

Ac₂O Acetic anhydride

ADCC Antibody-dependent cell cytotoxicity

AF488 Alexa Fluor 488

AIBN Azobisisobutyronitrile

APC Antigen presenting cell

ASC Antibody-secreting B cells

ATRP Atom transfer radical polymerization

BA Boronic acid

BCG Bacillus Calmette-Guérin

BCR B cell receptor

BnBr Benzyl bromide

BOP Benotriazole-1-yl-oxy-tris-(dimethylamino)-phosphonium

hexafluorophosphate

BPA Leguminous lectin Bauhinia purpurea agglutinin

bpy 2,2'-Bipyridine

BSA Bovine serum albumin

cat. Catalytic

CholA Cholesterylamine

CMFRP Cyanoxyl mediated free radical polymerization

Con A Concanavalin A

CS Chondroitin sulfate

CTA chain transfer agent

CTP 4-Cyano-4-methyl-4-thiobenzoylsulfanyl butyric acid

CuAAC Copper-catalyzed azide-alkyne cycloaddition

DBU 1,8-Diazabicyclo[5.4.0]undece-7-ene

DC Dendritic cell

DCM Dichloromethane

DC-SIGN Dendritic cell specific intracellular adhesion molecule-3 grabbing

nonintegrin

DIPEA Diisopropylethylamine

DLS Dynamic light scattering

DMAP 4-Dimethylaminopyridine

DMF Dimethylformamide

DMSO Dimethyl sulfoxide

DNP Dinitrophenyl

dOSM Desialylated ovine submaxillary mucin

DP Degree of polymerization

EBL Electron-beam lithography

ELISA Enzyme linked immunosorbent assay

Et Ethyl

EtOAc Ethyl acetate

FACS Fluorescence-activated cell sorting

FCS Fluorescent correlation spectroscopy

FDA Food and Drug Administration

FITC Fluorescein isothiocyanate

FLIC Fluorescence interference contrast microscopy

FRAP Fluorescence recovery after photobleaching

FRET Fluorescence resonance energy transfer

FucA Fucose acrylate

GAG Glycosaminoglycans

GalNAc N-acetylgalactosamine

GAMA 2-Gluconamidoethyl methacrylate

GPC Gel permeation chromatography

GPI Glycosylphosphatidyl-inositol

GulA Glucose acrylate

HAI Hemagglutination inhibition

HBSS Hank's balanced salt solution

HEPES 4-(2-Hydroxyethyl)-1-piperazineethanesulfonic acid

Hex Hexane

HIV Human immunodeficiency virus

HOBt hydroxybenzotriazole

HPLC High-performance liquid chromatography

HRMS High resolution mass spectrometry

HRP Horseradish peroxidase

HSA Human serum albumin

IACUC Institutional Animal Care and Use Committee

IFN Interferon

IL-6 Interleukin-6

IP₃ 1,4,5-Inositol triphosphate

ITC Isothermal titration calorimetry

K_d Dissociation constant

KLH Keyhole limpet haemocyanin

LDH Lactate dehydrogenase

LRP Living radical polymerization

MAGlu 2-Methacryloxyethyl glucoside

ManA Manose acrylate

MC-SPR Multichannel SPR

Me₆-TREN Tris[2-(dimethylamino)etheyl]amine

MeOH Methanol

MHC Major histocompatibility complex

MMA Methyl methacrylate

Mn Molecular weight

mPEG₃₀₀MA Methoxy(poly(ethylene glycol))₃₀₀ methacrylate

MUC1 Mucin 1

MWCO Molecular weight cut-off

NeuAc N-acetylneuraminic acid

NHS N-hydroxysuccinimide

NIP Nitro-iodophenol

NK Natural killer (cell)

NMFRP Nitroxide-mediated living free-radical polymerization

NMP N-methyl-2-pyrrolidone

NMR Nuclear magnetic resonance

OD Optical density

P-(HPMA) Poly (N-(2-hydroxypropyl)methacrylamide)

PAA Poly(acrylic acid)

PBS Phosphate-buffered saline

PDI Polydispersity index

PEG Polyethylene glycol

PMDETA N,N,N',N''-pentamethyldiethylenetriamine

PNA Peanut Arachis hypogaea agglutinin

poly(SET) Polystyrenyl ether trehalose

PPE Poly(*p*-phenylene ethynylene)

PSM Post synthetic modification

PV Polio virus

Py Pyridine

RAFT Reversible addition-fragmentation chain transfer polymerization

RCA I Ricinus communis I

ROMP Ring-opening metathesis polymerization

RPMI Roswell Park Memorial Institute medium

RT Room temperature

SBA Soybean agglutinin

SEC Size exclusion chromatography

SET-LRP Single-electron transfer living radical polymerization

SHP Src homology region 2 domain-containing phosphatase

SPR Surface plasmon resonance

TACA Tumor associated carbohydrate antigen

TBAF Tetra-*n*-butylammonium fluoride

TCEP Tris(2-carboxyethyl)phosphine hydrochloride

TEAI Tetraethylammonium iodide

Tf₂O Triflic anhydride

TFA Trifluoroacetic acid

Th Helper T (cell)

THF Tetrahydrofuran

TI T cell independent

TMB 3,3,5′,5′-Tetramethylbenzidine

TMSOTf Trimethylsilyl trifluoromethanesulfonate

Tn Thomsen-nouveau

TNF α Tumor necrosis factor alpha

TR Texas Red

TRIS Tris(hydroxymethyl)aminomethane

TSTU N,N,N',N'-tetramethyl-O-(N-succinimidyl)uronium tetrafluoroborate

TT Tetanus toxoid

V-501, ACVA 4,4'-Azobis(4-cyanovaleric acid)

VLP Virus-like particle

VNTR Variable number of tandem repeats

VVA *V. villosa* agglutinin

WFL W. floribunda lectin

 τ_D Diffusion time

τ_{FL} Fluorescence lifetime

CHAPTER 1: Synthetic linear glycopolymers and their biological applications

1.1: Introduction of glycopolymers and multivalent interactions

Carbohydrates play significant roles in a variety of biological recognition events, which are considered as the first step in a number of phenomena based on cell-cell interactions, including fertilization, embryogenesis, cell migration, organ formation, immune defense, microbial and viral infection, inflammation, and cancer metastasis.^{1,2} These recognition processes are thought to proceed by specific carbohydrate-protein interactions.³ Synthetic polymers with pendant carbohydrates (namely glycopolymers)⁴ have been developed to mimic this behavior. In recent years, glycopolymers have also been used as a tool for drug, gene and antigen delivery.⁵⁻⁹

Monovalent protein-carbohydrate interactions typically occur with low affinity $(K_D \sim 10^{-3} \text{ M})$. However, it is generally known that high affinity complexation is required for physiological recognition processes $(K_D \sim 10^{-9} \text{ M})$. Multivalency is defined to be the operation of multiple molecular recognition events of the same kind occurring simultaneously between two entities. Multivalency is necessary to achieve high binding affinity (avidity). It can be categorized into three different types: (a) bivalency, with two interactions between ligands and receptors, (b) oligovalency, with the number of interactions $i \le 10$, and (c) polyvalency, the number of interactions i > 10. The same kind occurring affinity (avidity).

From a thermodynamic perspective, binding affinity between a multivalent ligand and a multivalent receptor is much higher than that between a monovalent ligand and receptor (**Figure 1.1** showing monovalent binding and multivalent binding). A monovalent ligand-receptor interaction occurs with free energy change ΔG^{mono} ; N monovalent receptors interact separately with N monovalent ligands with a total free

energy change of $N\Delta G^{mono}$. A multivalent receptor with N binding sites interacts more strongly than with N times of monovalent ligands, where $K^{multi} >> (K^{mono})^{N}$. According to the van't Hoff equation: ΔG =-RTln(K), ΔG^{multi} of a multivalent interaction can be more favorable than $N\Delta G^{mono}$ (total free energy change of N monovalent interactions), ΔG^{multi} << $N\Delta G^{mono}$. The enthalpy of binding of a multivalent system can be more favorable than that of the monovalent species, with little or no corresponding increase in the unfavorable translational and rotational entropy of binding. 13,14

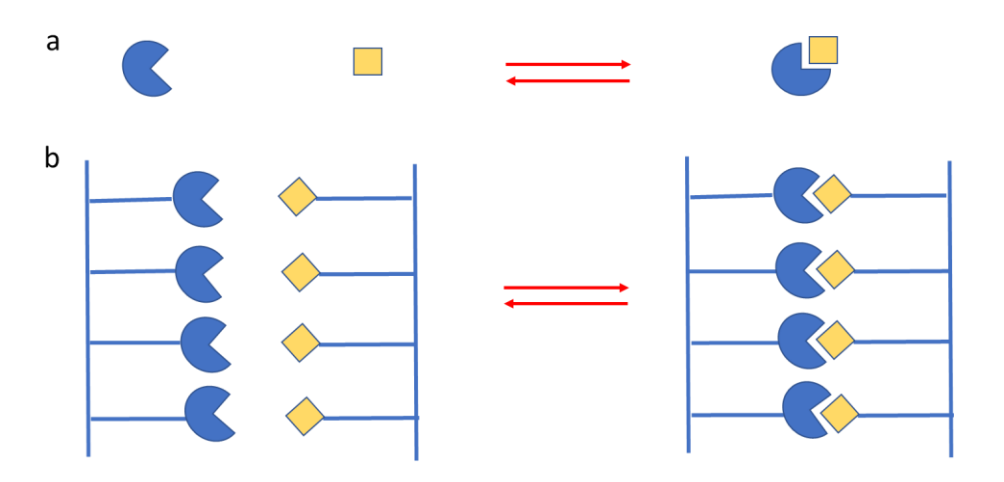


Figure 1.1: (a) monovalent ligand binds to monovalent receptor (b) multivalent ligands bind to multivalent receptors.

1.2: Synthesis of linear glycopolymers

1.2.1: Direct polymerization of glycomonomers

Linear glycopolymers can be synthesized via two methods: (1) direct polymerization of carbohydrate-containing monomers and (2) post-glycosylation of preformed polymers.¹⁵ A number of polymerization methods have been used for synthesis including atom transfer radical polymerization (ATRP), reversible addition-

fragmentation chain transfer polymerization (RAFT), ring-opening metathesis polymerization (ROMP), nitroxide-mediated living free-radical polymerization (NMFRP) and cyanoxyl mediated free radical polymerization (CMFRP).

Glycopolymers have been prepared by polymerization of protected sugar monomers with ring-opening,¹⁶ traditional free radical,¹⁷ ionic polymerization,¹⁸⁻²² coordination,²³ controlled radical polymerization²⁴⁻³⁰ followed by selective deprotection.

Kiessling and coworkers synthesized glycopolymers by ROMP as shown in **Scheme 1.1** with greater control of polymer size, structure and density of carbohydrate components.³¹

Scheme 1.1: Synthesis of glycopolymers by ROMP.

Chaikof et al. described the preparation of a series of model *N*-acetyl-D-glucosamine-containing glycomonomers. CMFRP was used to afford water-soluble glycopolymers with low polydispersity indexes (PDIs) and high monosaccharide contents.³² Statistical copolymers of acrylamide with either alkene- or acrylate-based glycomonomers and homoglycopolymers with some degree of control can be generated

by this polymerization method with **Scheme 1.2** showing the general mechanism of CMFRP of acrylic glycomonomers.

$$CI \longrightarrow NH_2 \xrightarrow{NaNO_2} T=0 \text{ °C/H}_2O$$

$$CI \longrightarrow N\equiv N^{\oplus} + ^{\ominus}OCN \xrightarrow{-N_2} CI \longrightarrow \bullet OCN$$

$$T=50 \text{ °C} \qquad n \text{ GM} \qquad OCN$$

$$CI \longrightarrow OCN \qquad CI \longrightarrow OCN \qquad OCN \qquad$$

Scheme 1.2: Homopolymerization of acrylic glycomonomers.

Narain and co-workers reported the first example of low polydispersity, controlled sugar methacrylate polymer structures prepared directly under mild conditions with ATRP without resorting to protecting group chemistry. The sugar monomer 2-gluconamidoethyl methacrylate (GAMA) was obtained by the ring-opening reaction of 2-aminoethyl methacrylate with D-gluconolactone as shown in **Scheme 1.3**, and the polymerization reaction (**Scheme 1.4**) was carried out at 20 °C in protic media (either

methanol, water or methanol/water mixtures).³³ While this method utilized carbohydrate based precursors, the pyranoside ring was opened in the polymer. Other synthetic routes have been developed to prepare sugar polymers in which the cyclic sugar is preserved during synthesis.

Scheme 1.3: Synthesis of monomer GAMA.

Scheme 1.4: ATRP of GAMA in protic media under mild conditions.

Maynard and coworkers synthesized glycopolymer via ATRP from biotinylated initiators either by direct polymerization of unprotected glycomonomer or by polymerization of protected glycomonomer as depicted in **Scheme 1.5**.³⁴

Scheme 1.5: Synthesis of glycopolymers from biotinylated initiator by ATRP.

Hawker et al. reported the synthesis of well-defined amphiphilic lipoglycopolymers by NMFRP (**Scheme 1.6**) in which the amphiphilic character is controlled and varied by the appropriate selection of monomers and initiating groups.²⁹

Scheme 1.6: Synthesis of a lipo-glycopolymer.

McCormick et al. reported the first example of direct polymerization of a sugar monomer (2-methacryloxyethyl glucoside (MAGlu)) without protecting group chemistry in aqueous media via RAFT as depicted in **Scheme 1.7**.35 4-Cyano-4-methyl-4-thiobenzoylsulfanyl butyric acid (CTP) was chosen as the RAFT chain transfer agent (CTA) due to its water-solubility and applicability for methacrylic monomers. In addition, they have shown the possibility of obtaining novel sugar-based AB-diblock copolymers in which MAGlu may be polymerized as the first or second block.

Scheme 1.7: The aqueous RAFT polymerization of MAGlu without protecting group. (V-501 = 4,4'-azobis(4-cyanovaleric acid).)

1.2.2: Post-glycosylation of pre-formed polymers

Haddleton et al. reported the synthesis of well-defined alkyne side chain functionalized polymers by living radical polymerization, followed by click chemistry with carbohydrate building blocks to afford the final glycopolymers (**Scheme 1.8**). 36

Scheme 1.8: Synthesis of glycopolymers by living radical polymerization and click chemistry. Reagents and conditions: (a) *N*-(n-ethyl)-2-pyridylmethanimine/CuBr, toluene, 70 °C; (b) *N*-(ethyl)-2-pyridylmethanimine/CuBr, methyl methacrylate (MMA) or methoxy(poly(ethylene glycol))₃₀₀ methacrylate (mPEG₃₀₀MA), toluene, 70 °C; (c) Tetra-*n*-butylammonium fluoride (TBAF), acetic acid, THF, -20 to +25 °C; (d) R¹N₃, (PPh₃)₃CuBr, diisopropylethylamine (DIPEA).

Later on, they developed the first copper-catalyzed azide-alkyne cycloaddition (CuAAC) and living radical polymerization (LRP) process to prepare glycopolymers

(Scheme 1.9). A number of parameters including solvent, catalyst concentration, temperature and the nature of the azide were varied to tune the relative rates of CuAAC and LRP.³⁷ With toluene at 60 °C and for both octyl azide and triethyleneglycol azide, the process followed path 1 as shown in Scheme 1.9. In DMSO, the two reactions proceeded concurrently, with the rate of CuAAC much slower and rate of LRP a little higher compared to those with toluene as the solvent. Using DMF as the solvent, CuAAC and LRP also occurred simultaneously, with the rate of CuAAC greatly higher than in DMSO and rate of LRP similar to in toluene. Mannose-functional polymers were prepared by this method using DMSO as the solvent with both reactions proceeded simultaneously. The rate of both reactions went up with increased catalyst concentration. With the increase of CuAAC reaction rate, the amount of un-clicked alkyne groups in the final polymer could be largely limited when relatively low concentration of catalyst was used

Scheme 1.9: Synthesis of glycopolymers by one-pot CuAAC/LRP process with three possible pathways (benzyl 2-bromoisobutyrate was employed as the polymerization initiator).

1.3: Glycopolymers as probes to study biological processes

1.3.1: Interaction with plant derived lectins

Lectins are carbohydrate binding proteins which are crucial elements in lots of biological processes. ^{38,39,40} This section will focus on glycopolymers binding to plant lectins. The commonly used plant derived lectins include: *Concanavalin A* (Con A) from the Jack bean, ⁴¹ peanut *Arachis hypogaea* agglutinin (PNA), ⁴² leguminous lectin *Bauhinia purpurea* agglutinin (BPA), ⁴³ soybean agglutinin (SBA) from the *G. max*, ⁴⁴ *W. floribunda* lectin (WFL), ⁴⁵ *V. villosa* agglutinin (VVA), ⁴⁶ *Ricinus communis* I (RCA I)

from castor beans,⁴⁷ and *Aleuria aurantea* lectin (AAL) from mushroom.⁴⁸

Lectins are known to be able to induce erythrocyte agglutination through interactions with cell surface glycoproteins. When glycopolymers are used as mimics of carbohydrate ligands, their binding to lectins would inhibit the agglutination processes. Using the hemagglutination inhibition assay, we would have a measurement of the binding abilities of different glycopolymers to lectins. With control of different factors including chain length, carbohydrate density (ligand spacing) and valency, different binding affinities were observed between glycopolymers and Con A by Kiessling and coworkers. They generated mannose- and glucose-derived neoglycopolymers via aqueous ROMP to inhibit Con A-facilitated agglutination. ⁴⁹ The inhibitory properties of the polyvalent ligands were proven to be better than those of the corresponding monosaccharides, which supported the multivalent effect.

Then they varied the monomer to catalyst ratio to produce polymers of increasing length, and studied the effect of chain length on the functional affinity of saturated and unsaturated neoglycopolymers (structures shown in **Figure 1.2**).⁵⁰ The potencies of the unsaturated polymers increased exponentially as the average length increased linearly for polymers up to DP (degree of polymerization) = 50 (analyzed on a saccharide residue basis), while further increase of chain length led to approximately equivalent inhibitory potencies. The saturated polymers showed a similar trend. The observed dependence of the inhibitory potency on the polymer length was largely due to a combination of statistical and chelation effects. ^{51,52}

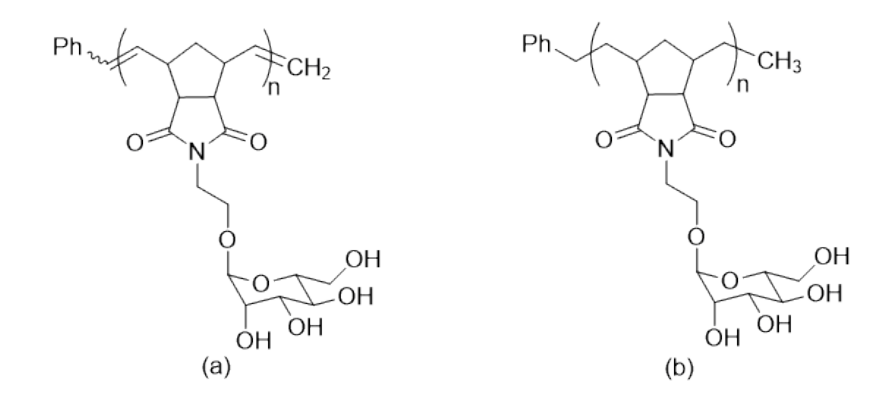


Figure 1.2: Structures of (a) unsaturated neoglycopolymer and (b) saturated neoglycopolymer.

Classical ROMP method to prepare defined materials with biological activities has several disadvantages. Each new polymer class requires a new, functionalized bicyclic substrate for ROMP. Rates of initiation, propagation, and nonproductive termination would be affected by the physical properties of each monomer. Moreover, purification of the polymer products can be complicated depending on the monomers. To address these issues, Kiessling and co-workers developed a general synthetic route (post synthetic modification (PSM)) for generation of libraries of oligomers and large-scale production. Con A inhibitory potencies of the materials generated by PSM and standard ROMP approaches were compared, and results indicated PSM protocol can afford biologically active materials with adequate or better potencies.

Their study showed that carbohydrate residue density could also affect the inhibitory activities.⁵⁴ For both the glucose and mannose-bearing polymers, the polymers with one sugar per repeat unit inhibited at an eight-fold lower saccharide concentration compared to polymers bearing two sugars per unit. This can be explained by the fact that the two saccharides connected to a single repeat unit are too close to bridge two binding sites on the same protein or two protein molecules according to molecular modeling

studies. This result unveiled the importance of carbohydrate ligand spacing in carbohydrate protein interactions.

The unfunctionalized monomer units employed in this study were smaller and more hydrophobic than the functionalized units, thus the glycopolymers did not present a uniform steric and electronic environment. To overcome this, they synthesized polymers with monomer units (mannose and galactose) that varied only in their binding activity. Con A binds to mannose selectively instead of galactose although they are sterically similar. Polymers with similar length, polarity and steric properties but different mannose densities were made by altering the ratio of mannose- and galactose-substituted monomers in copolymerization reactions. Con A was used as a model receptor to explore the impact of epitope density on receptor clustering including the stoichiometry of complexation, rate of cluster formation, and receptor proximity. It was found that polymers displaying the greatest number of binding sites generated the largest clusters, but those with the lowest density bound to the greatest number of receptors per residue. The highest density polymer was able to induce fastest clustering. However, increases in binding epitope density resulted in decreases in proximity of receptors within the clusters.

In addition, they also explored the use of glycopolymers as scaffolds to induce concentration-dependent precipitation of Con A.⁵⁷ The concentration required to induce precipitation was lower for higher-valency polymers than that required for shorter oligomers. Besides insoluble clusters, they also characterized the formation of soluble aggregates of Con A in solution by fluorescence resonance energy transfer (FRET). Similar trend was observed with varying valency. The efficiency of fluorescence quenching was also dependent on concentration. It went up first as the scaffold

concentration increased, but then started to drop as the concentration was increased further, which could be explained most likely by mannose binding site saturation. Furthermore, they studied the ability of Con A-scaffold complexes to aggregate Jurkat cells (models for aggregation shown in **Figure 1.3**). Based on the fact that the average size of a Jurkat cell is between 5,000 and 10,000 nm and the total length of the Con A-scaffold complex is about 20 nm, there is very little chance that the complex could span more than two cell surfaces simultaneously. They postulated that the enhancements in cell aggregation by multivalent ligands probably resulted from the increase of avidity of the Con A-scaffold complex for cell surface glycans.

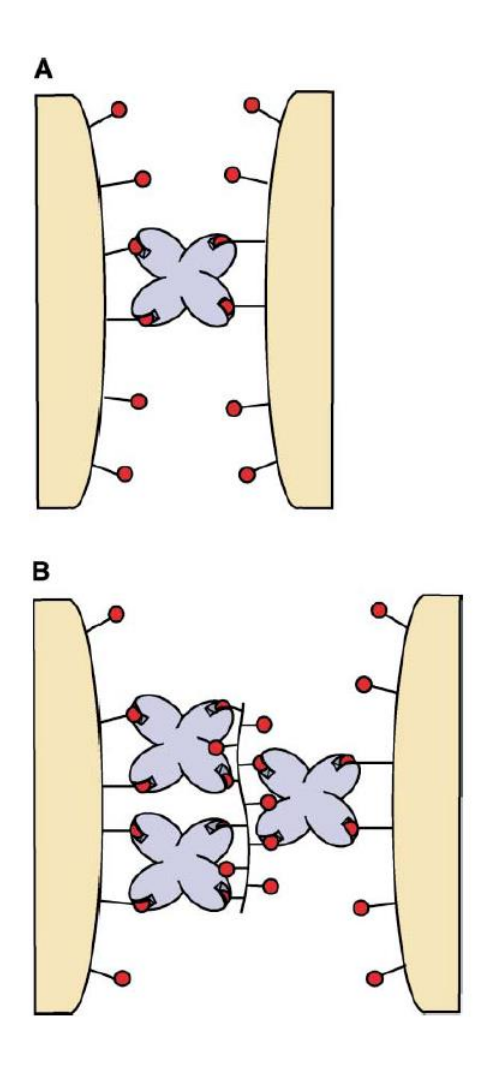


Figure 1.3: Models for cell aggregation by Con A. (A) Two hypothetical cell surfaces bearing multiple mannose-terminated glycans (red circles) can be aggregated by Con A. (B) The observed enhancements in cell aggregation in the presence of multivalent ligands is highly likely due to the increased avidity of the Con A-scaffold complex for the cell surface. Reproduced with permission from reference⁵⁷ Copyright 2002, Elsevier.

Stolnik and co-workers synthesized glycopolymer pGalEMA by either polymerization of the deprotected glycomonomer GalEMA or deprotection of the corresponding peracetylated polymer pAcGalEMA (**Scheme 1.10**),⁵⁸ and studied the interaction between the glycopolymers and the lectin PNA by UV-difference spectroscopy and isothermal titration calorimetry (ITC).⁵⁹ This was the first time ITC was used to investigate the interaction of a lectin with synthetic glycopolymers.

Scheme 1.10: Polymer synthesis. Reagents and conditions: (a), NaOCH₃ [cat.], dry CH₃OH, room temperature (RT), under N₂; (b), AIBN, CHCl₃, 65 °C, 48 h; (c), K₂S₂O₈, H₂O: CH₃OH (4: 1), 65 °C, 48 h; (d), NaOCH₃ [cat.], CH₃OH: CHCl₃ (1: 1), RT, under N₂.

1.3.2: Glycoarray

Glycopolymers can be integrated into microarrays for probing glycan-binding proteins due to their similarities to natural glycoproteins. Glycopolymers could be prepared by RAFT in a similar manner as described before, with one end bearing an alkyne group for attachment to azide-functionalized surface and a fluorophore at the other end (Scheme 1.11).⁶⁰ Micropatterns of these polymers can be generated by covalent microcontact printing (Scheme 1.12), and the glycopolymers displayed can bind specific lectins (e.g., HPA). With this new microarray platform, the densities and orientations of the glycan ligands are more controllable compared to traditional glycan arrays, which have very little control over how glycans are presented (Figure 1.4).⁶¹

Scheme 1.11: Synthesis of dual-end-functionalized glycopolymers as mucin mimics by RAFT (ACVA = 4,4'-Azobis(4-cyanovaleric acid)).

A CONVENTIONAL ARRAY B MUCIN MIMETIC ARRAY

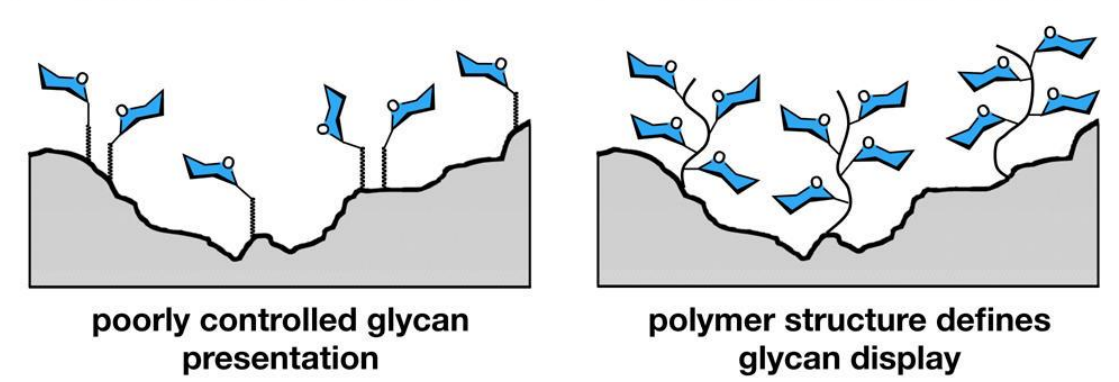
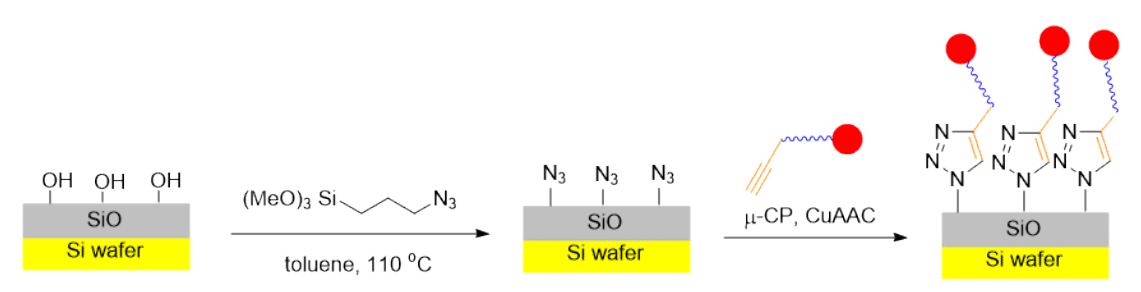


Figure 1.4: Mucin mimetic glycopolymer arrays. (A) Conventional glycan arrays with poor control over glycan spatial presentation. (B) New glycan arrays using polymeric scaffolds are able to mimic native mucins more closely. Reproduced with permission from reference⁶¹ Copyright 2012, American Chemical Society.



Scheme 1.12: Preparation of mucin mimic glycan array by covalent microcontact printing (μ -CP) of glycopolymer on azide-functionalized silicon oxide wafers.

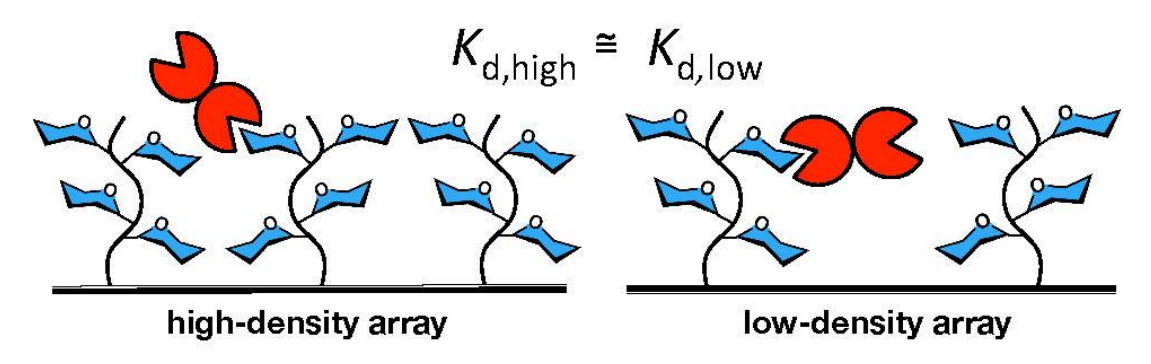
Later on Bertozzi group developed a general synthetic strategy for rapid, high-throughput generation of glycopolymer libraries for microarrays.⁶² The biotinylated glycopolymers were prepared via ligation of reducing sugars to hydrazide groups on the polymers synthesized by RAFT (**Scheme 1.13**). Since free reducing sugars are often available from natural sources, this approach can avoid laborious carbohydrate prefunctionalization, which is required for most glycopolymer synthesis. The glycopolymer ligands in these microarrays were able to bind lectins (ConA, RCA I, and AAL) according to the structures of their pendent glycans.

Scheme 1.13: Synthesis of biotinylated glycopolymers by RAFT followed by ligation of reducing sugars to hydrazide groups on the polymers.

With great control over glycan valency, density and presentation, Godula and coworkers used mucin mimetic glycopolymer microarrays to evaluate the ability of different Tn antigen-binding lectins (SBA, WFL, VVA and HPA) to cross-link mucin-like glycoconjugates by varying glycopolymer surface densities. As illustrated in **Figure 1.5**, if cross-linking did not occur, the observed dissociation constant K_d should not change much with regard to glycopolymer spacing. However, if lectins did cross-link multiple glycopolymers, weaker binding (higher K_d) in the low-density array would be observed. They found out that high avidity lectins (e.g., HPA), especially those that engage their ligands in a "face-to-face" mode as shown in **Figure 1.6** in which two GalNAc residues on the same polymer bound to two adjacent binding sites were unlikely to cross-link. On the other hand, more weakly associating lectins (e.g., SBA) whose binding sites are likely too far apart to engage "face-to-face" interactions, would have an

opportunity to form well-organized cross-linked networks.

A DISCRETE COMPLEX FORMATION:



B CROSSLINKING:

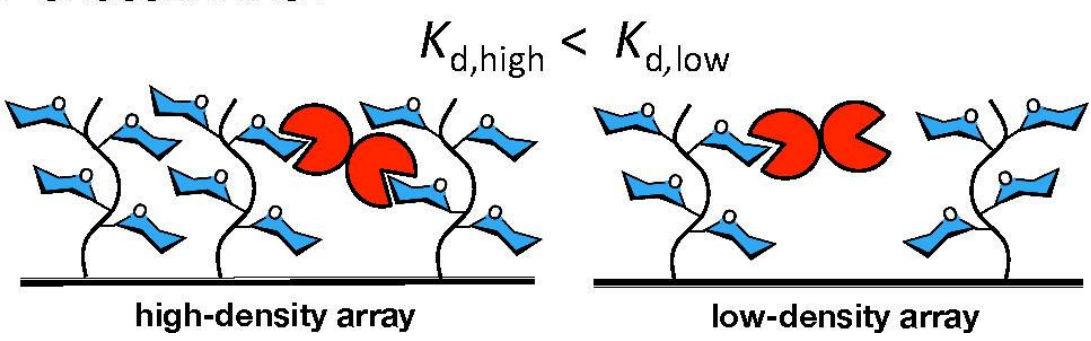


Figure 1.5: Determination of cross-linking by lectins in mucin mimic glycopolymer microarrays. (A) When cross-linking does not occur, the observed dissociation constant should be independent of glycopolymer surface density. (B) When cross-linking happens, weaker binding should be observed with increasing spacing between neighboring glycopolymers ($K_{d,high}$ and $K_{d,low}$ denote dissociation constants for a lectin in a high and a low glycopolymer surface density array, respectively). Reproduced with permission from reference⁶¹ Copyright 2012, American Chemical Society.

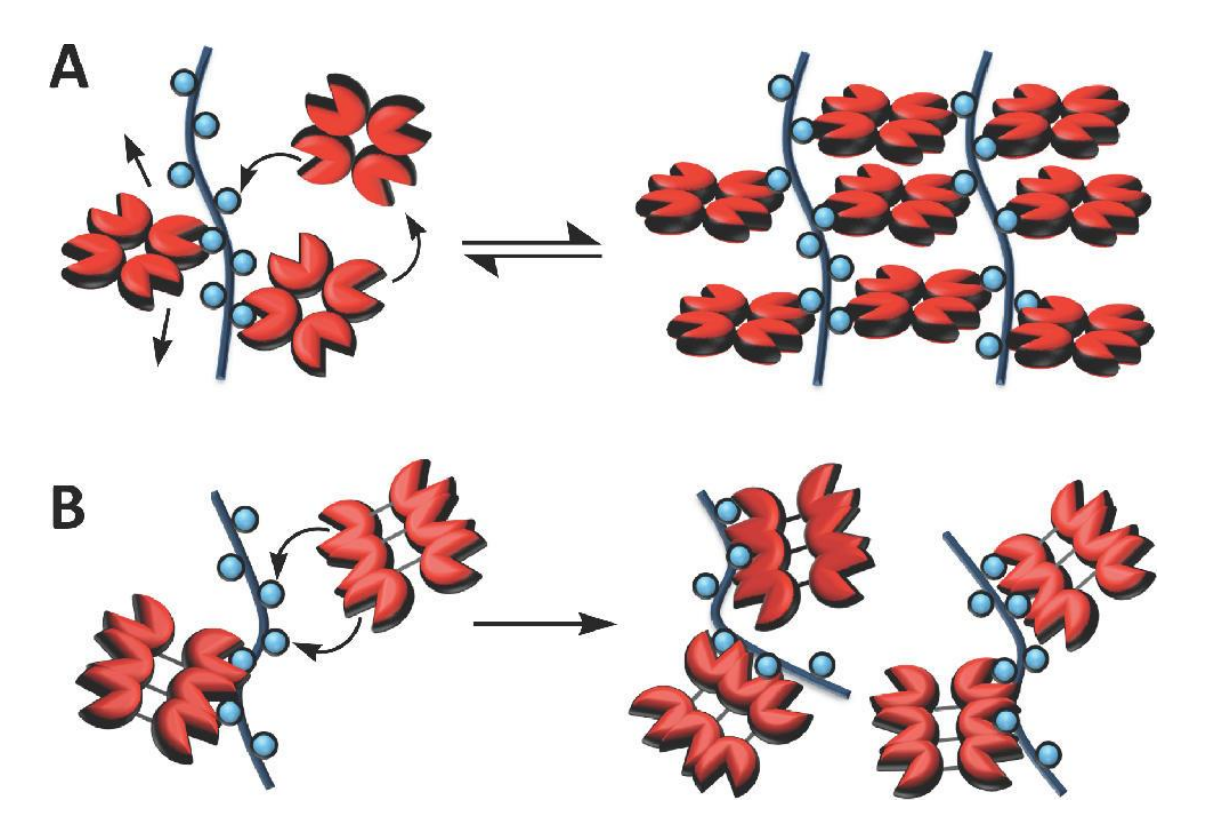


Figure 1.6: Models for different cross-linking activities of SBA and HPA. (A) More weakly associating SBA engages in a reversible "bind-and-slide" mechanism with the glycopolymers which maximizes binding interactions through cross-linking. (B) High avidity HPA interacts with the glycopolymers in a strong "face-to-face" mode, possibly leading to the formation of kinetically trapped species with not enough unbound GalNAc residues available for cross-linking. Reproduced with permission from reference⁶¹ Copyright 2012, American Chemical Society.

Xuelong Sun's group reported immobilization of an *O*-cyanate chain-end functionalized glycopolymer bearing multivalent lactose units synthesized by one-pot CMFRP with amine functionalized glass slides via *O*-cyanate-based isourea bond formation for glycoarray application (**Figure 1.7**).⁶³ In a similar way, they also immobilized sialyllactose-containing glycopolymer prepared via chemoenzymetic synthesis for glycoarray and surface plasmon resonance (SPR)-based glyco-biosensor applications.⁶⁴

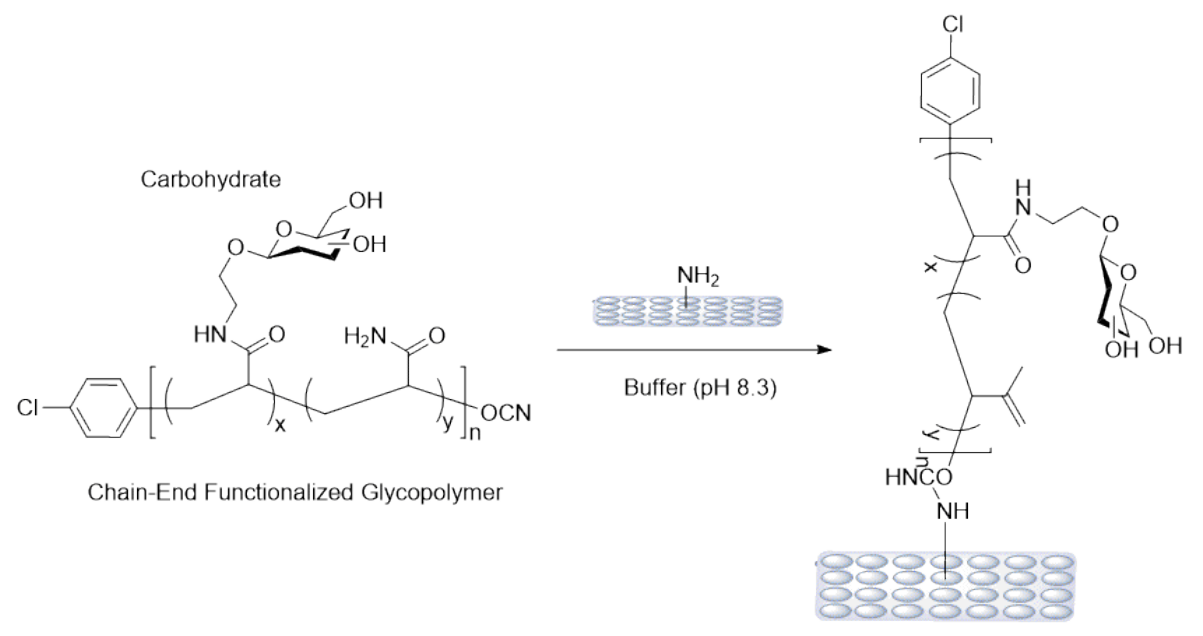


Figure 1.7: Preparation of glycoarray by immobilization of the *O*-cyanate chain-end functionalized glycopolymer with amine functionalized glass slides *via* isourea bond formation.

To better control glycan orientation and density, they designed boronic acid (BA) ligands in different sizes as detachable "temporary molecular spacers" as illustrated in **Figure 1.8**.65 First, the lactose-containing glycopolymer was pre-complexed with polyacrylamide-BA, lysozyme-BA, and bovine serum albumin (BSA)-BA conjugates respectively, and then immobilized onto glass slide at pH 10.3. When pH changed to 7.4, the macromolecular spacers were detached to afford the oriented and density controlled glycopolymer microarrays.

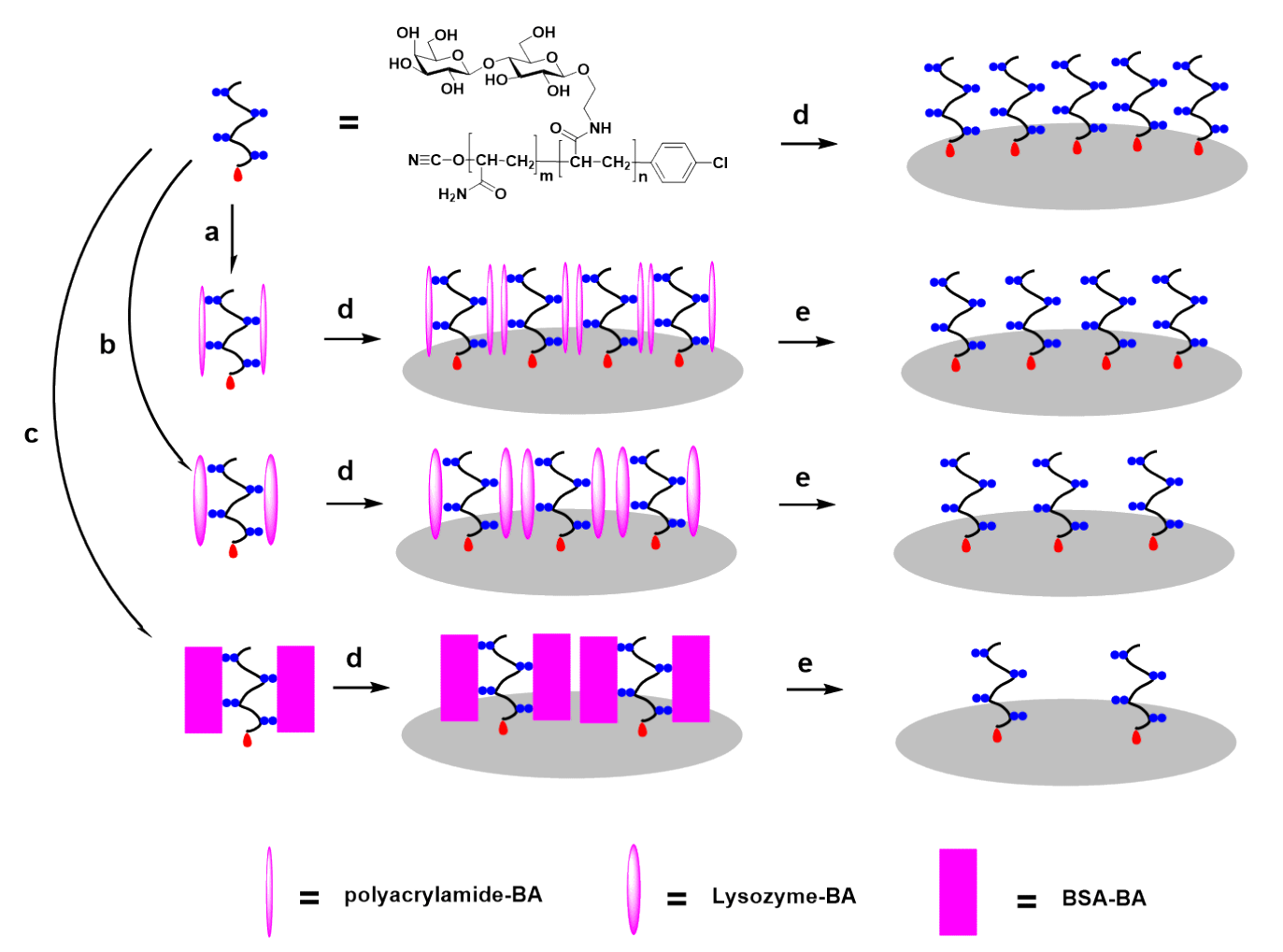


Figure 1.8: Orientation and density controlled glycopolymer microarray. Reaction conditions: (a) polyacrylamide-BA, NaHCO₃ buffer (pH 10.3), (b) lysozyme-BA, NaHCO₃ buffer (pH 10.3), (c) BSA-BA, NaHCO₃ buffer (pH 10.3), (d) NaHCO₃ buffer (pH 10.3), (e) 1 mM glucose, phosphate-buffered saline (PBS) buffer (pH 7.4).

Glycosaminoglycans (GAGs) are polysaccharide with 10-200 repeating sulfated disaccharide units (**Figure 1.9A**), which play important roles in biological processes ranging from cell division and viral invasion to cancer and neuroregeneration.⁶⁶ Hsieh-Wilson group integrated a new class of ROMP polymers that mimic chondroitin sulfate (CS) proteoglycans with microarray (**Figure 1.9B**) and SPR platforms, and demonstrated that these glycopolymers were able to retain their binding specificities to protein receptors such as monoclonal antibodies 2D11 and 2D5.⁶⁷

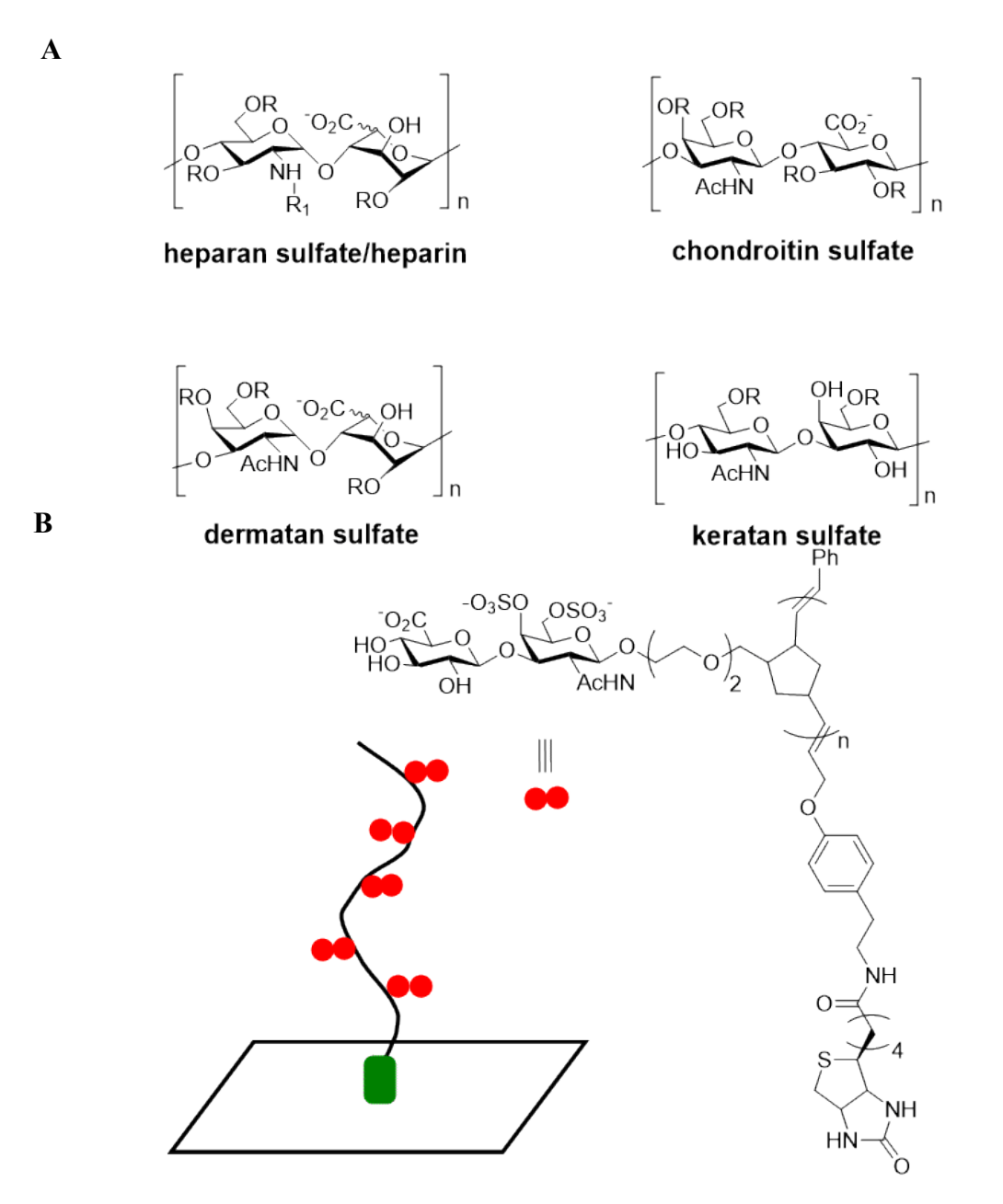


Figure 1.9: (A) Structures of representative GAGs. $R = SO_3^-$ or H; $R_1 = SO_3^-$, H, or Ac; $n = \sim 10\text{-}200$. (B) Biotin end-functionalized polymers as mimetics of CS proteoglycans. $n = \sim 80\text{-}280$.

1.3.3: Mimics of cell-associated glycans

Mucins are cell-surface glycoproteins responsible for cell-cell interactions.⁶⁸ Approaches for molecular-level studies of glycan function including genetic and metabolic engineering have been reported.^{69,70,71,72,73} However, since both methods take

advantage of cells' internal machinery, it is possible that they would perturb the cell's biological responses during the process. In some cases, certain cell types are not prone to genetic or metabolic modification. For these reasons, passive insertion of chemically modified structures into cellular membranes is considered to be an attractive alternative approach. Bertozzi group first reported anchoring glycopolymers end-functionalized with lipid groups as mucin mimics to a supported lipid bilayers, and they studied the ability of these mucin mimetics to bind carbohydrate-binding proteins.⁷⁴ However, with first generation glycopolymers (structures shown in Figure 1.10) only a small amount of them were able to be incorporated into the membrane. To address this problem, they designed second-generation end-functionalized polymers with increased lipophilicity of the end groups (structures shown in Figure 1.11). These polymers were incorporated into fluid lipid bilayers, and the mobility of the mucin mimetics were investigated with the fluorescence recovery after photobleaching (FRAP) technique, and similar results were obtained as the intrinsic lipid mobility of the membranes suggesting that the glycopolymers were anchored to the membrane only by its lipid moiety rather than through lipid-sugar interactions. The abilities of polymers (Figure 1.11a and Figure 1.11b) on supported bilayers to bind carbohydrate-binding proteins were tested. HPA and BPA were selected respectively for mucin mimetics Figure 1.11a and Figure 1.11b, and the specificities of the lectins were accurately recapitulated in this biomimetic system.

a
$$\begin{array}{c}
AcHNO
\\
R
\end{array}$$
b, c
$$\begin{array}{c}
OH \\
CN
\\
N
\end{array}$$

$$\begin{array}{c}
OH \\
AcHNO
\\
N
\end{array}$$

$$\begin{array}{c}
OH \\
AcHNO
\\
N
\end{array}$$

$$\begin{array}{c}
NH_2
\end{array}$$

$$\begin{array}{c}
SO_2NHNH_2
\end{array}$$

$$\begin{array}{c}
CN
\\
SO_2NHNH_2
\end{array}$$

$$\begin{array}{c}
CN
\\
SO_2NHNH_2
\end{array}$$

Figure 1.10: Structures of first generation glycopolymers with low lipophilicity of the end groups.

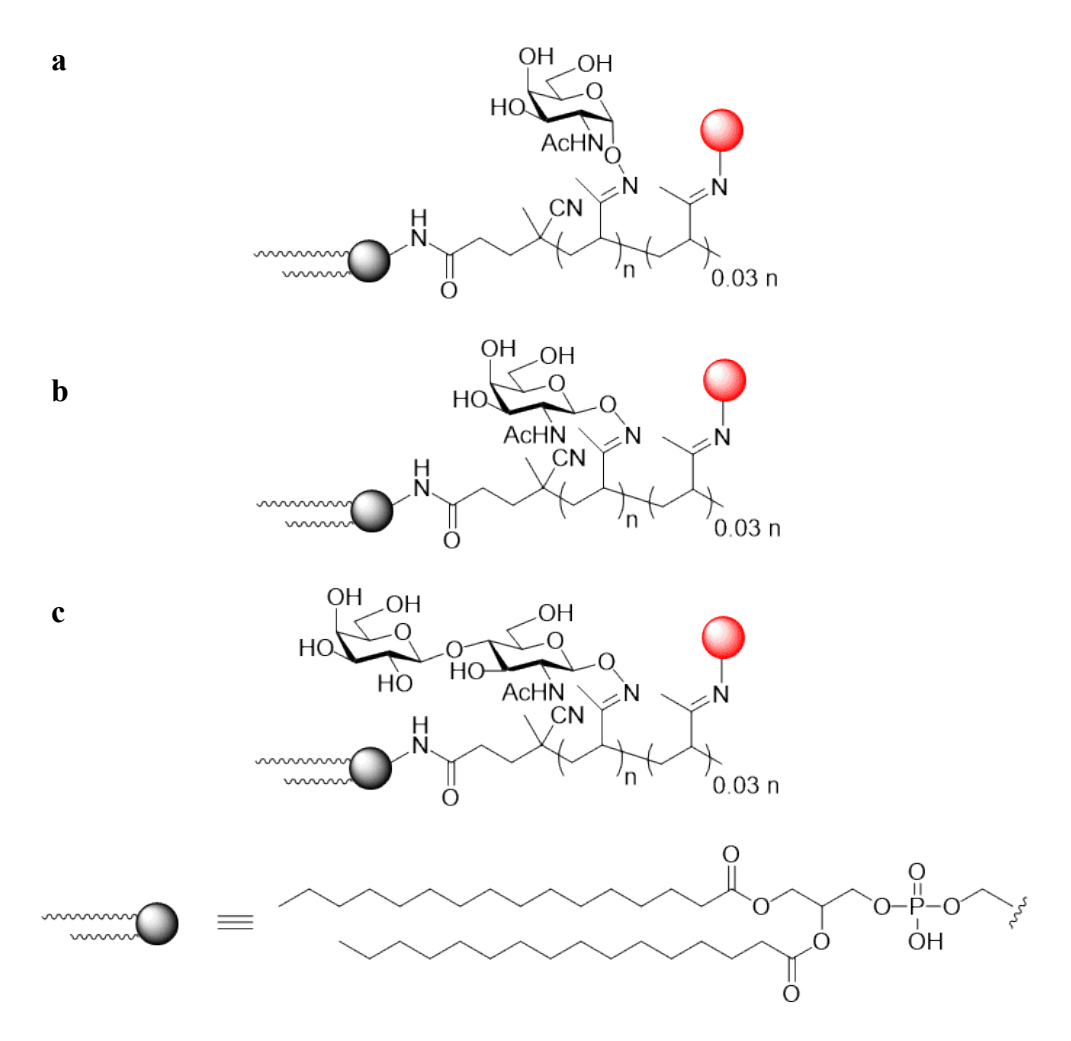


Figure 1.11: Structures of second generation glycopolymers.

The Bertozzi group further demonstrated that these glycopolymers can be inserted into the plasma membrane of *ldlD* CHO cells, which are devoid of endogenous mucins. Fluorescent correlation spectroscopy (FCS) was used to determine the density of cell surface mucin mimics. Membrane insertion efficiency and mobility of the mucin mimics were not affected by changes in the glycan structure. However, insertion efficiency was dependent on hydrophobic end-functionality. Among glycopolymers with a phospholipid tail similar to biological membrane lipids (**Figure 1.11a**), a straight alkyl tail (**Figure 1.10b**) and a pyrene group (**Figure 1.10c**), glyopolymer with a phospholipid

tail (Figure 1.11a) showed the highest insertion efficiency although their diffusion coefficients were similar. Thus this polymer (Figure 1.11a) was used for subsequent studies. Then they compared the mobility and cell surface density of the polymer with those of native proteins, and in this study glycosylphosphatidyl-inositol (GPI)-anchored proteins were used since they have similar lipid insertion behaviors as their synthetic polymers. The polymers had slightly slower mobilities and lower densities than the GPIanchored proteins, but their surface densities were much more consistent from cell to cell. They also assessed the ability of the mucin mimics (Figure 1.11a and Figure 1.11b) to bind lectin HPA while being presented on live cell surfaces. HPA only binds α-linked GalNAc residues instead of their β-linked isomers. Since both polymers (Figure 1.11a and Figure 1.11b) had similar densities on cell membrane as mentioned above, the result that HPA specifically bound to cells displaying α -linked GalNAc polymer (Figure 1.11a) on surface but not to cells displaying β-linked GalNAc polymer (Figure 1.11b) matched the intrinsic specificity of the lectin for the α -linked GalNAc polymer. Furthermore, they confirmed the mucin mimics were internalized through endocytic pathways, and the trafficking properties were similar to those of native mucins.

For this generation of the mucin mimics, the fluorescent dyes were randomly distributed along the body of the polymer ("body-labeled") (**Figure 1.12a**), and the polymers showed a supine orientation by interferometric measurements.⁷⁶ They synthesized the polymers by RAFT to get narrow chain-length distributions, and also modified the position and type of the polymer's fluorescent probe to create a new generation of mucin mimics. The "end-labeled" polymers have a single fluorescent probe at the opposite end of a lipid anchor (**Figure 1.12b**). With the precise end-localization of

the fluorophore, the height determined by fluorescence interference contrast microscopy (FLIC) is the height of the molecule rather than being the average signals from fluorophores distributed along the polymer backbone. Polymers with different fluorescent probes, Texas Red (TR) and Alexa Fluor 488 (AF488) were synthesized. P2-TR and P2-AF488 were incorporated into supported lipid bilayers. It was surprising to find that the orientation of the glycopolymers was dependent on the properties of the fluorophores. P2-AF488 projected out from the membrane surface while P2-TR lied flat. This study showed that macromolecular orientation at membranes can be controlled by small modifications of chemical structures.

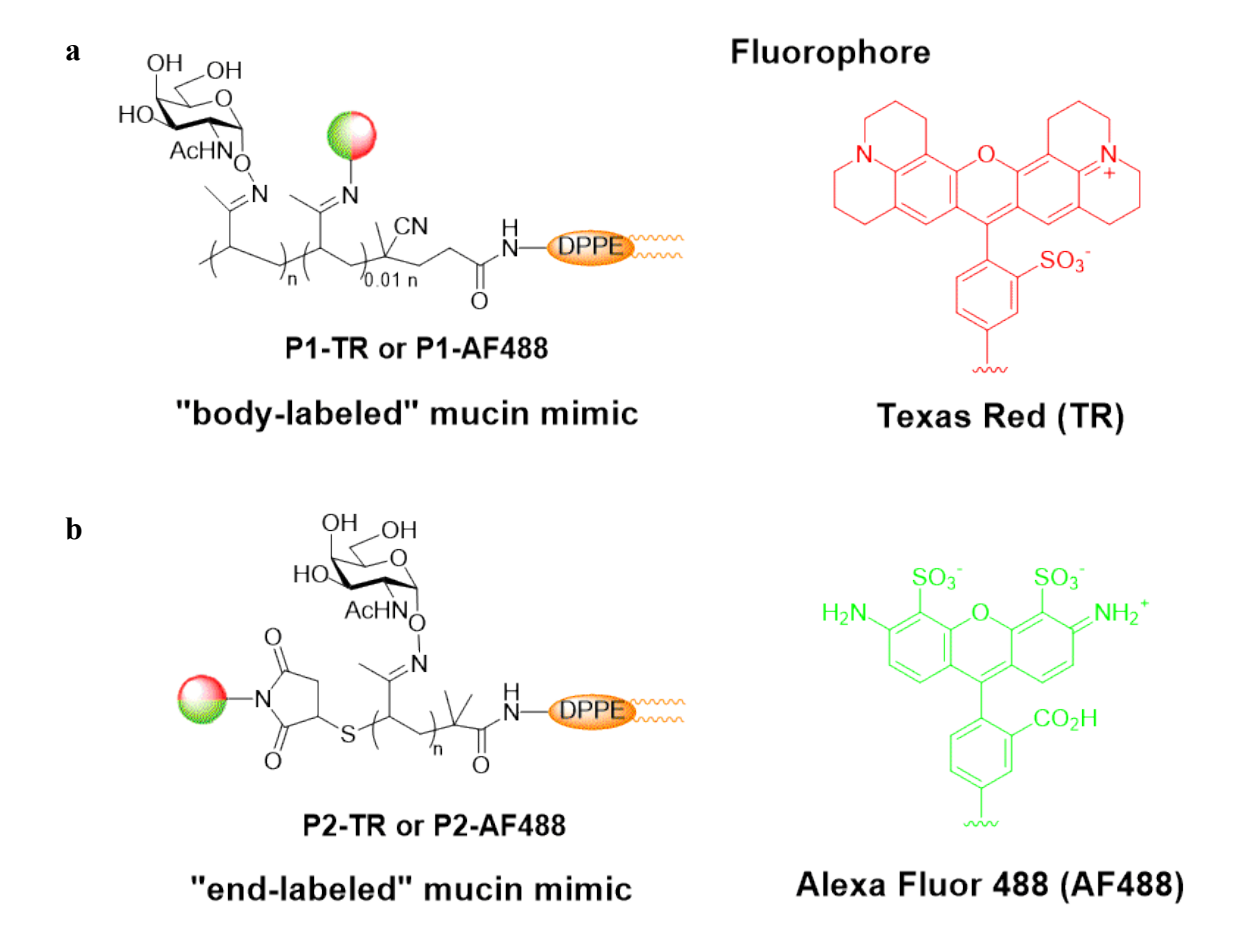


Figure 1.12: Structures of two types of phospholipid-terminated mucin mimetics: (a) "body-labeled" glycopolymers with a small number (2-3) of fluorophores distributed along the glycopolymer backbone (n \sim 240), and (b) "end-labeled" glycopolymers with only one terminal fluorescent dye per polymer chain (green = AF488, red = TR).

This new generation of glycopolymers can be utilized to study a variety of cell surface interactions. Galectins are a family of glycan-binding proteins, which can oligomerize cell surface glycoproteins and glycolipids into higher-order aggregates in order to mediate many cellular processes. However, due to the heterogeneous nature of galectin's endogenous ligands, the study of galectin ligand behaviors on live cell surfaces had been limited. The Bertozzi group prepared glycopolymers with galectin-binding glycans distributed along the polymer backbone, a lipid anchor at one end, and a FRET

donor or acceptor at the other end.⁷⁸ After insertion into the cell membrane, the glycopolymers' fluorescence lifetime (τ_{FL}) and diffusion time (τ_{D}) were measured with and without galectin-1 (**Figure 1.13**). They observed galectin-dependent decrease in τ_{FL} and increase in τ_{D} , which provided the first experimental evidence for galectin-1 mediated cross-linking on a cell surface.

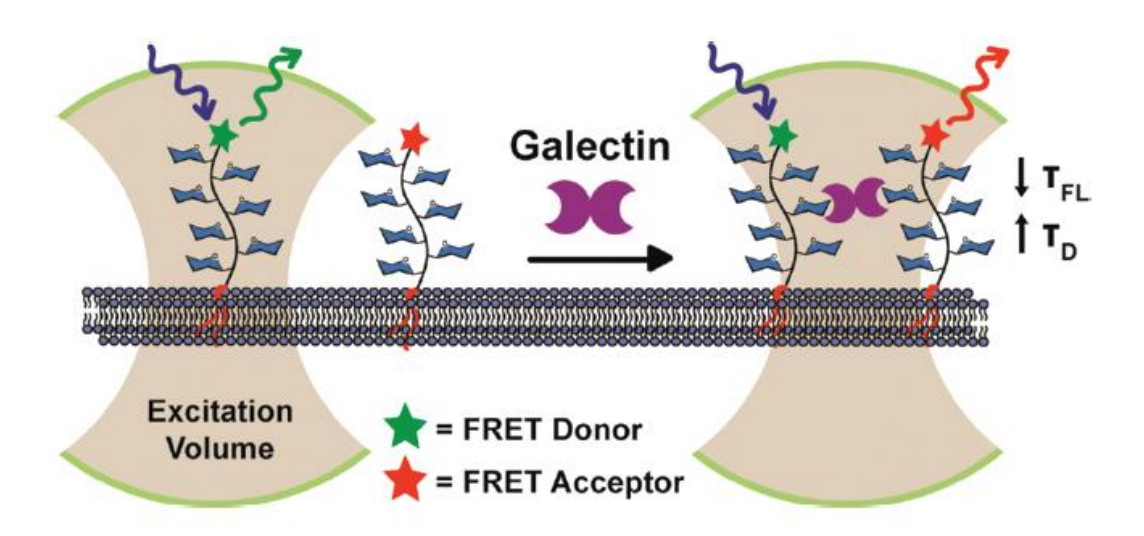


Figure 1.13: A schematic model for probing galectin-mediated ligand cross-linking on live cell surfaces. Synthetic glycopolymers bearing galectin-binding glycans (blue hexagons) with a lipid anchor on one end and either a FRET donor or acceptor dye on the other end were inserted into live cell membranes, and their τ_{FL}) and τ_{D} were monitored. Reproduced with permission from reference⁷⁸ Copyright 2012, American Chemical Society.

Later on, they looked into how glycopolymers affect galectin-3 binding.⁷⁹ The glycocalyx in the apical membrane of epithelial cells plays a critical role in maintaining barrier function on mucosal surfaces, but in the other way it also limits the bioavailability of drugs and vaccines targeting epithelial cells.⁸⁰ By interacting with galectin-3 on the apical surface of epithelial cells, mucin O-glycans contribute to maintaining barrier function in the cornea.⁸¹ In this study, cellobiose- and lactose-decorated polymers were

used to test the effect of glycopolymer insertion on barrier function of stratified human corneal epithelial cells. Results showed that surface insertion of cellobiose glycopolymers interfered with surface recognition of endogenous lactosyl residues, which resulted in disruption of the glycocalyx barrier. Unexpectedly lactose glycopolymers, which can bind galectin-3, did not enhance barrier function possibly as a result of failing to compete for galectin-3 binding in the presence of natural ligands or incorporation into undifferentiated apical cells with poorly glycosylated mucins but in insufficient quantities. This study indicated that galectin-3 multimerization and surface recognition of lactosyl residues were required to maintain glycocalyx barrier function at the ocular surface.

1.3.4: Interaction with the immune system

Many cell surface receptors and lectins in the immune system can recognize multivalent carbohydrate ligands, thus triggering either immune system activation or down-regulation including suppression and inhibition. Glycopolymers can be used as multivalent carbohydrate ligands to play a role in immune system function.

1.3.4.1: Glycopolymers for immune activation

Carbohydrate antigens can bind to B cell receptors (BCRs) and activate B cells. Glycopolymers bearing desired carbohydrate antigens can interact with BCRs and elicit immune responses against the carbohydrate antigens. In this way, the glycopolymers act as vaccines to target specific carbohydrate antigens.

Bundle and co-workers synthesized polyacrylamide with β -mannan trisaccharide hapten, and conjugated the glycopolymer to carrier protein chicken serum albumin

(Scheme 1.14).⁸² The conjugate vaccine was able to induce a robust T cell dependent immune responses with high titers of antibodies capable of recognizing native cell wall antigen β -mannan. This is the first report of fully functional glycopolymer conjugate vaccine with B-cell epitopes from the glycopolymer and T-cell epitopes from the carrier protein.

Scheme 1.14: Synthesis of glycopolymer and its conjugation to chicken serum albumin.

Cameron and co-workers synthesized well-defined glycopolymers bearing Thomsen-nouveau (Tn) antigens by RAFT, and then conjugated the polymers to gold nanoparticles to afford "multicopy-multivalent' nanoscale glycoconjugates (**Figure 1.14**). These glycoconjugates were able to generate significant and long-lasting antibodies, which can recognize natural Tn-antigens and mammalian-mucin glycoproteins. This is the first report of fully synthetic protein- and peptide-free glycoconjugate vaccines through layered multivalent polymer display.⁸³

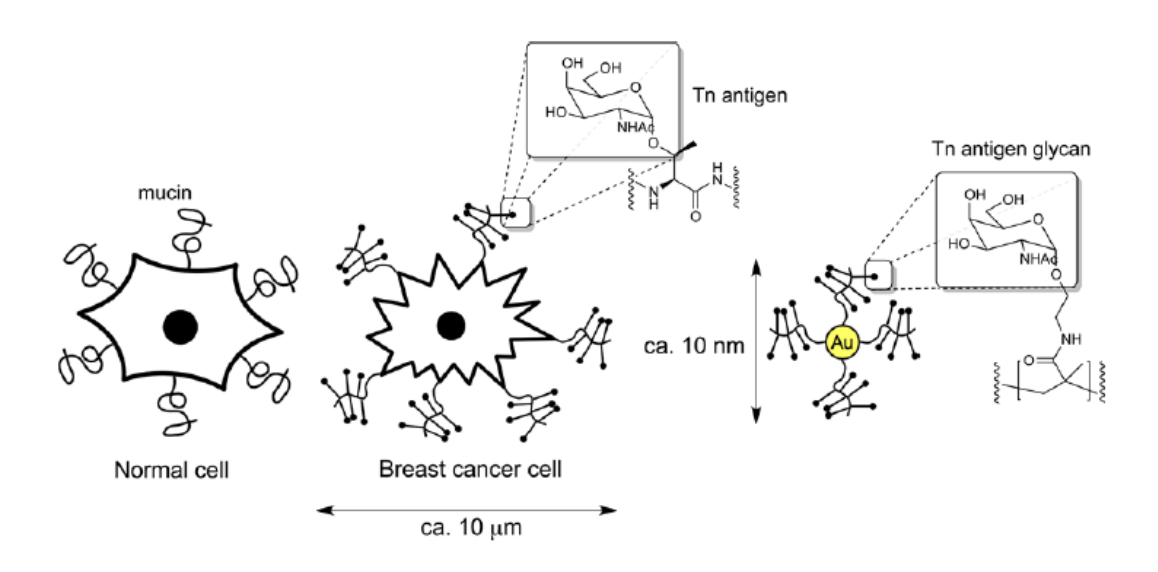


Figure 1.14: Overview of approach to develop gold nanoparticle-based synthetic glycopolymer anticancer vaccines. Breast cancer cells express aberrant mucins displaying Core 1 glycans such as Tn-antigen. The glycopolymers bearing Tn-antigens conjugated to gold nanoparticles can mimic the 'multicopy-multivalent' presentation. Reproduced with permission from reference⁸³ Copyright 2013, American Chemical Society.

Kunz et al. reported water soluble poly (N-(2-hydroxypropyl)methacrylamide) (P-(HPMA)) polymers prepared via RAFT bearing a tumor-associated MUC1 tandem-repeat glycopeptide as the B-cell epitope and a helper T cell peptide epitope (P2 peptide) as

potential antitumor vaccines (**Figure 1.15**).⁸⁴ The attachment of the P2 peptide onto the polymer induced self-assembly to micelle-like nanoobjects. The vaccines were able to elicit significant T cell dependent immune responses and IgG antibodies generated could recognize MCF-7 breast tumor cells. It is worth to mention that polymer with additional nanostructure-promoting domains (**Figure 1.15b**) induced antibodies that had even higher affinity to MUC1 bearing tumor cells.

Figure 1.15: Structures of polymer glycopeptide conjugate vaccines bearing tumor-associated MUC1 glycopeptide and the T-helpercell epitope P2 peptide.

1.3.4.2: Glycopolymers for immune down-regulation

Glycopolymers can bind to immune cell surface lectins, which can either inhibit lectin binding to other ligands or suppress the immune cell activation processes.

Dendritic cell specific intracellular adhesion molecule-3 grabbing nonintegrin (DC-SIGN) is a C-type lectin abundantly expressed on dendritic cells (DCs), which can bind to human immunodeficiency virus (HIV)-1 envelope glycoprotein gp120 enhancing their infection of target cells. 85,86 Haddleton and co-workers created a library of glycopolymers with identical chain length and chain length distribution but different percentages of mannose and galactose by post-polymerization modifications. 87,88,89,90,91,92 They used multichannel SPR (MC-SPR) to study the binding affinity of the glycopolymers with human DC-SIGN tetramers, and found that glycopolymers could inhibit DC-SIGN binding to gp120. This approach may provide new therapeutics against HIV infection. 93

To gain a better control over the relative position of the sugars on the polymer, they used a controlled polymerization technique called single-electron transfer living radical polymerization (SET-LRP) as shown in **Figure 1.16**. 94 Furthermore, they introduced a third glycomonomer fucose acrylate (FucA) to make a hexablock copolymer of mannose acrylate (ManA), glucose acrylate (GluA) and FucA. SPR was used to measure the interactions between the glycopolymers and DC-SIGN. Polymers with higher mannose content had higher binding affinity, and with nanomolar concentrations the glycopolymers could inhibit DC-SIGN binding to HIV gp120.

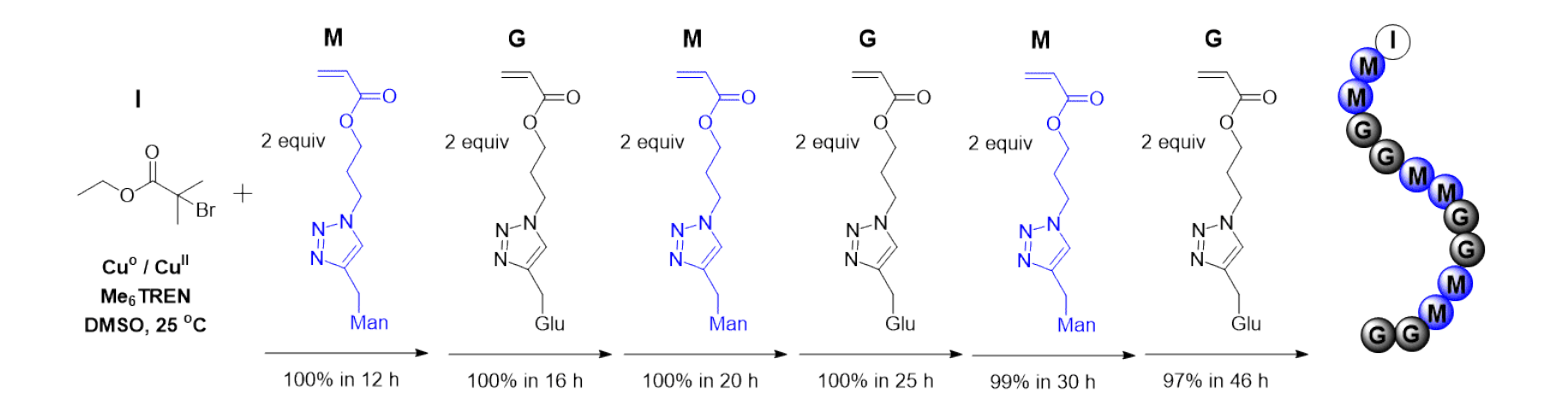


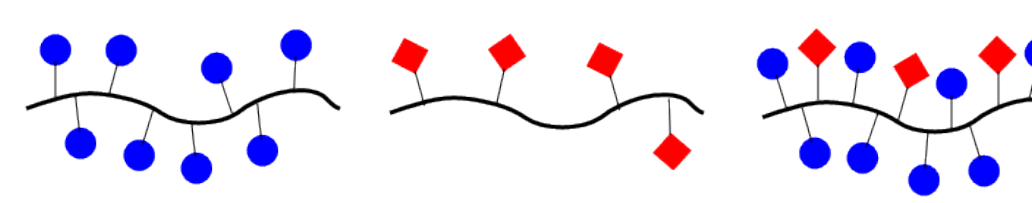
Figure 1.16: Schematic representation of the sequence-controlled multi-block copolymerization of ManA (M) and GluA (G).

CD22 (Siglec-2) is a B-cell inhibitory receptor that attenuates B cell activation, ⁹⁵ and it binds to cell surface sialylated glycoproteins with preference for α2,6-linked sialylated glycans. ⁹⁶ Kiessling and co-workers prepared glycopolymers (**Figure 1.17**) that can bind to cells through the BCR alone, CD22 alone, or both to study the roles of cell-surface (*cis*) and antigen-presented (*trans*) CD22 ligands on B cell activation (**Figure 1.18**). ⁹⁷ Their results showed that dinitrophenyl (DNP)/CD22L copolymer **3** suppressed B cell activation through *trans* interaction with CD22 as monitored by intracellular calcium ion concentration and phosphor-tyrosine level changes, which are two critical indicators of B cell activation (**Figure 1.19**). Later, they used the glycopolymers as probes of BCR endocytosis during inhibitory signaling. ⁹⁸

DNP homopolymer 1

CD22L homopolymer 2

DNP/CD22L copolymer 3



 $R_1 \chi = 0.33$; $R_2 \chi = 0$; $R_3 \chi = 0.67$

 $R_1 \chi = 0$; $R_2 \chi = 0.23$; $R_3 \chi = 0.77$

 $R_1 \chi = 0.36$; $R_2 \chi = 0.24$; $R_3 \chi = 0.40$

Figure 1.17: Structures of polymers used to investigate CD22 recognition. Polymers with a DP of 250 (n \approx 250) were used. The substituents include the DNP group (R₁, blue), the CD22 ligand Neu5Ac α 2,6Gal β 1,4Glc (CD22L, R₂, red), or the spacer unit derived from ethanolamine coupling. The level of substitution of each group (mole fraction χ) is labeled for each polymer.

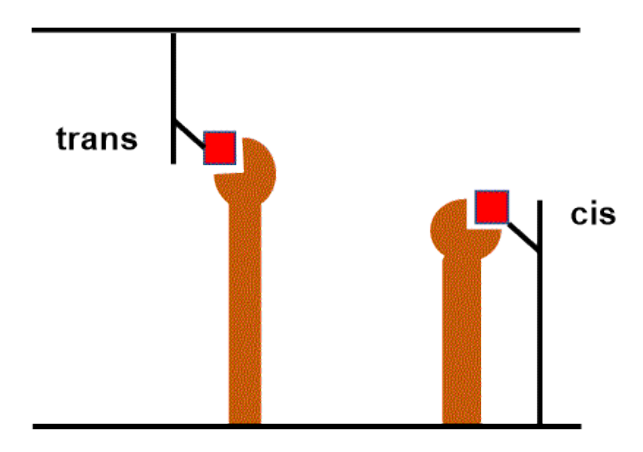


Figure 1.18: CD22 can interact with B cell surface glycoproteins that have terminal α 2,6-linked sialic acid residues (*cis* interactions), which can mask CD22's interactions with exogenous ligands (*trans* interactions).

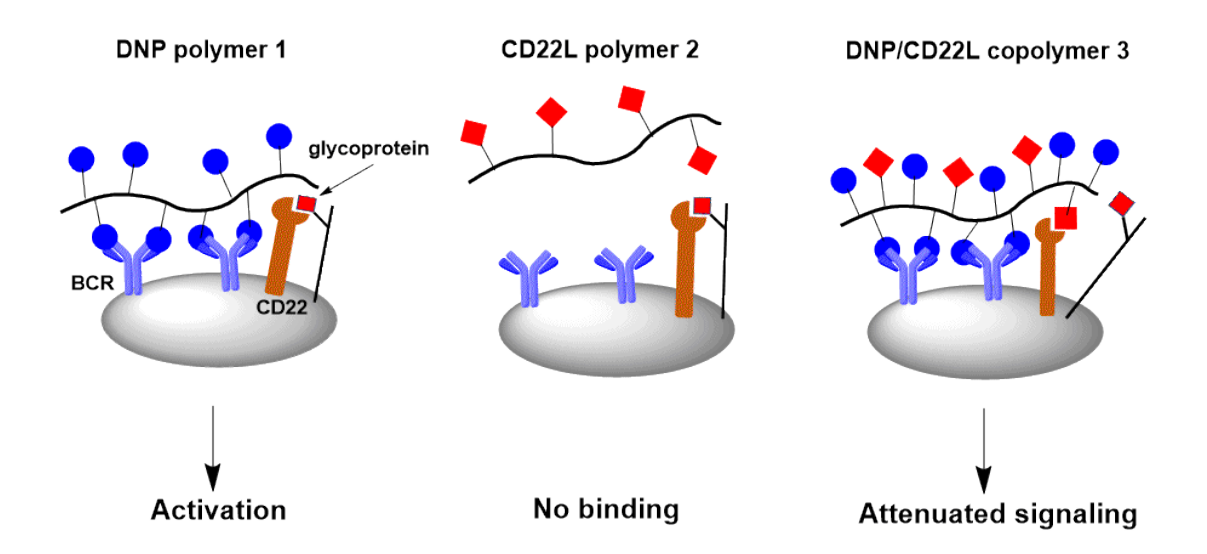


Figure 1.19: DNP polymer can initiate activation of early B cell signaling events. Copolymers bearing DNP and a ligand for CD22 result in the attenuation of B cell activation.

Bertozzi group applied glycocalyx engineering approach to study how specific sialosides mediate Siglec-based immunoevasion from natural killer (NK) cells. 99 Cancer cells engineered to display sialylated glycopolymers were able to evade NK cell killing

among which the polymer containing the monosaccharide sialic acid alone (Sia polymer, Figure 1.20b) offered the strongest protection against killing. It was found that NK cell activation was suppressed by inhibiting both degranulation and interferon (IFN)- γ production by NK cells. During the process, Siglec-7 was recruited to the NK-target immune synapse to promote a strong inhibitory signal (Figure 1.20a). Their results showed that cell surface Siglec-7 ligands can protect cancer cells from not only innate responses but also therapeutically relevant antibody-dependent cell cytotoxicity (ADCC). The sialic acid polymers were also able to protect allogeneic and xenogeneic primary cells from NK-mediated killing suggesting that Siglec-7 engagement may also inhibit NK recognition in the context of xenogeneic transplants.

a

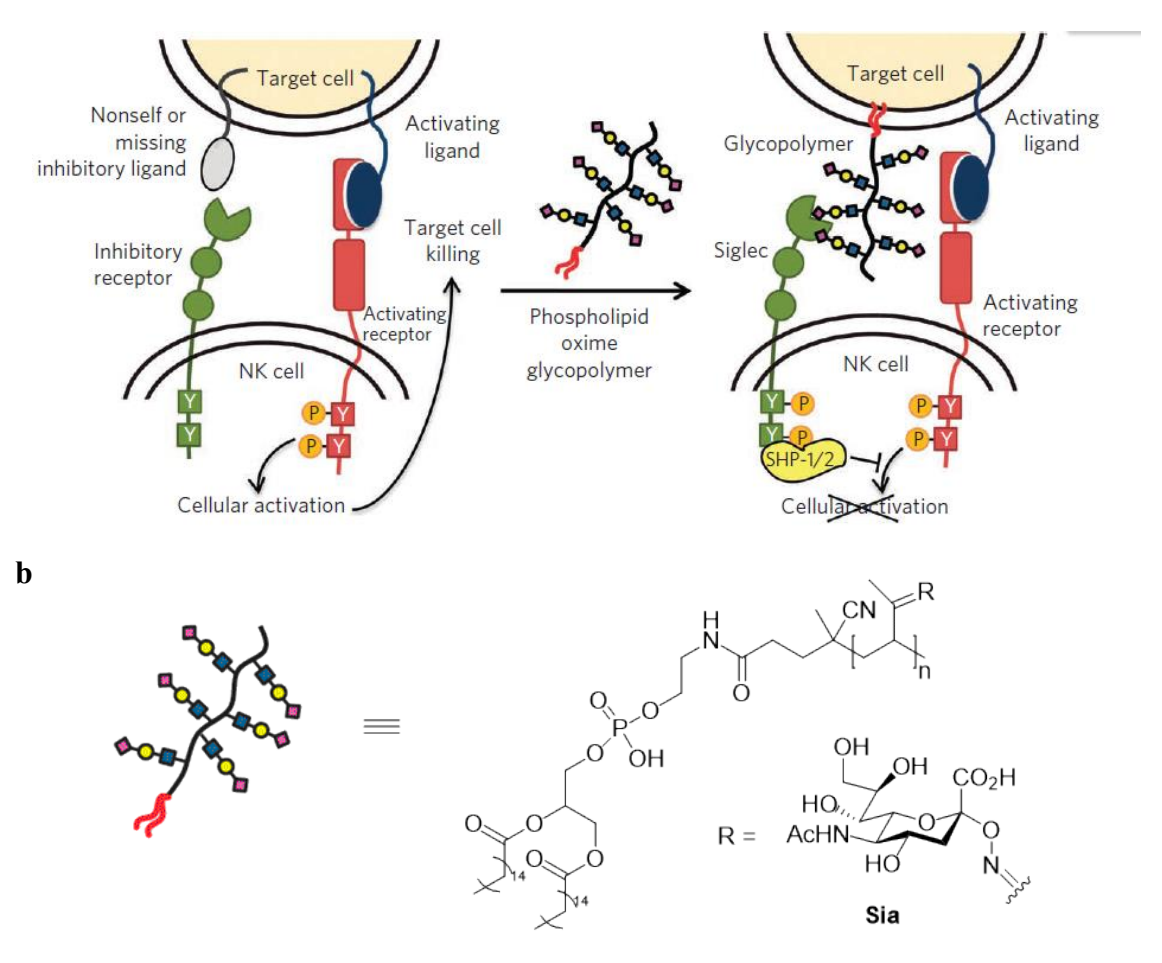


Figure 1.20: A glycocalyx engineering approach to study sialoside-mediated immunoevasion from NK cells. (a) NK cells can be activated after binding to activating ligands when there are no inhibitory ligands on the target cell. When sialylated glycopolymers are inserted onto cancer cell membrane, they can bind to the Siglec family of inhibitory receptors and localize Siglecs to the site of activation, which results in Src homology region 2 domain-containing phosphatase (SHP)-1 and SHP-2 recruitment to prevent cellular activation. (b) Structure of phospholipid oxime glycopolymer. Reproduced with permission from reference ⁹⁹ Copyright 2013, Springer Nature.

The selectins are a family of cell-cell adhesion proteins that mediate leukocyte attachment to endothelial cells and to platelets. ¹⁰⁰ P-selectin is one member of the selectin family, which recognizes sulfated saccharide residues. ¹⁰¹ In order to investigate P-selectin carbohydrate interactions, Kiessling group developed a protocol to generate glycopolymers with sulfated saccharide residues via ROMP. ¹⁰² The sulfated

neoglycopolymers could potently and specifically block P-selectin binding with cells.

1.3.5: Interaction with viral and bacterial proteins

Whitesides et al. reported a microscale strategy that allows for rapid generation and convenient screening of libraries of poly(acrylic acid) (PAA) presenting multiple copies of *N*-acetylneuraminic acid (NeuAc or sialic acid) as polyvalent inhibitors of influenza-mediated hemagglutination in microtiter plates. They also applied this method to generate libraries of ter-polymers, pAA-(NeuAc-L; R). The R groups were non-sialoside groups, which had no hemagglutination inhibition (HAI) activities by themselves. However, the ter-polymers showed enhanced potency compared to pAA(NeuAc), which are partly due to increased affinity of polymer for the viral surface as a result of binding of non-sialoside groups to non-HA sites.

Many bacteria, in particular those of the Enterobacteriaceae family, have multiple filamentous protein appendages called fimbriae or pili, which have lectins with different sugar specificity. 104 Seeberger et al. reported using fluorescent glycopolymers for detection of *E. coli* by multivalent interactions. 105 The glycopolymers were obtained by coupling of the 2'-aminoethyl mannoside and galactoside to poly(*p*-phenylene ethynylene) (PPE). The mannose specific lectin interacts with the glycopolymers resulting in brightly fluorescent cell clusters. This method can detect the presence of a pathogen in as little as 10 to 15 minutes, and many different carbohydrates can be coupled to polymers for detection of multiple pathogens.

Kiessling and coworkers generated multivalent galactose-bearing polymers with

different valencies, and examined their abilities to cluster chemoreceptors on the plasma membranes of both *E. Coli* and *Bacillus subtilis*, and to elicit a chemotactic response. ¹⁰⁶ They proposed a mechanism in which ligand valency increases lead to changes in chemotactic responses by the incorporation of more receptors into clusters (**Figure 1.21**).

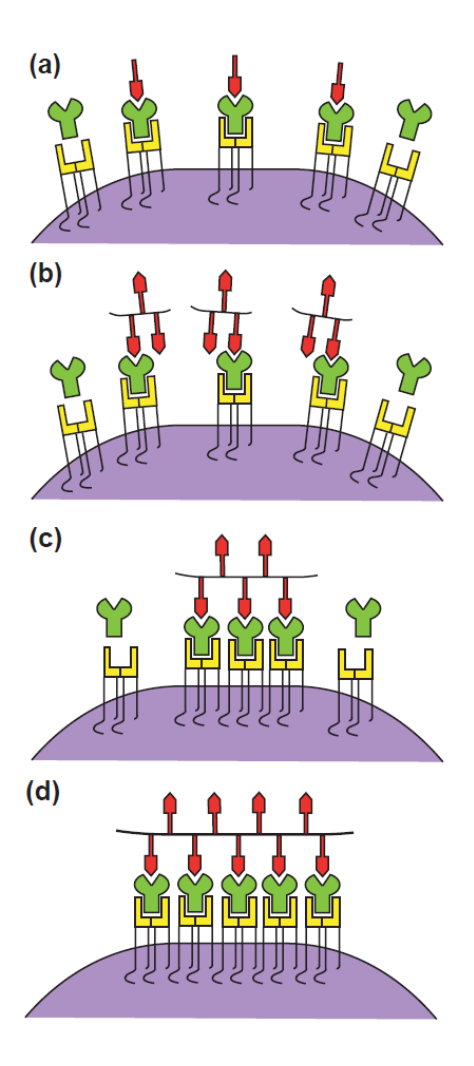


Figure 1.21: Model of receptor clustering by synthetic ligands. (a) Chemoreceptors form dimers in the plasma membrane of E. coli and each dimer appears to interact with a single ligand. (b) Multivalent ligands that cannot span the distance needed to cluster the receptors can only bind to individual dimers, as in (a). (c) Multivalent ligands of sufficient lengths are able to cluster the chemoreceptors. (d) Increasing the valency of a multivalent ligand can engage more receptor clustering, thus enhancing the bacterial response. Reproduced with permission from reference 106 Copyright 2000, Elsevier.

In addition, Kiessling group reported the design, synthesis and use of

glycopolymers bearing galactose, glucose or mannose as chemoattractants to study the mechanism of chemotactic response amplification in different bacteria including *E. coli*, *S. aurantia*, *V. furnissii*, and *B. subtilis*. ¹⁰⁷

1.4: Other biological applications of glycopolymers

Besides interactions with different proteins, glycopolymers have other biological applications as well. In this section, we will review a few other bio-applications of glycopolymers.

Previous glycopolymers were prone to be internalized by cells within hours, which limited their application in probing biological processes spanning longer time scales. In order to improve the plasma membrane residence time, Bertozzi group tested a number of glycopolymers bearing different lipid anchors that varied in length, regiochemistry, unsaturation, or the linkage type to glycerol. The polymers were biotin-capped that could be detected with a membrane-impermeant AF488-labeled anti-biotin antibody for the purpose of quantitating the cell surface residence time. Unlike other lipids, the surface population of cholesterylamine (CholA)-anchored glycopolymers stabilized and remained at much higher levels up to ten days after labeling despite an initial drop. They built a model for the mechanism by which CholA-anchored glycopolymers were recycled and delivered back to cell surface (Figure 1.22). Their experiments also revealed that similar to native mucins, the long CholA-anchored glycopolymers were excluded from the sites of adhesion formation, and were able to drive integrin clustering by a kinetic funnel effect (Figure 1.23). It has been postulated

that mucin overexpression would promote tumor metastasis by this mechanism, and their experiments showed that the long CholA-anchored glycopolymers could similarly enhance the cell survival in a zebrafish model of metastasis.

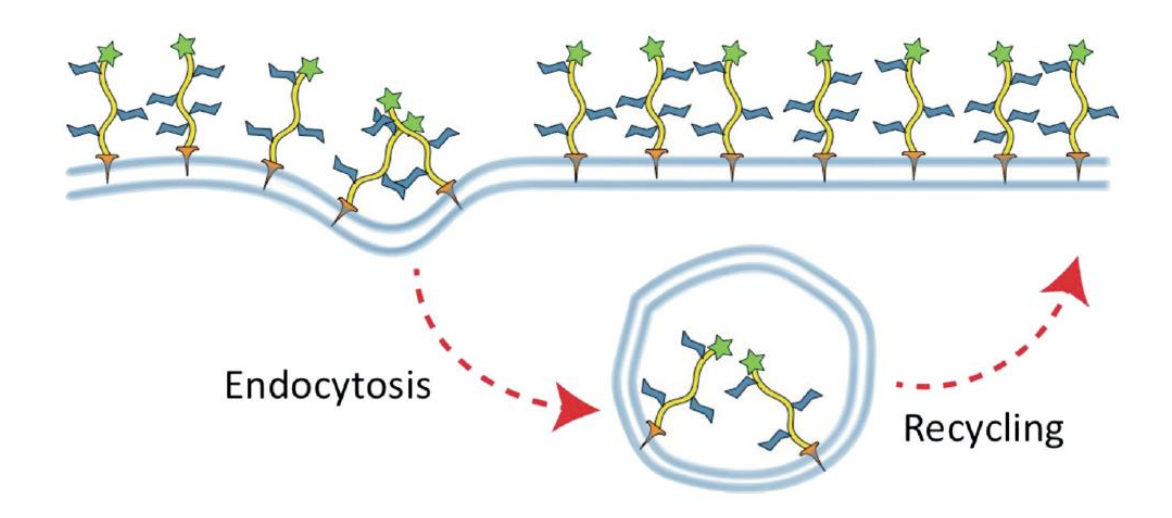


Figure 1.22: CholA-anchored glycopolymers are recycled and return back to the cell surface. Reproduced with permission from reference¹⁰⁸ Copyright 2015, John Wiley and Sons.

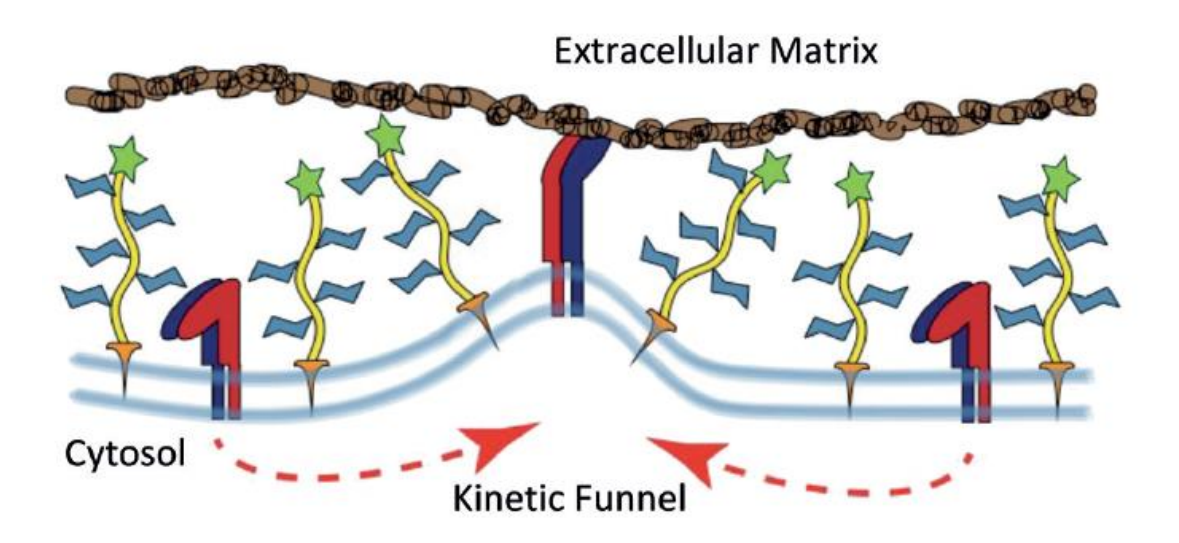


Figure 1.23: CholA-anchored glycopolymers are excluded from sites of adhesion formation and drive integrin clustering by a kinetic funnel effect. Reproduced with permission from reference ¹⁰⁸ Copyright 2015, John Wiley and Sons.

Maynard group reported the first well-defined trehalose glycopolymer synthesized via RAFT (Figure 1.24).¹⁰⁹ The glycopolymers of different molecular weights (Figure 1.25 P1) were conjugated to hen egg white lysozyme and the stabilities of the conjugates were tested. Their results showed that the trehalose polymers were more effective than PEG for stabilization of protein to lyophilization and heat. They also investigated three additional trehalose glycopolymers (Figure 1.25) with different attachment sites, linkage chemistry and polymer backbones, and their application as excipients to stabilize proteins to heat and during lyophilization. They found out that all glycopolymers were able to stabilize the proteins better than no additive or trehalose, and they had no cytotoxicity to four different cell lines. All the polymers performed similarly at high concentrations. While at lower concentrations, differences in performance were observed due to the polymer backbone rather than the site of attachment or chemistry of the linkages. The polymethacrylate backbone polymers P2 and P4 were able to better stabilize HRP under heat treatment, while the styrenyl polymers P1 and P3 performed better for lyophilization of β -Gal. These trehalose glycopolymers have great potential to be used as excipients for protein stabilization. 110

Figure 1.24: Schematic presentation of trehalose glycopolymers synthesized by RAFT.

Figure 1.25: Structure of the trehalose polymers.

Besides applications in protein stabilization, by applying the polystyrene backbone trehalose glycopolymer to protect proteins during electron-beam lithography (EBL), surfaces with complex patterns of multiple proteins at the micrometer and nanometer scales were generated without requiring cleanroom conditions (**Figure 1.26**). This glycopolymer has also been used as a resist for direct writing of interleukin-6 (IL-6) or tumor necrosis factor alpha (TNF α) antibodies for detection of these cytokines secreted from macrophages. The protein patterning technique will have important

applications in various areas including bioanalytical assays, biosensors, microreactors, and bioactive interfaces for cell culture.

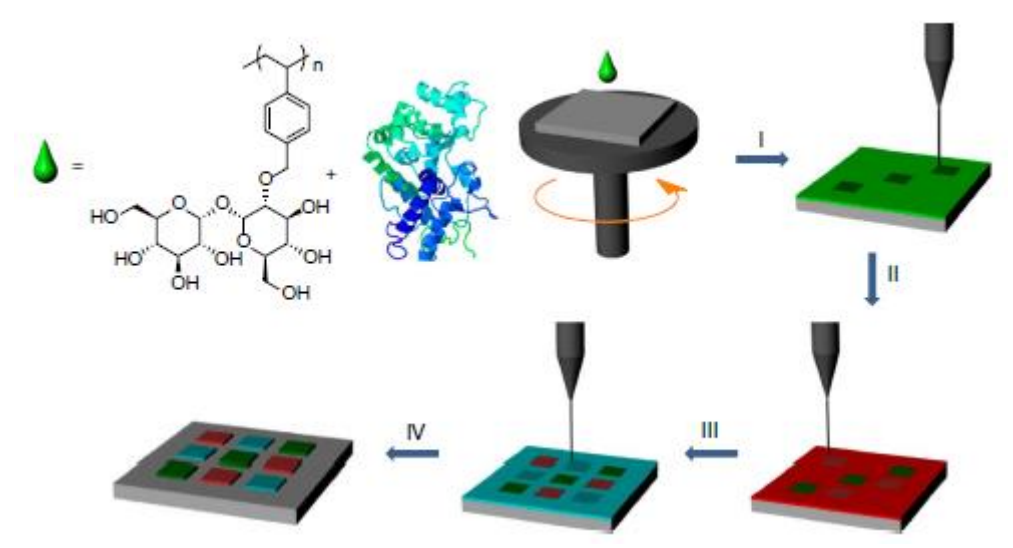


Figure 1.26: Steps for generating multiple protein patterns. (I), spin coating with polystyrenyl ether trehalose (poly(SET))-protein-1 solution and writing of the first layer. (II), rinsing of the unexposed poly(SET)-protein-1 followed by spin coating poly(SET)-protein-2, alignment to the first layer and writing of the second layer. (III-IV), multiple protein patterns can be obtained by repeated spin coating, alignment, writing and rinsing steps. All of the above steps including EBL do not require cleanroom conditions. Reproduced with permission from reference¹¹¹ Copyright 2015, Springer Nature.

1.5: Summary

Glycopolymers overcome the disadvantage of the weak interactions of monomeric glycans with their multivalent effects. By controlled polymerization methods, glycopolymers with well controlled chain length, monomer density and low PDI could be prepared. They have been widely used as tools to study carbohydrate protein interactions including binding with lectins, viral proteins and transmembrane receptors. In addition, their applications in other biological areas such as immune modulation and protein stabilization have also been explored.

REFRENCES

REFERENCES

- 1. Dwek, R. A., Glycobiology: Toward understanding the function of sugars. *Chem. Rev.* **1996,** *96*, 683–720.
- 2. Sharon, N.; Lis, H., Carbohydrates in cell recognition. Sci. Am. 1993, 268, 82-89.
- 3. Ladmiral, V.; Melia, E.; Haddleton, D. M., Synthetic glycopolymers: an overview. *Eur. Polym. J.* **2004**, *40*, 431-449.
- 4. Pearson, S.; Chen, G.; Stenzel, M. H., Synthesis of Glycopolymers. In *Engineered Carbohydrate-Based Materials for Biomedical Applications*, John Wiley & Sons, Inc.: Hoboken, NJ, USA, 2011; pp 1–118.
- 5. Davis, B. G.; Robinson, M. A., Drug delivery systems based on sugar-macromolecule conjugates. *Curr. Opin. Drug. Discov. Devel.* **2002**, *5*, 279-288.
- 6. Suriano, F.; Pratt, R.; Tan, J. P.; Wiradharma, N.; Nelson, A.; Yang, Y.; Dubois, P.; Hedrick, J. L., Synthesis of a family of amphiphilic glycopolymers *via* controlled ring-opening polymerization of functionalized cyclic carbonates and their application in drug delivery. *Biomaterials* **2010**, *31*, 2637-2645.
- 7. Zheng, C.; Guo, Q.; Wu, Z.; Sun, L.; Zhang, Z.; Li, C.; Zhang, X., Amphiphilic glycopolymer nanoparticles as vehicles for nasal delivery of peptides and proteins. *Eur. J. Pharm. Sci.* **2013**, *49*, 474-482.
- 8. Ahmed, M.; Jawanda, M.; Ishihara, K.; Narain, R., Impact of the nature, size and chain topologies of carbohydrate-phosphorylcholine polymeric gene delivery systems. *Biomaterials* **2012**, *33*, 7858-7870.
- 9. Thapa, B.; Kumar, P.; Zeng, H.; Narain, R., Asialoglycoprotein receptor-mediated gene delivery to hepatocytes using galactosylated polymers. *Biomacromolecules* **2015**, *16*, 3008-3020.
- 10. Kiessling, L. L.; Young, T.; Gruber, T. D.; Mortell, K. H., Multivalency in Protein-Carbohydrate Recognition. In *Glycoscience*, Fraser-Reid, B.; Tatsuta, K.; Thiem, J., Eds. Springer-Verlag Berlin Heidelberg: 2008; pp 2484-2523.
- 11. Krishnamurthy, V. M.; Estroff, L. A.; Whitesides, G. M., Multivalency in Ligand Design. In *Fragment-based Approaches in Drug Discovery*, Jahnke, W.; Erlanson, D. A., Eds. Wiley-VCH Verlag GmbH & Co. KGaA, Weinheim, FRG. : 2006.
- 12. Shan, M. Design, synthesis, and evaluation of bivalent estrogen ligands. Doctoral disssertation, Freie Universität Berlin, 2011.
- 13. Mammen, M.; Choi, S.; Whitesides, G. M., Polyvalent interactions in biological

- systems: implications for design and use of multivalent lignads and inhibitors. *Angew. Chem. Int. Ed.* **1998,** *37*, 2754-2794.
- 14. Jencks, W. P., On the attribution and additivity of binding energies. *Proc. Natl. Acad. Sci.* **1981,** 78, 4046-4050.
- 15. Spain, S. G.; Gibson, M. I.; Cameron, N. R., Recent advances in the synthesis of well-defined glycopolymers. *J. Polym. Sci. Part A: Polym. Chem.* **2007**, *45*, 2059-2072.
- 16. Aoi, K.; Tsutsumiuchi, K.; Aoki, E.; Okada, M., First synthesis of glycopeptide macromonomers and graft-type sugar-containing polymers with glycopeptide side chains. *Macromolecules* **1996**, *29*, 4456-4458.
- 17. Taguchi, T.; Kishida, A.; Sakamoto, N.; Akashi, M., Preparation of a novel functional hydrogel consisting of sulfated glucoside-bearing polymer: Activation of basic fibroblast growth factor. *J. Biomed. mater. Res.* **1998**, *41*, 386-391.
- 18. Labeau, M.; Cramail, H.; Deffieux, A., Amphiphilic block copolymers of controlled dimensions with hydrophilic glycosidic vinyl ether moieties. *Macromol. Chem. Phys.* **1998**, *199*, 335–342.
- 19. Yamada, K.; Minoda, M.; Miyamoto, T., Controlled synthesis of amphiphilic block copolymers with pendant N-Acetyl-d-glucosamine residues by living cationic polymerization and their interaction with WGA lectin. *Macromolecules* **1999**, *32*, 3553–3558.
- 20. Ye, W.; Wells, S.; Desimone, J. M., Well-defined glycopolymer amphiphiles for liquid and supercritical carbon dioxide applications. *J. Polym. Sci. Polym. Chem.* **2001**, *39*, 3841-3849.
- 21. D'Agosto, F.; Charreyre, M.; Pichot, C.; Mandrand, B., Polymer of controlled chain length carrying hydrophilic galactose moieties for immobilization of DNA probes. *Macromol. Chem. Phys.* **2002**, *203*, 146-154.
- 22. D'Agosto, F.; Charreyre, M.; Delolme, F.; Dessalces, G.; Cramail, H.; Deffieux, A.; Pichot, C., Kinetic study of the "living" cationic polymerization of a galactose carrying vinyl ether. MALDI-TOF MS analysis of the resulting glycopolymers. *Macromolecules* **2002**, *35*, 7911–7918.
- 23. Wang, J.; Tomita, I.; Endo, T., Synthesis of well-defined glycopolymers by π -allylnickel-catalyzed living coordination polymerization. *Macromolecules* **2001**, *34*, 4294-4295.
- 24. Ohno, K.; Tsujii, Y.; Miyamoto, T.; Fukuda, T.; Goto, M.; Kobayashi, K.; Akaike, T., Synthesis of a well-defined glycopolymer by nitroxide-controlled free radical polymerization. *Macromolecules* **1998**, *31*, 1064-1069.
- 25. Ohno, K.; Tsujii, Y.; Fukuda, T., Synthesis of a well-defined glycopolymer by atom

- transfer radical polymerization. J. Polym. Sci., Part A: Polym. Chem. 1998, 36, 2473-2481.
- 26. Ejaz, M.; Ohno, K.; Tsujii, Y.; Fukuda, T., Controlled grafting of a well-defined glycopolymer on a solid surface by surface-initiated atom transfer radical polymerization. *Macromolecules* **2000**, *33*, 2870–2874.
- 27. Chen, Y.; Wulff, G., Amphiphilic block copolymers with pendent sugar as hydrophilic segments and their surface properties. *Macromol. Chem. Phys.* **2001**, *202*, 3273-3278.
- 28. Chen, Y.; Wulff, G., Synthesis of poly(styryl sugar)s by TEMPO mediated free radical polymerization. *Macromol. Chem. Phys.* **2001**, *202*, 3426–3431.
- 29. GÖtz, H.; Harth, E.; Schiller, S. M.; Frank, C. W.; Knoll, W.; Hawker, C. J., Synthesis of lipo-glycopolymer amphiphiles by nitroxide-mediated living free-radical polymerization. *J. Polym. Sci., Part A: Polym. Chem.* **2002,** *40*, 3379-3391.
- 30. Chen, Y.; Wulff, G., ABA and star amphiphilic block copolymers composed of polymethacrylate bearing a galactose fragment and poly(ε-caprolactone). *Macromol. Rapid Commun.* **2002**, *23*, 59-63.
- 31. Mortell, K. H.; Gingras, M.; Kiessling, L. L., Synthesis of cell agglutination inhibitors by aqueous ring-opening metathesis polymerization. *J. Am. Chem. Soc.* **1994**, *116*, 12053-12054.
- 32. Grande, D.; Baskaran, S.; Chaikof, E. L., Glycosaminoglycan mimetic biomaterials. 2. alkene- and acrylate-derivatized glycopolymers via cyanoxyl-mediated free-radical polymerization. *Macromolecules* **2001**, *34*, 1640-1646.
- 33. Narain, R.; Armes, S. P., Synthesis of low polydispersity, controlled-structure sugar methacrylate polymers under mild conditions without protecting group chemistry. *Chem. Commun.* **2002**, *23*, 2776-2777.
- 34. Vázquez-Dorbatt, V.; Maynard, H. D., Biotinylated glycopolymers synthesized by atom transfer radical polymerization. *Biomacromolecules* **2006**, *7*, 2297-2302.
- 35. Lowe, A. B.; Sumerlin, B. S.; McCormick, C. L., The direct polymerization of 2-methacryloxyethyl glucoside via aqueous reversible addition-fragmentation chain transfer (RAFT) polymerization. *Polymer* **2003**, *44*, 6761-6765.
- 36. Ladmiral, V.; Mantovani, G.; Clarkson, G. J.; Cauet, S.; Irwin, J. L.; Haddleton, D. M., Synthesis of neoglycopolymers by a combination of "click chemistry" and living radical polymerization. *J. Am. Chem. Soc.* **2006**, *128*, 4823-4830.
- 37. Geng, J.; Lindqvist, J.; Mantovani, G.; Haddleton, D. M., Simultaneous copper (I)-catalyzed azide-alkyne cycloaddition (CuAAC) and living radical polymerization. *Angew. Chem. Int. Ed.* **2008**, *47*, 4180-4183.

- 38. Sharon, N.; Lis, H., History of lectins: from hemagglutinins to biological recognition molecules. *Glycobiology* **2004**, *14*, 53R-62R.
- 39. Sharon, N.; Lis, H., Lectins as cell recognition molecules. *Science* **1989**, *246*, 227-234.
- 40. Ashwell, G.; Harford, J., Carbohydrate-specific receptors of the liver. *Annu. Rev. Biochem.* **1982**, *51*, 531-554.
- 41. Pieters, R., Maximising multivalency effects in protein-carbohydrate interactions. *Org. Biomol. Chem.* **2009**, *7*, 2013-2025.
- 42. Young, N. M.; Johnston, R. A.; Watson, D. C., The amino acid sequence of peanut agglutinin. *Eur. J. Biochem.* **1991**, *196*, 631-637.
- 43. Wu, A. M.; Wu, J. H.; Liu, J.; Singh, T., Recognition profile of *Bauhinia purpurea* agglutinin (BPA). *Life Sciences* **2004**, *74*, 1763-1779.
- 44. Lotan, R.; Siegelman, H. W.; Lis, H.; Sharon, N., Subunit structure of soybean agglutinin. *J. Biol. Chem.* **1974**, *249*, 1219-1224.
- 45. Sugii, S.; Kabat, E. A., Immunochemical specificity of the combining site of *Wistaria floribunda* hemagglutinin. *Biochemistry* **1980**, *19*, 1192-1199.
- 46. Tollefsen, S. E.; Kornfeld, R., Isolation and characterization of lectins from *Vicia villosa*. *J. Biol. Chem.* **1983**, *258*, 5165-5171.
- 47. You, W.; Kasman, I.; Hu-Lowe, D. D.; McDonald, D. M., *Ricinus communis* Agglutinin I leads to rapid down-regulation of VEGFR-2 and endothelial cell apoptosis in tumor blood vessels. *Am. J. Pathol.* **2010**, *176*, 1927-1940.
- 48. Matsumura, K.; Higashida, K.; Ishida, H.; Hata, Y.; Yamamoto, K.; Shigeta, M.; Mizuno-Horikawa, Y.; Wang, X.; Miyoshi, E.; Gu, J.; Taniguchi, N., Carbohydrate binding specificity of a fucose-specific lectin from *Aspergillus oryzae*: a novel probe for core fucose. *J. Biol. Chem.* **2007**, *282*, 15700-15708.
- 49. Mortell, K. H.; Weatherman, R. V.; Kiessling, L. L., Recognition specificity of neoglycopolymers prepared by ring-opeing metathesis polymerization. *J. Am. Chem. Soc.* **1996**, *118*, 2297-2298.
- 50. Kanai, M.; Mortell, K. H.; Kiessling, L. L., Varying the size of multivalent ligands: the dependence of Concanavalin A binding on neoglycopolymer length. *J. Am. Chem. Soc.* **1997**, *119*, 9931-9932.
- 51. Mandal, D. K.; Brewer, C. F., Interactions of concanavalin A with glycoproteins: formation of homogeneous glycoprotein-lectin cross-linked complexes in mixed precipitation systems. *Biochemistry* **1992**, *31*, 12602-12609.

- 52. Mandal, D. K.; Brewer, C. F., Differences in the binding affinities of dimeric concanavalin A (including acetyl and succinyl derivatives) and tetrameric concanavalin A with large oligomannose-type glycopeptides. *Biochemistry* **1993**, *32*, 5116-5120.
- 53. Strong, L. E.; Kiessling, L. L., A general synthetic route to defined, biologically active multivalent arrays *J. Am. Chem. Soc.* **1999**, *121*, 6193-6196.
- 54. Schuster, M. C.; Mortell, K. H.; Hegeman, A. D.; Kiessling, L. L., Neoglycopolymers produced by aqueous ring-opening metathesis polymerization: decreasing saccharide density increases activity. *J. Mol. Catal. A.* **1997**, *116*, 209-216.
- 55. Cairo, C. W.; Gestwicki, J. E.; Kanai, M.; Kiessling, L. L., Control of multivalent interactions by binding epitope density. *J. Am. Chem. Soc.* **2002**, *124*, 1615-1619.
- 56. Goldstein, I. J.; Poretz, R. D., In *The Lectins: Properties, functions and applications in biology and medicine*, Liener, I. E.; Sharon, N.; Goldstein, I. J., Eds. Academic Press: Orlando, FL, 1986; p 35.
- 57. Gestwicki, J. E.; Strong, L. E.; Cairo, C. W.; Boehm, F. J.; Kiessling, L. L., Cell aggregation by scaffolded receptor clusters. *Chem. Biol.* **2002**, *9*, 163-169.
- 58. Ambrosi, M.; Batsanov, A.; Cameron, N. R.; Davis, B. G.; Howard, J. A.; Hunter, R., Influence of preparation procedure on polymer composition: synthesis and characterisation of polymethacrylates bearing β -D-glucopyranoside and β -D-glacopyranoside residues. *J. Chem. Soc., Perkin Trans. 1* **2002**, 45-52.
- 59. Ambrosi, M.; Cameron, N. R.; Davis, B. G.; Stolnik, S., Investigation of the interaction between peanut agglutinin and synthetic glycopolymeric multivalent ligands. *Org. Biomol. Chem.* **2005**, *3*, 1476-1480.
- 60. Godula, K.; Rabuka, D.; Nam, K. T.; Bertozzi, C. R., Synthesis and microcontact printing of dual end-functionalized mucin-like glycopolymers for microarray applications. *Angew. Chem. Int. Ed.* **2009**, *48*, 4973-4976.
- 61. Godula, K.; Bertozzi, C. R., Density variant glycan microarray for evaluating cross-linking of mucin-like glycoconjugates by lectins. *J. Am. Chem. Soc.* **2012**, *134*, 15732-15742.
- 62. Godula, K.; Bertozzi, C. R., Synthesis of glycopolymers for microarray applications via ligation of reducing sugars to a poly (acryloyl hydrazide) scaffold. *J. Am. Chem. Soc.* **2010**, *132*, 9963-9965.
- 63. Narla, S. N.; Sun, X., Orientated glyco-macroligand formation based on site-specific immobilization of O-cyanate chain-end functionalized glycopolymer. *Org. Biomol. Chem.* **2011**, *9*, 845-850.
- 64. Narla, S. N.; Sun, X., Immobilized sialyloligo-macroligand and its protein binding specificity. *Biomacromolecules* **2012**, *13*, 1675-1682.

- 65. Narla, S. N.; Sun, X., Glyco-macroligand microarray with controlled orientation and glycan density. *Lab Chip* **2012**, *12*, 1656-1663.
- 66. Gama, C. I.; Hsieh-Wilson, L. C., Chemical approaches to deciphering the glycosaminoglycan code. *Curr. Opin. Chem. Biol.* **2005**, *9*, 609-619.
- 67. Lee, S.; Brown, J. M.; Rogers, C. J.; Matson, J. B.; Krishnamurthy, C.; Rawat, M.; Hsieh-Wilson, L. C., End-functionalized glycopolymers as mimetics of chondroitin sulfate proteoglycans. *Chem. Sci.* **2010**, *1*, 322-325.
- 68. Hang, H. C.; Bertozzi, C. R., The chemistry and biology of mucin-type O-linked glycosylation. *Bioorg. Med. Chem.* **2005**, *13*, 5021-5034.
- 69. Mahal, L. K.; Bertozzi, C. R., Engineered cell surfaces: fertile ground for molecular landscaping. *Chem. Biol.* **1997**, *4*, 415-422.
- 70. Sadamoto, R.; Niikura, K.; Sears, P. S.; Liu, H.; Wong, C.; Suksomcheep, A.; Tomita, F.; Monde, K.; Nishimura, S., Cell-wall engineering of living bacteria. *J. Am. Chem. Soc.* **2002**, *124*, 9018-9019.
- 71. Link, A. J.; Tirrell, D. A., Cell surface labeling of Escherichia coli via Copper (I)-catalyzed [3+2] cycloaddition. *J. Am. Chem. Soc.* **2003**, *125*, 11164-11165.
- 72. Prescher, J.; Bertozzi, C. R., Chemistry in living systems. *Nat. Chem. Biol.* **2005**, *1*, 13-21.
- 73. Campbell, C. T.; Sampathkumar, S. G.; Yarema, K. J., Metabolic oligosaccharide engineering: perspectives, applications, and future directions. *Mol. Biosyst.* **2007**, *3*, 187-194.
- 74. Rabuka, D.; Parthasarathy, R.; Lee, G. S.; Chen, X.; Groves, J. T.; Bertozzi, C. R., Hierarchical assembly of model cell surfaces: synthesis of mucin mimetic polymers and their display on supported bilayers. . J. Am. Chem. Soc. 2007, 129, 5462-5471.
- 75. Rabuka, D.; Forstner, M. B.; Groves, J. T.; Bertozzi, C. R., Noncovalent cell surface engineering: incoporation of bioactive synthetic glycopolymers into cellular membranes. *J. Am. Chem. Soc.* **2008**, *130*, 5947-5953.
- 76. Parthasarathy, R.; Rabuka, D.; Bertozzi, C. R.; Groves, J. T., Molecular orientation of membrane-anchored mucin glycoprotein mimics. *J. Phys. Chem. B* **2007**, *111*, 12133-12135.
- 77. Godula, K.; Umbel, M. L.; Rabuka, D.; Botyanszki, Z.; Bertozzi, C. R.; Parthasarathy, R., Control of the molecular orientation of membrane-anchored biomimetic glycopolymers. *J. Am. Chem. Soc.* **2009**, *131*, 10263-10268.
- 78. Belardi, B.; O'Donoghue, G. P.; Smith, A. W.; Groves, J. T.; Bertozzi, C. R., Investigating cell surface galectin-mediated cross-linking on glycoengineered cells. J.

- Am. Chem. Soc. 2012, 134, 9549-9552.
- 79. Mauris, J.; Mantelli, F.; Woodward, A. M.; Cao, Z.; Bertozzi, C. R.; Panjwani, N.; Godula, K.; Argueso, P., Modulation of ocular surface glycocalyx barrier function by a galectin-3 N-terminal deletion mutant and membrane-anchored sythetic glycopolymers. *PloS ONE* **2013**, *8*, e72304.
- 80. Frey, A.; Giannasca, K. T.; Weltzin, R.; Giannasca, P. J.; Reggio, H.; Lencer, W. I.; Neutra, M. R., Role of the glycocalyx in regulating access of microparticles to apical plasma membranes of intestinal epithelial cells: implications for microbial attachment and oral vaccine targeting. *J. Exp. Med.* **1996**, *184*, 1045-1059.
- 81. Argueso, P.; Guzman-Aranguez, A.; Mantelli, F.; Cao, Z.; Ricciuto, J.; Panjwani, N., Association of cell surface mucins with galectin-3 contributes to the ocular surface epithelial barrier. *J. Biol. Chem.* **2009**, *284*, 23037-23045.
- 82. Lipinski, T.; Kitov, P. I.; Szpacenko, A.; Paszkiewicz, E.; Bundle, D. R., Synthesis and Immunogenicity of a Glycopolymer Conjugate. *Bioconjugate Chem.* **2011**, *22*, 274-281.
- 83. Parry, A. L.; Clemson, N. A.; Ellis, J.; Bernhard, S. R.; Davis, B. G.; Cameron, N. R., 'Multicopy multivalent' glycopolymer-stabilized gold nanoparticles as potential synthetic cancer vaccines. *J. Am. Chem. Soc.* **2013**, *135*, 9362-9365.
- 84. Nuhn, L. H., S.; Palitzsch, B.; Gerlitzke, B.; Schmitt, E.; Zentel, R.; Kunz, H., Watersoluble polymers coupled with glycopeptide antigens and T-cell epitopes as potential antitumor vaccines. *Angew. Chem. Int. Ed.* **2013**, *52*, 10652-10656.
- 85. Geijtenbeek, T. B.; Torensma, R.; van Vliet, S. J.; van Duijnhoven, G. C.; Adema, G. J.; van Kooyk, Y.; Figdor, C. G., Identification of DC-SIGN, a novel dendritic cell-specific ICAM-3 receptor that supports primary immune responses. *Cell* **2000**, *100*, 575-585.
- 86. Geijtenbeek, T. B.; Kwon, D. S.; Torensma, R.; van Vliet, S. J.; van Duijnhoven, G. C.; Middel, J.; Cornelissen, I. L.; Nottet, H. S.; KewalRamani, V. N.; Littman, D. R.; Figdor, C. G.; van Kooyk, Y., DC-SIGN, a dendritic cell-specific HIV-1-binding protein that enhances trans-infection of T cells. *Cell* **2000**, *100*, 587-597.
- 87. Gauthier, M. A.; Gibson, M. I.; Klok, H., Synthesis of functional polymers by post-polymerization modification. *Angew. Chem. Int. Ed.* **2008**, *48*, 48-58.
- 88. Becer, C. R.; Hoogenboom, R.; Schubert, U. S., Click chemistry beyond metal-catalyzed cycloaddition. *Angew. Chem. Int. Ed.* **2009**, *48*, 4900-4908.
- 89. Geng, J.; Lindqvist, J.; Mantovani, G.; Chen, G.; Sayers, C. T.; Clarkson, G. J.; Haddleton, D. M., Well-defined poly(N-glycosyl 1,2,3-triazole) multivalent ligands: design, synthesis and lectin binding studies. *QSAR Comb. Sci.* **2007**, *26*, 1220-1228.

- 90. Chen, G.; Tao, L.; Mantovani, G.; Geng, J.; Nystrom, D.; Haddleton, D. M., A modular click approach to glycosylated polymeric beads: design, synthesis and preliminary lectin recognition studies. *Macromolecules* **2007**, *40*, 7513-7520.
- 91. Becer, C. R.; Babiuch, K.; Pilz, D.; Hornig, S.; Heinze, T.; Gottschaldt, M.; Schubert, U. S., Clicking pentafluorostyrene copolymers: synthesis, nanoprecipitation, and glycosylation. *Macromolecules* **2009**, *42*, 2387-2394.
- 92. Nurmi, L.; Linkdqvist, J.; Randev, R.; Syrett, J.; Haddleton, D. M., Glycopolymers via catalytic chain transfer polymerization (CCTP), Huisgens cycloaddition and thiol-ene double click reactions. *Chem. Commun.* **2009**, 2727-2729.
- 93. Becer, C. R.; Gibson, M. I.; Geng, J.; Ilyas, R.; Wallis, R.; Mitchell, D. A.; Haddleton, D. M., High-affinity glycopolymer binding to human DC-SIGN and disruption of DC-SIGN interactions with HIV envelope glycoprotein. *J. Am. Chem. Soc.* **2010**, *132*, 15130-15132.
- 94. Zhang, Q.; Collins, J.; Anastasaki, A.; Wallis, R.; Mitchell, D. A.; Becer, C. R.; Haddleton, D. M., Sequence-controlled multi-block glycopolymers to inhibit DC-SIGN-gp120 binding. *Angew. Chem. Int. Ed.* **2013**, *52*, 4435-4439.
- 95. Crocker, P. R.; Paulson, J. C.; Varki, A., Siglecs and their roles in the immune system. *Nat. Rev. Immunol.* **2007**, *7*, 255-266.
- 96. Stamenkovic, I.; Sgroi, D.; Aruffo, A., CD22 binds to alpha-2,6-sialyltransferase-dependent epitopes on COS cells. *Cell* **1992**, *68*, 1003-1004.
- 97. Courtney, A. H.; Puffer, E. B.; Pontrello, J. K.; Yang, Z.; Kiessling, L. L., Sialylated multivalent antigens engage CD22 in trans and inhibit B cell activation. *PNAS* **2009**, *106*, 2500-2505.
- 98. Courtney, A. H.; Bennett, N. R.; Zwick, D. B.; Hudon, J.; Kiessling, L. L., Synthetic antigens reveal dynamics of BCR endocytosis during inhibitory signaling. *ACS Chem. Biol.* **2014**, *9*, 202-210.
- 99. Hudak, J. E.; Canham, S. M.; Bertozzi, C. R., Glycocalyx engineering reveals a Siglec-based mechanism for NK cell immunoevasion. *Nat. Chem. Biol.* **2014**, *10*, 69-75.
- 100. Rosen, S. D.; Bertozzi, C. R., The selectins and their ligands. *Curr. Opin. Cell. Biol.* **1994**, *6*, 663-673.
- 101. Rosen, S. D.; Bertozzi, C. R., Leukocyte adhesion: two selectins converge on sulphate. *Curr. Biol.* **1996**, *6*, 261-264.
- 102. Manning, D. D.; Hu, X.; Beck, P.; Kiessling, L. L., Synthesis of sulfated neoglycopolymers: selective P-selectin inhibitor. *J. Am. Chem. Soc.* **1997**, *119*, 3161-3162.

- 103. Choi, S.; Mammen, M.; Whitesides, G. M., Generation and in situ evaluation of libraries of poly(acrylic acid) presenting sialosides as side chains as polyvalent inhibitors of influenza-mediated hemagglutination. *J. Am. Chem. Soc.* **1997**, *119*, 4103-4111.
- 104. Sharon, N., Bacterial lectins, cell-cell recognition and infectious disease. *FEBS Lett.* **1987**, *217*, 145-157.
- 105. Disney, M. D.; Zheng, J.; Swager, T. M.; Seeberger, P. H., Detection of bacteria with carbohydrate-functionalized fluorescent polymers. *J. Am. Chem. Soc.* **2004**, *126*, 13343-13346.
- 106. Gestwicki, J. E.; Strong, L. E.; Kiessling, L. L., Tuning chemotactic responses with synthetic multivalent ligands. *Chem. Biol.* **2000**, *7*, 583-591.
- 107. Lamanna, A. C.; Gestwicki, J. E.; Strong, L. E.; Borchardt, S. L.; Owen, R. M.; Kiessling, L. L., Conserved amplification of chemotactic responses through chemoreceptor interactions. *J. Bacteriol.* **2002**, *184*, 4981-4987.
- 108. Woods, E. C.; Yee, N. A.; Shen, J.; Bertozzi, C. R., Glycocalyx engineering with a recycling glycopolymer that increases cell survival in vivo. *Angew. Chem. Int. Ed.* **2015**, *54*, 15782-15788.
- 109. Mancini, R. J.; Lee, J.; Maynard, H. D., Trehalose glycopolymers for stabilization of protein conjugates to environmental stressors. *J. Am. Chem. Soc.* **2012**, *134*, 8474-8479.
- 110. Lee, J.; Lin, E.; Lau, U. Y.; Hedrick, J. L.; Bat, E.; Maynard, H. D., Trehalose glycopolymers as excipients for protein stabilization. *Biomacromolecules* **2013**, *14*, 2561-2569.
- 111. Bat, E.; Lee, J.; Lau, U. Y.; Maynard, H. D., Trehalose glycopolymer resists allow direct writing of protein patterns by electron-beam lithography. *Nat. Commun.* **2015**, *6*, 6654.
- 112. Lau, U. Y.; Saxer, S. S.; Lee, J.; Bat, E.; Maynard, H. D., Direct write protein patterns for multiplexed cytokine detection from live cells using electron beam lithography. *ACS Nano* **2016**, *10*, 723-729.

CHAPTER 2: Carbohydrate antigen delivery by water soluble copolymers as potential anti-cancer vaccines

2.1: Introduction

2.1.1: Tumor associated carbohydrate antigens (TACAs)

The stimulation of immune systems through the use of a construct that can elicit a specific immune response against cancer is the basis of anti-cancer vaccines.¹ Cancer cells often bear characteristic carbohydrate structures on cell surface.^{2,3} These TACAs are shared by a variety of cancer cell types (**Table 2.1**), which make them attractive for anti-cancer vaccine development.^{4,5,6,7,8,9,10,11}

As we can see from **Table 2.1**, there are more than one type of TACAs on cell surface. Due to the heterogeneity of cell surface glycan structures, it is difficult to isolate sufficient TACAs from natural resources, while synthetic chemistry can afford large scale of pure functionalized TACAs (representative structures shown in **Figure 2.1**). 12

Cancer Type	Tumor Antigens
Melanoma	GM2, GM3, GD2
Neuroblastoma	GM2, GD2, polysialic acid
Sarcoma	GM2, GD2, GD3
B cell lymphoma	GM2, GD2
Small-cell lung	GM2, fucosyl-GM1, polysialic acid, Globo-H
Breast	GM2, Globo-H, TF(c), Tn(c), Le ^y
Prostate	GM2, Globo-H, Tn(c), TF(c), STn(c), Le ^y
Lung	GM2, Globo-H, Le ^y
Colon	GM2, Tn, STn(c), TF(c), Le ^y
Ovary	GM2, Globo-H, STn(c), TF(c), Le ^y
Stomach	GM2, Le ^y , Le ^a , SLe ^a

Table 2.1: Major TACAs identified in cancer tissues

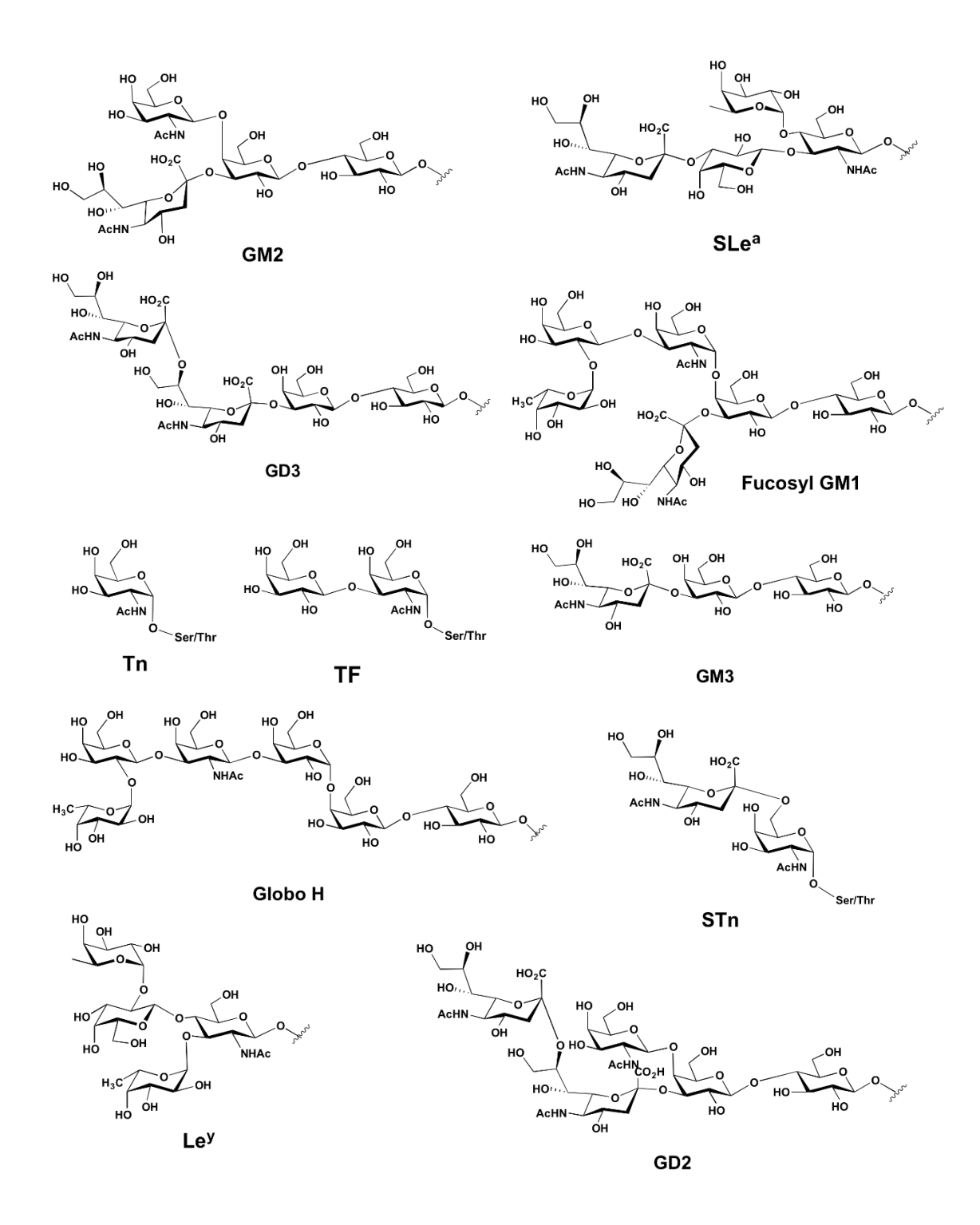


Figure 2.1: Representative structures of TACAs.

2.1.2: Challenges in TACA delivery and overview of different carrier platforms

When an antigen enters the body, there is an immediate response known as innate immunity, which will be followed by a secondary response known as adaptive immunity. Both branches of the immune system are important toward the prevention of the disease state. However, of most interest toward the development of a successful vaccine would be the adaptive branch. Once an antigen is presented to a naïve B cell by an antigen presenting cell (APC), the B cell matures into an activated B cell and can begin secreting low affinity antibodies of the IgM subtype. This response will only last for a few weeks; however, if a successful vaccine is to be developed, a long-term response is required. For this to occur, there must be a class switch from low affinity IgM isotypes to high affinity IgG isotypes. This can occur when both a naïve B-cell and a naïve T cell recognize the same antigen and differentiate into an activated B cell and an effector CD4+ helper T (Th) cell respectively. Once this has happened, the B cell can act as an APC and display the antigen to the effector Th cell by means of a major histocompatibility complex (MHC) class II. However, most carbohydrate epitopes cannot directly activate Th cells. As a result, the immune response to most carbohydrates is an exclusively primary immune response with low-affinity IgM production without class switch to high affinity IgG antibodies. Therefore, it is believed that conjugating a carbohydrate antigen to a protein containing these Th peptide epitopes should allow the dual activation and communication of B cells and Th cells. Once this complex has formed, the effector T cells will secrete cytokines that can induce isotype switching and cause the generation of memory B cells. These memory B cells are desired in order to establish long-term immunity. This is important because each additional time the body is exposed to the same

antigen, the immune response generated will be stronger and faster.¹³

However, serious challenges exist in order to elicit powerful anti-TACA immunity. As TACAs are also expressed at lower levels on normal cells, they are perceived as "self-antigens" by the immune system. 14,15 Direct vaccination with TACA alone typically can only induce weak activation of antibody secreting B cells with no cooperation from Th cells. 16 As a result, the antibodies secreted are mainly the low affinity IgM type. Since T cells typically recognize peptide epitopes, conjugating TACA to a Th cell peptide epitope should allow the stimulation of both B cells and Th cells. The matched Th cells provide stimulatory signals that can induce the B cells to undergo isotype switching leading to high affinity IgG antibodies. 17 Many innovative carriers have been developed to co-deliver TACAs with Th epitopes. The most common type of carrier is immunogenic proteins such as keyhole limpet haemocyanin (KLH), 18,19,20,21 tetanus toxoid (TT),^{22,23} and Bacillus Calmette-Guérin (BCG).²⁴ Other antigen presenting dendrimers, 25,26 regioselectively addressable functionalized platforms include templates, ²⁷ nanomaterials, ^{28,29} liposomes and proteoliposomes ^{30,31} polysaccharides ³² and virus-like particles (VLPs).33,34

A potential approach to enhance the anti-TACA immune response is to increase the local concentration of TACAs by clustering of the epitope in the vaccine construct. Livingston and co-workers demonstrated the cluster effect with Tn antigen.³⁵ Mice immunized with Tn-KLH could only raise few antibodies against the Tn cluster (Tn(c)) conjugated to human serum albumin (HSA) or desiallylated ovine submaxillary mucin (dOSM)--a natural source of Tn, although the loading of Tn on KLH was as high as 1,330 copies of Tn per KLH. And the antiserum showed little binding to Tn-expressing tumor

cell LSC. However, the Tn(c)-KLH (**Figure 2.2**) generated high IgG titers toward both Tn(c)-HAS and dOSM with moderated recognition of LSC. In phase I clinical trials with prostate cancer patients,³⁶ Tn(c)-KLH elicited significant titers of IgM and IgG.

Figure 2.2: Tn-KLH and Tn(c)-KLH vaccine.

From **Table 2.1** we know that many cancer cells express more than one type of TACAs. In order to elicit a much stronger immune response we can target several TACAs associated with a certain type of cancer at the same time by developing a unimolecular polyvalent vaccine containing various TACAs within one construct. Danishefsky and coworkers designed and synthesized antigenic glyco-conjugates containing multiple TACAs within one construct (**Figure 2.3**).³⁷ Overall the antibody titers generated were quite low; however, it is interesting that the antibodies generated were not only against the trivalent constructs but also against each individual TACA. They predicted that the organization of the various over-expressed carbohydrate motifs on the cancer cell surface

is very heterogeneous like a vaccine presenting multiple TACAs. Following this research, their group synthesized a first generation unimolecular pentavalent construct, which consists of breast cancer associated TACAs Globo-H, GM2, STn, TF and Tn.³⁸ Immunization results showed that IgM and IgG antibody titers against Globo-H were superior, but those against Tn were inferior compared with a noncovalent mixture of the monovalent constructs and no immune response was generated against Le^y. It is possible that the position of TACAs on the construct is important in determining the immunogenicity. So further research is needed in order to develop a more effective construct, which can elicit significant immune responses against many TACAs at the same time.

Figure 2.3: Unimolecular trivalent antigen constructs.

MUC1 is a membrane-bound glycoprotein.³⁹ The "variable number of tandem repeats (VNTR)" of MUC1, which consists of a 20-amino acid extracellular domain, can be used as a B-cell epitope. This sequence HGVTSAPDTRPAPGSTAPPA has several potential glycosylation sites at serine and threonine residues.⁴⁰ For many epithelial cancers like breast, ovarian, pancreatic and prostate, the O-glycans of MUC1 are limited

to short carbohydrate chains such as Tn, TF, and corresponding sialylated STn and STF. 41 Currently MUC1 glycopeptide has become a heated target for anti-tumor vaccine development. The Kunz group has prepared a series of MUC1 glycopeptide constructs for immunological evaluations. 42 In their latest work, two MUC1 glycopeptides bearing an STn disaccharide at separate locations were synthesized and conjugated with TT as the carrier protein. Very strong antibody responses (mainly IgG1) were obtained upon immunization of mice with these two constructs. The binding of the antiserum with MCF-7 cell was very strong, which could be inhibited by competitive binding with the free glycopeptide suggesting the specificity of the biological recognition.

Polymers are a class of synthetic carrier that has multiple potential advantages for TACA delivery. A polymer chain can carry many TACA molecules, which can enhance the avidities between the antigen and B cell receptors through the polyvalency effect and lead to strong activation of B cells. Furthermore, Th epitopes can be introduced into the glycopolymer to potentiate Th cells generating a long lasting humoral immune response. Although synthetic glycopolymers have been utilized in a variety of applications^{43,44} including biosensing,⁴⁵ delivery of therapeutic,^{46,47} modulation of natural killer cell function⁴⁸ and cellular signaling,⁴⁹ it is only recently that they have been explored as a TACA carrier.^{50,51} Herein, we present our results on using water soluble block copolymers as a platform to codeliver TACA and a Th epitope as a potential anti-cancer vaccine.

2.2: Results and discussion

2.2.1: Synthesis of Tn antigen (Scheme 2.1)

Starting with the commercially available D-galactosamine hydrochloride 1, diazo

transfer followed by global acetylation gave compound 3. Next selective deacylation to liberate the anomeric hydroxyl group yielded 4. Trichloroacetonitrile was used to convert 4 to donor 5. Selective benzylation of the carboxylic residue of Fmoc-Serine 6 resulted in acceptor 7. Glycosylation of donor 5 and acceptor 7 yielded glycoside 8 with an α/β ratio of 4.7:1. One pot reduction and acetylation of α-anomer azide 8 gave acetamide 9. Catalytic hydrogenation of benzyl ester provided carboxylic acid 10, and in this step acetic acid was added to obtain a pH of 3~4 to prevent Fmoc cleavage. 10 was capped with ethanolamine to get ethanolamide 11. Concentrated ammonia (7N) in methanol solution was used to furnish fully deprotected 12. Diazo transfer of 6-amino caproic acid 13 made 6-azido caproic acid 14. Linker 14 was coupled to free amine 12 to obtain the final Tn analog 15.

Scheme 2.1: Synthesis of azido-Tn analog.

Scheme 2.1 (cont'd)

2.2.2: Design, synthesis and characterization of glycopolymers

We selected the cyanoxyl-mediated free radical polymerization method^{52,53,54,55} for polymer construction due to the mild reaction condition. In order to incorporate both TACAs

and Th epitope, the copolymer was designed to contain a block with multiple ammonium moieties followed by a methyl ester block (see polymer 22 in Scheme 2.2). The polymerization was initiated by the treatment of aniline 16 with sodium nitrite and fluoroboric acid, which was followed by the addition of a mixture of sodium cyanate, acrylamide 18 and methacrylamide amine 19 and heating at 50 °C for 40 hours leading to intermediate polymer 20 (Scheme 2.2). Subsequently, acrylamide 18 and acrylamide methyl ester monomer 21 were added to the reaction mixture with further heating for another 40 hours. The resulting mixture was dialyzed in water to obtain copolymer 22. Based on integrations of ¹H-nuclear magnetic resonance (NMR) peaks from the polymers using the aromatic peaks from the terminal phenyl ring as the internal standard, there were on average 45 ammonium ions and 4 methyl esters per polymer chain of 22. Gel permeation chromatography (GPC) showed that polymer 22 has a molecular weight (Mn) of 13,800 with a polydispersity index of 1.14. (Polymer reaction yields are listed in Table 2.2).

Scheme 2.2: Synthesis of polymer **22**.

To test the efficiency of TACA delivery, a representative TACA, *i.e.*, the Tn antigen was introduced into the polymer. The Tn antigen, found over-expressed on a variety of cancer cell surface including 90% of breast cancer carcinoma, is an appealing target for TACA based anti-cancer vaccine development. A flexible amide linker was designed to conjugate Tn with the polymer to avoid potential humoral responses to the linker. In order to accomplish this, Tn derivative 23 in the form of N-hydroxysuccinimide (NHS) activated ester was synthesized and linked with the amines in polymer 22 promoted by DIPEA leading to glycopolymer 24 in 65% yield (Scheme 2.3). On average, 31 copies of Tn were introduced per chain based on H-NMR analysis. Polymer 24 was then treated with LiOH to hydrolyze all the methyl esters, which was supported by H-NMR analysis showing the

complete disappearance of the methyl groups. The resulting polymer was functionalized with pyridyl disulfide **25**, which then reacted with a cysteine modified oligopeptide from polio virus (PV) to introduce the helper T cell epitope^{30, 61} through the formation of disulfide bonds. The number of PV peptide per glycopolymer **28** was determined to be 2 peptides per chain by cleaving the disulfide linkage between the peptide and the glycopolymer followed by high-performance liquid chromatography (HPLC) quantification. As a control, polymer **29** was synthesized by capping the amine groups of polymer **22** with methoxyacetic acid, which was followed by introduction of two PV peptides per chain utilizing a similar protocol as in the construction of polymer **28**.

Scheme 2.3: Synthesis of glycopolymer 28.

Polymer	Yield
22	50%
24	65%
26	62%
28	79%

Table 2.2: Reaction yields for polymers 22, 24, 26 and 28

2.2.3: Immunological studies to evaluate vaccine efficacy

With the peptidic glyco-copolymer **28** in hand, its ability to elicit antibodies was evaluated. Mice were injected with glycopolymer **28** (4 µg Tn per dose) subcutaneously

with Freund's adjuvant followed by two booster injections at intervals of two weeks (days 14 and 28). Sera were drawn from mice one week after the final injection (day 35). The control group was vaccinated with polymer 29 following an identical protocol. To test anti-Tn antibody levels in sera, enzyme linked immunosorbent assay (ELISA) was performed using Tn functionalized BSA immobilized on microtiter plates. Analysis showed that the main antibodies induced by 28 were the IgG type with an IgG titer of 4,432 (Figure 2.4a. IgM titers are shown in Figure 2.4d). In comparison, the sera from mice receiving control polymer 29 contained extremely low titers of anti-Tn IgG antibodies (mean titer = 100) (Figure 2.4a). The fact that high titers of IgG antibodies were induced by 28 implies the Tn-specific B cells have undergone isotype switching. Another important characteristic of a successful vaccine is the maintenance of immune responses. To evaluate this, mice immunized with 28 were bled on day 89. ELISA analysis showed that the anti-Tn IgG titers remained at a similar level (Figure 2.4a, mean titer = 4,369) suggesting long lasting humoral immunity was generated.

For many TACA constructs with highly immunogenic protein carriers, antibodies specific against the carrier are induced as well, the titers of which can be hundreds times higher than that against the desired TACA.^{59, 62} The strong anti-carrier responses can potentially interfere with the generation of glycan specific antibodies due to antigen competition.^{63,64,65} The antibodies generated against the polymer backbone were analyzed. As shown in **Figure 2.4b**, immunization with glycopolymer **28** or control polymer **29** elicited similar amounts of anti-polymer IgG antibodies with titers around 700 as compared to a titer of 400 pre-immunization. The relatively low anti-polymer titers induced suggest the polymer backbone most likely does not compete significantly for B cell interactions.

As ELISA tests antibody binding to an artificial BSA-Tn construct, it is important to determine whether the antibodies elicited can recognize Tn expressed in its native environment, *i.e.*, cancer cells. Jurkat cells are known to express large amounts of Tn antigen on their surfaces. The post-immune serum from mice immunized with glycopolymer 28 exhibited significant binding with Jurkat cells, while those from the control polymer did not react with the cells (**Figure 2.4c**).

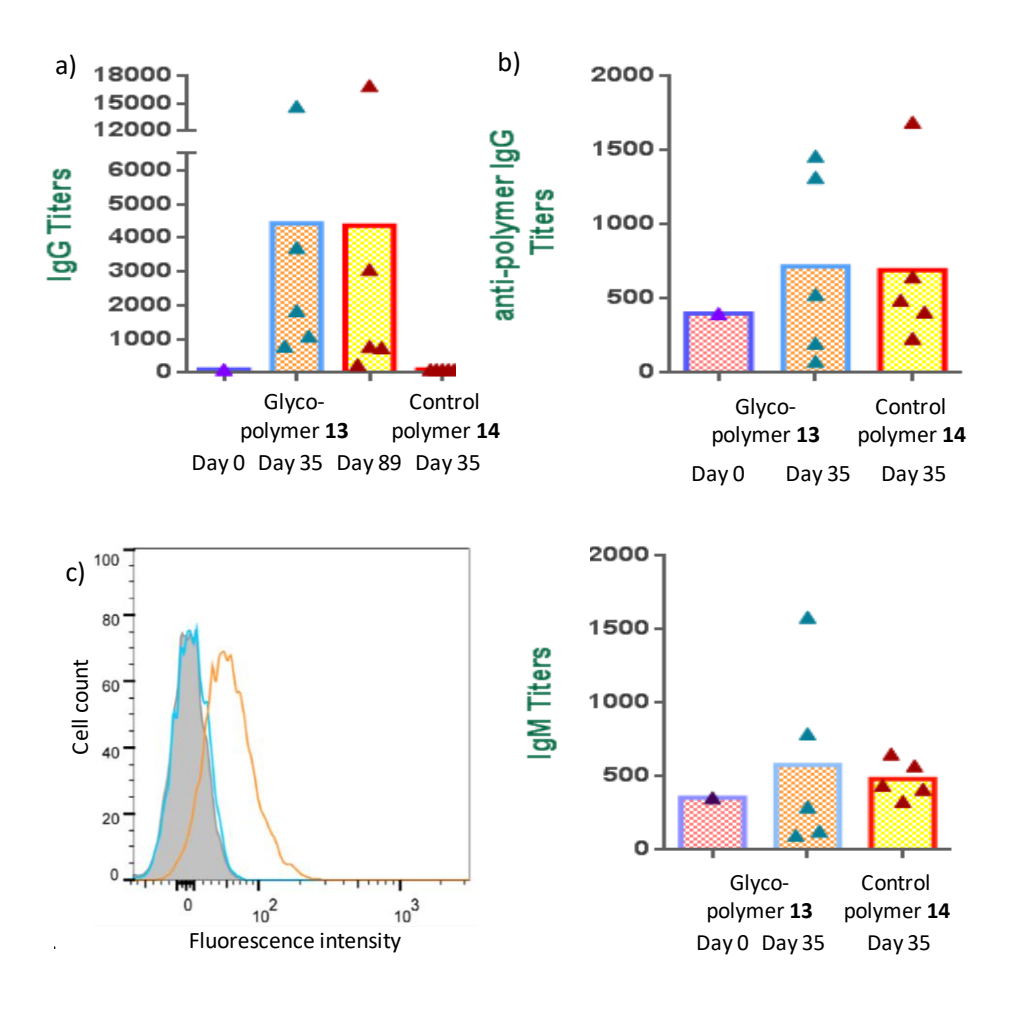


Figure 2.4: (a) Anti-Tn IgG titers on days 0, 35 and 89 from mice immunized with glycopolymer 28 and the anti-Tn IgG titers on day 35 from mice receiving control polymer 29. (b) Anti-polymer backbone IgG titers on days 0 and 35 from mice immunized with glycopolymer 28 and anti-polymer backbone IgG titers on day 35 from mice receiving control polymer 29. (c) Flow cytometry analysis of Jurkat cell binding by IgG antibodies in sera from representative mice immunized with glycopolymer 28 (orange curve) and control polymer 29 (blue curve). The shaded curve was from pre-immune serum binding with Jurkat cells. (d) Anti-Tn IgM titers on days 0, and 35 from mice immunized with glycopolymer 28 and the anti-Tn IgM titers on day 35 from mice receiving control polymer 29.

2.3: Conclusions

In conclusion, a fully synthetic glycopolymer vaccine incorporating multiple Tn antigen and Th cell peptide epitope has been prepared, which elicited significant and long-lasting anti-Tn IgG antibody titers. The antibodies generated recognized Tn antigens on tumor cells. Compared with other delivery platforms such as virus like particles, ^{33,34,60} the anti-Tn antibody titers generated by the glycopolymer constructs were modest. However, the polymer platform offers great flexibilities to adjust antigen densities and valency as well as the ratio of TACA *vs.* Th epitope. In addition, the immunogenicity of the polymer backbone is not high, which likely will not compete significantly with the desired TACA for B cell activation. These attributes bode well for further optimization of the glycopolymer construct to enhance the humoral responses against the TACAs.

2.4: Experimental section

2.4.1: General experimental procedures and methods for synthesis

All reactions were carried out under nitrogen with anhydrous solvents in flame-dried glassware, unless otherwise noted. Chemicals used were reagent grade as supplied except where noted. Centrifugal filter units of 3,000 molecular weight cut-off (MWCO) were purchased from EMD Millipore. Compounds were visualized by UV light (254 nm) and by staining with a yellow solution containing Ce(NH₄)₂(NO₃)₆ (0.5 g) and (NH₄)₆Mo₇O₂₄4H₂O (24.0 g) in 6% H₂SO₄ (500mL). Flash column chromatography was performed on silica gel 60 (230-400 Mesh). NMR spectra were referenced using residual CHCl₃ (δ ¹H-NMR 7.26 ppm), D₂O (δ ¹H-NMR 4.79 ppm). The molecular weight and polydispersity of the block copolymer were determined by GPC at 35 °C using two PLgel 10-μm mixed-B columns with DMF as the eluting solvent. The PV Th cell epitope peptide (CKLFAVWKITYKDT) was synthesized by RS Synthesis.

2.4.2: Synthesis of Tn antigen

Compound 3: 1,3,4,6-tetraacetyl-2-deoxy-2-azidogalactopyranose

Sodium azide (15.1 g, 232 mmol, 10 eq) was dissolved in water and cooled to 0 0 C. Then toluene (37.5 mL) was added, followed by drop wise addition of triflic anhydride (Tf₂O) (7.7 mL, 46.4 mmol, 2 eq). The reaction mixture was stirred at 0 0 C for 2 h. Then saturated sodium bicarbonate was added till no bubbles left. The organic phase was separated and the aqueous phase was extracted with toluene twice. The combined organic phase was dried over anhydrous sodium sulfate, (Note: this solution should never

be concentrated.) and used directly for the next step without further purification.

Galactosamine hydrochloride (1) (5 g, 23.2 mmol, 1 eq) was dissolved in water (30 mL), and potassium carbonate (4.8 g, 3.8 mmol, 1.5 eq), copper sulfate pentahydrate (57.9 mg, 0.232 mmol, 0.01 eq) and MeOH (50 mL) were added. Then the triflic azide solution from last step was added followed by addition of more MeOH until homogeneity. The mixture was allowed to stir at RT overnight, and the color changes from blue to green. Evaporate and coevaporate with toluene several times until almost dryness. Then pyridine (Py) (25 mL, 302 mmol, 13 eq) was added and the reaction was cooled to 0 °C followed by addition of acetic anhydride (Ac₂O) (50 mL, 464 mmol, 20 eq) slowly and 4-dimethylaminopyridine (DMAP) (0.718 g, 5.8 mmol, 0.25 eq). The reaction was allowed to warm to RT slowly and continued to stir at RT for 3~5 days. Upon completion, excess acetic anhydride was quenched by slow addition of MeOH. Then the mixture was concentrated under vacuum, diluted with DCM and washed with 1M HCl, Na₂CO₃ and H₂O. The organic phase was then dried over anhydrous Na₂SO₄, filtered and concentrated. After purified by column chromatography (Hex:EtOAc, 1:1), compound 3 was obtained as a white foam in an overall yield of 70%. Comparison with literature data⁶⁷ confirms its identity.

Compound 4: 3,4,6-tetra-*O*-acetyl-2-deoxy-2-azido-D-galactopyranose

Compound 3 (5.98 g, 16 mmol) was dissolved in THF (200 mL), and hydrazine acetate (2.15 g, 24 mmol, 1.5 eq) was added. Upon completion the reaction was diluted with DCM and washed with water twice. The organic phase was dried, and purified by column chromatography (Hex:EtOAc, 3:2) to obtain compound 4 as colorless oil in an

83% yield. Comparison with literature data⁶⁸ confirms its identity.

Compound **5**: *O*-(3,4,6-tri-*O*-acetyl-2-azido-2-deoxy-D-galactopyranoside) trichloroacetimidate

Compound 4 (4.7 g, 4.2 mmol) was dissolved in anhydrous DCM (63 mL), and 1,8-diazabicyclo[5.4.0]undec-7-ene (DBU) (0.22mL, 0.42 mmol, 0.1 eq) was added. To this mixture, trichloroacetonitrile (14 mL, 42 mmol, 10 eq) was added drop wise. The reaction was stirred at RT for ~2 h. Upon completion, the reaction was concentrated and purified by fast column chromatography (Hex:EtOAc, 3:2). Compound 5 was obtained as clear oil in an 88% yield. Comparison with literature data⁶⁸ confirms its identity.

Compound 7: Fmoc-Ser-OBn

Fmoc protected serine (6) (1 g, 3 mmol) was dissolved in DMSO (6 mL), and KHCO₃ (0.465 g, 4.5 mmol, 1.5 eq) and tetraethylammonium iodide (TEAI) (0.114 g, 0.3 mmol, 0.1 eq) were added. The reaction was stirred at RT for ~10 min and then benzyl bromide (BnBr) (1.11 mL, 9 mmol, 3 eq) was added, and the reaction was stirred at RT overnight. The reaction was quenched by addition of 50 mL of water and was extracted with DCM three times. The combined organic phase was washed with NaHCO₃, Na₂S₂O₃ and brine, dried over anhydrous Na₂SO₄, and concentrated under vacuum. Then after purification by column chromatography (Hex:EtOAc, 3:1→Hex: EtOAc, 1:1), compound 7 was obtained as a white solid in a 77% yield. Comparison with literature data⁶⁹ confirms its identity.

Compound **8**: *N*-(9-fluorenylmethyloxycarbonyl)-*O*-(3,4,6-tri-*O*-acetyl-2-azido-2-deoxy-α-D-galactopyranosyl)-L-serine benzylester

Compound 5 (5.95 g, 13.1 mmol, 1.5 eq) and compound 7 (3.62 g, 8.73 mmol, 1 eq) were mixed with freshly activated molecular sieves 4A (20.8 g), and dissolved in a mixture of anhydrous DCM:Et₂O (1:1) 240 mL. The reaction was stirred for 1 h, and then cooled to -30 0 C, and trimethylsilyl trifluoromethanesulfonate (TMSOTf) (0.32 mL, 1.78 mmol, 0.205 eq) was added drop wise. The reaction was kept stirring at -30 0 C for ~2 h. Upon completion, DIPEA was added to neutralize the pH. The reaction was diluted with DCM and washed with 0.1 M HCl and water and then dried, filtered and concentrated. Compound 8 was obtained in a 5:1 α/β mixture with an overall yield of 61% after using column chromatography (Hex:EtOAc, 3:1). Comparison with literature data⁶⁸ confirms its identity.

Compound **9**: N-(9-fluorenylmethyloxycarbonyl)-O-(3,4,6-tri-O-acetyl-2-acetamido-2-deoxy- α -D-galactopyranosyl)-L-serine benzylester

Compound 8α (2.36 g, 3.2 mmol, 1 eq), zinc dust (1 g, 64.7 mmol, 20 eq), acetic acid (1.85 mL, 32.4 mmol, 10 eq) and acetic anhydride (3.05 mL, 32.4 mmol, 10 eq) were added to THF (25 mL). The reaction mixture was stirred at RT overnight. Upon completion, the reaction was filtered through celite, and extracted with DCM and saturated NaHCO₃. The organic phase was dried, filtered and concentrated. The crude product was purified by column chromatography (Hex:EtOAc, 1:2) to obtain compound 9 with a 52% yield. Comparison with literature data³⁴ confirms its identity.

Compound **10**: *N*-(9-fluorenylmethyloxycarbonyl)-*O*-(3,4,6-tri-*O*-acetyl-2-acetamido-2-deoxy-α-D-galactopyranosyl)-L-serine

Compound 9 (0.864 g, 1.15 mmol, 1 eq) was dissolved in MeOH (54 mL) and the reaction flask was evacuated and flushed with nitrogen gas. Then palladium on activated carbon (0.09 g) was added followed by drop wise addition of acetic acid until the pH was ~3-4. The reaction was stirred under a hydrogen atmosphere for ~1 h. Upon completion, the reaction was filtered through celite, concentrated and purified by column chromatography (MeOH:DCM, 1:30→MeOH:DCM:AcOH, 5:94.5:0.5). Compound 10 was obtained as white foam with a 58% yield. Comparison with literature data³⁴ confirms its identity.

Compound 11: N-(9-fluorenylmethyloxycarbonyl)-O-(3,4,6-tri-O-acetyl-2-acetamido-2-deoxy- α -D-galactopyranosyl)-L-serine ethanolamide

Compound **10** (0.551 g, 0.85 mmol, 1 eq), benzotriazole-1-yl-oxy-tris-(dimethylamino)-phosphonium hexafluorophosphate (BOP) (0.744 g, 1.68 mmol, 2 eq) and DIPEA (0.28 mL, 1.71 mmol, 2 eq) were dissolved in a 42 mL mixture of THF:DCM (1:1), and stirred at RT for 1 h. Then ethanolamine (0.26 mL, 4.23 mmol, 5 eq) was added drop wise and the reaction was stirred for another 5 h. Once complete, the reaction was diluted with DCM and extracted with saturated ammonium chloride twice. The organic phase was dried, filtered and concentrated. Column chromatography (DCM:MeOH, 19:1 \rightarrow DCM:MeOH, 9:1) was used to obtain compound **11** as a white solid in a 60% yield. Comparison with literature data³⁴ confirms its identity.

Compound 12: *O*-(2-Acetamido-2-deoxy-α-D-galactopyranosyl)-L-serine ethanolamide

Compound 11 (207 mg, 0.3 mmol, 1 eq) was dissolved in a 7N ammonia in MeOH solution (10 mL) and the reaction was stirred at 0 °C for 6 h and allowed to warm to RT overnight. The reaction was concentrated to almost dryness and was purified by column chromatography (DCM:MeOH, 4:1 →DCM:MeOH:NH₄OH, 4:4:1). Compound 12 was obtained as a white solid with a 50% yield. Comparison with literature data³⁴ confirms its identity.

Compound 14: 6-azido-hexanoic acid

Sodium azide (6.5 g, 100 mmol) was dissolved in water (22 mL) and DCM (44 mL) was added. The mixture was cooled to 0 °C, and triflic anhydride (Tf₂O) (3.32 mL, 20 mmol, 2 eq) was added drop wise followed by stirring at 0 °C for 2 h. The aqueous phase was extracted twice with DCM and the combined organic phase was washed with saturated NaHCO₃ and dried over anhydrous Na₂SO₄. This solution was used for the next step without any further purification.

6-Amino caproic acid (13) (1.31 g, 10 mmol) was dissolved in MeOH (26 mL), K₂CO₃ (2.76 g, 20 mmol, 2 eq) and copper sulfate pentahydrate (0.025 g, 0.1 mmol, 0.01 eq) dissolved in water (10 mL) were added to the mixture. Then triflic azide solution from last step was added followed by addition of MeOH until homogeneity, and the reaction was stirred at RT overnight. The organic solvents were then evaporated under vacuum and the residue diluted with water and washed with DCM. 10% HCl was added to the aqueous phase to get a pH ~2 and EtOAc was used to extract several times. The combined organic phase was dried, filtered and concentrated followed by column

chromatography. Compound **14** was obtained as colorless oil with an 85% yield. Comparison with literature data⁷⁰ confirms its identity.

Compound **15**: 6-(azido)hexanoate-*O*-(2-acetamido-2-deoxy-alpha-D-galactopyranosyl)-L-serine ethanolamide

Compound 12 (31.2 mg, 0.0887 mmol, 1 eq), compound 14 (19.5 mg, 0.124 mmol, 1.4 benotriazole-1-yl-oxy-tris-(dimethylamino)-phosphonium eq), hexafluorophosphate (BOP) (47.7 mg, 0.108 mmol, 1.22 eq), hydroxybenzotriazole (HOBt) (15.0 mg, 0.111 mmol, 1.24 eq) and DIPEA (30 μL, 0.177 mmol, 1.97 eq) were dissolved in N-methyl-2-pyrrolidone (NMP). The reaction was stirred at RT overnight. Once complete, a large excess of ice-cold ether was added to precipitate out the product. After vacuum filtration and column chromatography (DCM:MeOH:NH₄OH, 12:5:1), the product was dissolved in water and lyophilized. Compound 15 was obtained as a white solid with a 32% yield. ¹H NMR (500 MHz, D₂O): $\delta = 4.79$ (d, 1H, H-1, J = 4.0 Hz), 4.48 (t, 1H, H-8, J = 5.5 Hz), 4.05 (dd, 1H, H-2, J = 3.5, 11.0 Hz), 3.86 (d, 1H, H-5, J = 3.0Hz), 3.82-3.74 (m, 3H, H-7, H-3, H-4), 3.69 (dd, 1H, H'-7, J=5.5, 10.5 Hz), 3.64-3.62(m, 2H, 2H-6, H'-6), 3.54-3.51 (m, 2H, 2H-3"), 3.25-3.19 (m, 4H, 2H-2", 2H-6'), 2.25 (t, 2H, 2H-2', J = 6.5 Hz), 1.92 (s, 1H, 3H-10), 1.55-1.57 (m, 4H, 2H-3', 2H-5'), 1.30-1.24 ppm (m, 2H, 2H-4'); 13 C NMR (600 MHz, D₂O): $\delta = 176.8$ (C-1'), 174.1 (C-9), 171.2 (C-1"), 97.4(C-1), 71.0 (C-4), 68.1 (C-5), 67.3 (C-3), 66.9 (C-7), 60.7 (C-6), 59.4 (C-3"), 53.4 (C-8), 50.5 (C-6'), 49.4 (C-2), 41.2 (C-2"), 34.9 (C-2'), 27.3 (C-5'), 25.1 (C-4'), 24.4 (C-4'), 21.6 ppm (C-3'); high resolution mass spectrometry (HRMS): m/z calculated for C₁₉H₃₅N₆O₉: 491.2466; found: 491.2460 [M+H]⁺.

2.4.3: Synthesis of block copolymer

Monomer 21 was prepared following a literature procedure. 71 All solutions used for polymer synthesis were treated with three freeze-pump-thaw cycles and the reaction was performed under nitrogen atmosphere. A solution of 4-(4-aminophenyl) butyric acid (17.9 mg, 0.1 mmol), sodium nitrite (8.3 mg, 0.12 mmol), and a 50% aqueous fluoroboric acid solution (18.7 µL, 0.15 mmol) in a 1:1 mixture of H₂O and THF (2 mL total) was cooled to 0 °C for 30 minutes. At this time, sodium cyanate (6.5 mg, 0.1 mmol), monomer N-(2-aminoethyl)methacrylamide hydrochloride (984.4 mg, 6 mmol) and acrylamide (213.2 mg, 3 mmol) dissolved in water (2 mL) were added. The reaction mixture was heated to 50 °C for 40 hours. A small aliquot of the mixture was removed and polymer 20 was purified and characterized. To the remaining mixture, monomer 21 (797 mg, 4 mmol) and acrylamide (213 mg, 3 mmol) were added and reaction was allowed to proceed at 50 °C for another 40 h. The copolymer was dialyzed against water and then lyophilized. ¹H-NMR: δ 0.75-1.10 (br m, CH₃ of amine monomer), 1.10-2.25 (br m, aliphatic **H**, from C**H** and C**H**₂ of polymer backbone), 2.75-3.40 (br m, aliphatic **H**, from CH₂ on the amine and ester monomer), 3.60 (s, CH₃ of ester monomer), 6.75 (br s, aromatic **H**), 7.00 (br s, aromatic **H**).

We normalized our peak integration to the small aromatic peaks at ~6.75 ppm (2 protons) and ~7.00 ppm (2 protons). For copolymer **20**, the amount of amine monomer per chain was calculated by the integration of the broad peak at ~1.0 ppm, which corresponds to methyl group on the amine monomer **19**. This matches the integration of the broad peak at ~3.25 ppm and ~3.00 ppm, which correspond to CH₂ on the amine monomer **19**. The broad peak at ~1.50 ppm is responsible for CH in the polymer

backbone (from acrylamide) and CH₂ in the polymer backbone (from both arylamide and monomer **19**). Subtracting the number of CH₂ protons on amine monomer **19** from the integration of this peak and then dividing by 3 gives the number of acrylamide monomer per chain. For copolymer **22**, the number of ester monomer per chain was determined from integration of the peak at ~3.60 ppm, which corresponds to the methyl group on the ester monomer. And the number of acrylamide was calculated in the same way as mentioned above.

Copolymer 22 was reacted with a large excess of phenylacetic acid (8 eq) to obtain the derivatized polymer which was soluble in DMF for GPC analysis. The Mn of polymer 22 was calculated by subtracting the molecular weight of the modified group from the Mn got for the derivatized polymer. We assumed all the amine groups have been derivatized so the PDI value would stay the same.

2.4.4: Synthesis of peptidic glycopolymer

To a solution of copolymer **22** (12.6 mg) and DIPEA (16.6 μL, 0.095 mmol) in anhydrous DMF (1 mL) was added Tn-NHS ester **23** (53 mg, 0.072 mmol)⁶⁰ at RT. The reaction mixture was stirred at RT for 2 days. The glycopolymer **24** obtained was dialyzed against water and lyophilized. ¹H-NMR: δ 0.75-1.10 (br m, CH₃ of amine monomer), 1.50 (br s, aliphatic **H** from Tn linker), 1.90 (s, CH₃ from Tn), 1.10-2.25 (br m, aliphatic **H**, from CH and CH₂ of polymer backbone and Tn linker), 2.10-2.30 (br m, aliphatic **H** from Tn linker), 2.75-3.40 (br m, aliphatic **H**, from CH₂ on the amine and ester monomer and Tn linker), 3.50-3.85 (br m, **H** from Tn), 4.50 (s, **H** from Tn), 4.05 (br m, **H** from Tn), 4.75 (s, anomeric **H** from Tn).

To a solution of glycopolymer **24** (14.9 mg) in water (1 mL), 0.1 M LiOH solution was added till pH~11. The mixture was stirred overnight followed by neutralization with hydrochloric acid to pH ~ 7. After dialysis and lyophilization, the residue was dissolved in anhydrous DMF (1 mL), to which DIPEA (3.8 μL, 0.022 mmol), *N,N,N',N'*-tetramethyl-*O*-(*N*-succinimidyl)uronium tetrafluoroborate (TSTU) (1 mg, 0.003 mmol) and *S*-(2-pyridylthio)cysteamine hydrochloride (1.2 mg, 0.005 mmol) were added. Stirring was continued for 2 days, and the resulting solution was dialyzed against water and lyophilized to obtain polymer **26**. ¹H-NMR: 0.75-1.10 (br m, CH₃ of amine monomer), 1.50 (br s, aliphatic **H** from Tn linker), 1.90 (s, CH₃ from Tn), 1.10-2.25 (br m, aliphatic **H**, from CH and CH₂ of polymer backbone and Tn linker), 2.10-2.30 (br m, aliphatic **H** from Tn linker), 2.75-3.40 (br m, aliphatic **H**, from CH₂ on the amine and ester monomer and Tn linker), 3.50-3.85 (br m, **H** from Tn), 4.50 (s, **H** from Tn), 4.05 (br m, **H** from Tn), 4.75 (s, anomeric **H** from Tn), 7.25 (br s, aromatic **H**), 7.75 (br m, aromatic **H**), 8.25 (br s, aromatic **H**).

Polymer 26 (7.3 mg) and PV peptide 27 (7.4 mg, 0.004 mmol) were dissolved in water and 1M NaOH solution was added until pH~9. After incubation for 2 days, the solution was dialyzed against water and lyophilized to obtain peptidic glycopolymer 28. In order to quantify the average amount of PV peptide per polymer, a calibration curve was constructed using known amounts of PV peptide by integrating the respective UV traces on reverse phase HPLC chromatograms. The peptidic glycopolymer 28 was treated with tris(2-carboxyethyl)phosphine hydrochloride (TCEP) to cleave the PV peptide from 28. After centrifuge filtration (3,000 MWCO) to remove TCEP, the 10,000 MWCO centrifugal filter was used to collect the solution containing the PV peptide. The amount

of PV peptide coupled to peptidic glycopolymer **28** was determined through HPLC analysis by comparison with the calibration curve.

2.4.5: Synthesis of the control polymer

DIPEA (38.4 μ L, 0.22 mmol), TSTU (33 mg, 0.11 mmol) and methoxyacetic acid (8.5 μ L, 0.11 mmol) were added to copolymer **22** (14.6 mg) in anhydrous DMF (1 mL) solution. Further modification and PV peptide conjugation were performed following similar procedures as synthesis of polymer **28**.

2.4.6: Mouse immunization

Pathogen-free female mice age 6–10 weeks were obtained from Charles River and maintained in the University Laboratory Animal Resources facility of Michigan State University. All animal care procedures and experimental protocols have been approved by the Institutional Animal Care and Use Committee (IACUC) of Michigan State University. Groups of five mice were injected subcutaneously on day 0 with 0.1 mL of the polymer as emulsions in complete Freund's adjuvant (Fisher), according to the manufacturer's instructions. Boosters were given subcutaneously on days 14 and 28 with the glycopolymer as emulsions in incomplete Freund's adjuvant (0.1 mL). Serum samples were collected on days 0 (before immunization), 35, and 89.

2.4.7: ELISA assays

A 96-well microtiter plate was coated with a solution of bovine serum albumin-Tn conjugate (BSA-Tn)⁶⁰ in PBS buffer (10 µg mL⁻¹) and then incubated at 4 °C overnight. The plate was washed four times with PBS/0.5% Tween-20 (PBST), followed by the addition of 1% (w/v) BSA in PBS to each well and incubation at RT for one hour. The plate was washed again with PBST and mice sera were added in 0.1% (w/v) BSA/PBS. The plate was incubated for two hours at 37 °C and washed. A 1:2000 dilution of horseradish peroxidase (HRP)-conjugated goat antimouse IgG (Jackson ImmunoResearch Laboratory) in 0.1% BSA/PBS was added to each well. The plate was incubated for one hour at 37 °C, washed and a solution of 3,3,5',5'-tetramethylbenzidine (TMB) was added. Color was allowed to develop for 15 min, and then a solution of 0.5 M H₂SO₄ was added to quench the reaction. The optical density was then measured at 450 nm. The titer was determined by regression analysis with log₁₀ dilution plotted with optical density. The titer was calculated as the highest dilution that gave three times the absorbance of normal mouse sera diluted at 1:1600 (about 0.1 for all sera). The antibody titers against the polymer backbone were determined by ELISA against polymer 7 immobilized on ELISA plates.

2.4.8: Fluorescence-activated cell sorting (FACS)

Human lymphoma Jurkat cells (kindly provided by Profs. Barbara Kaplan and Norbert Kaminski, Michigan State University) were cultured in Roswell Park Memorial Institute medium (RPMI) 1640 supplemented with 10% FBS, 2 mM L-glutamine, 1 mM sodium pyruvate, minimal essential medium nonessential amino acid, 100 units/mL each of penicillin G and streptomycin (all from Invitrogen). Mouse sera collected on day 89

were diluted 2-fold and incubated with 10⁵ Jurkat cells for 30 minutes at 4 °C. The cells were washed twice with FACS buffer (1% BSA + 0.1% NaN₃/PBS) and incubated with a 1:100 diluted goat anti-mouse IgG labeled with fluorescein isothiocyanate (FITC) (Jackson ImmunoResearch Laboratory, catalog #115-095-164) for 30 min at 4 °C. The cells were washed again twice with FACS buffer and re-suspended in FACS buffer. Data analysis was done with LSR II (BD Biosciences).

APPENDIX

APPENDIX

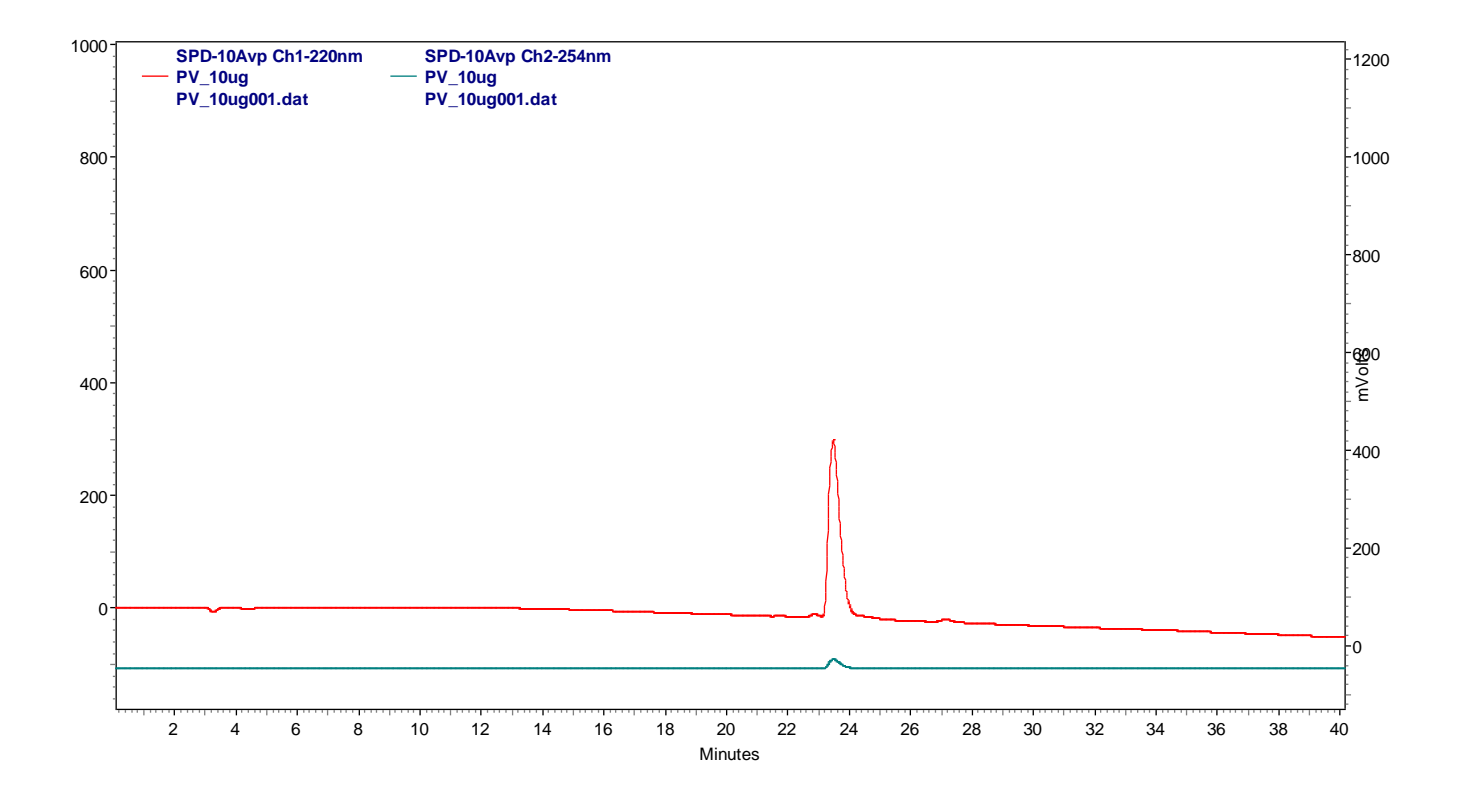


Figure 2.5: HPLC-UV spectrum of 10 μg PV peptide. Peak appears at ~24 min.

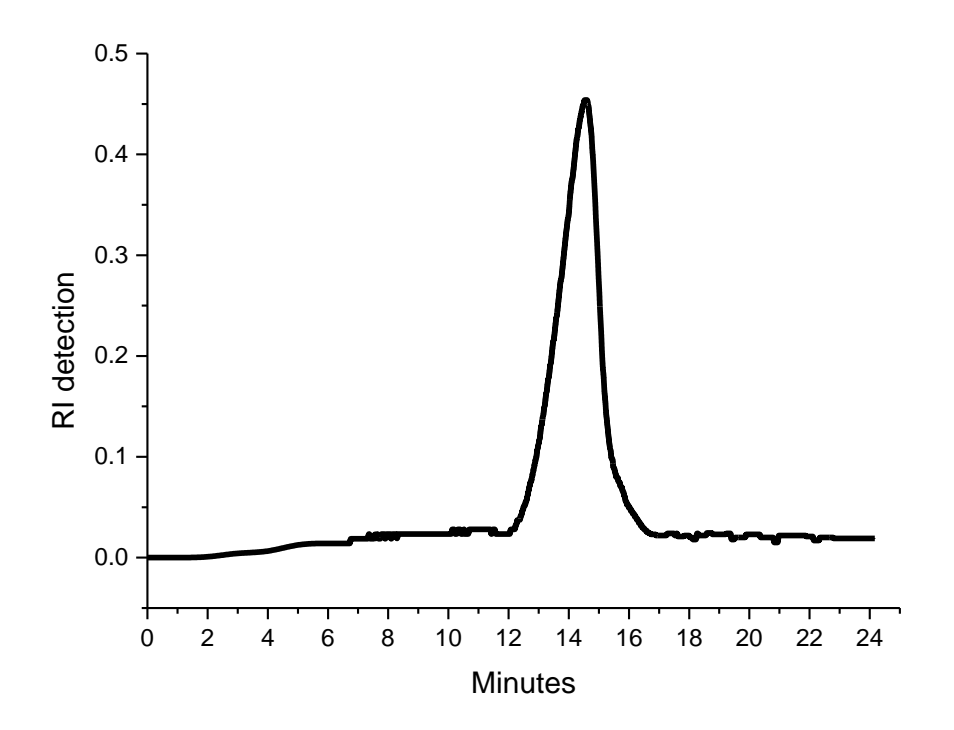


Figure 2.6: GPC of the phenyl acetic acid derivative of copolymer 22 (eluent: DMF).

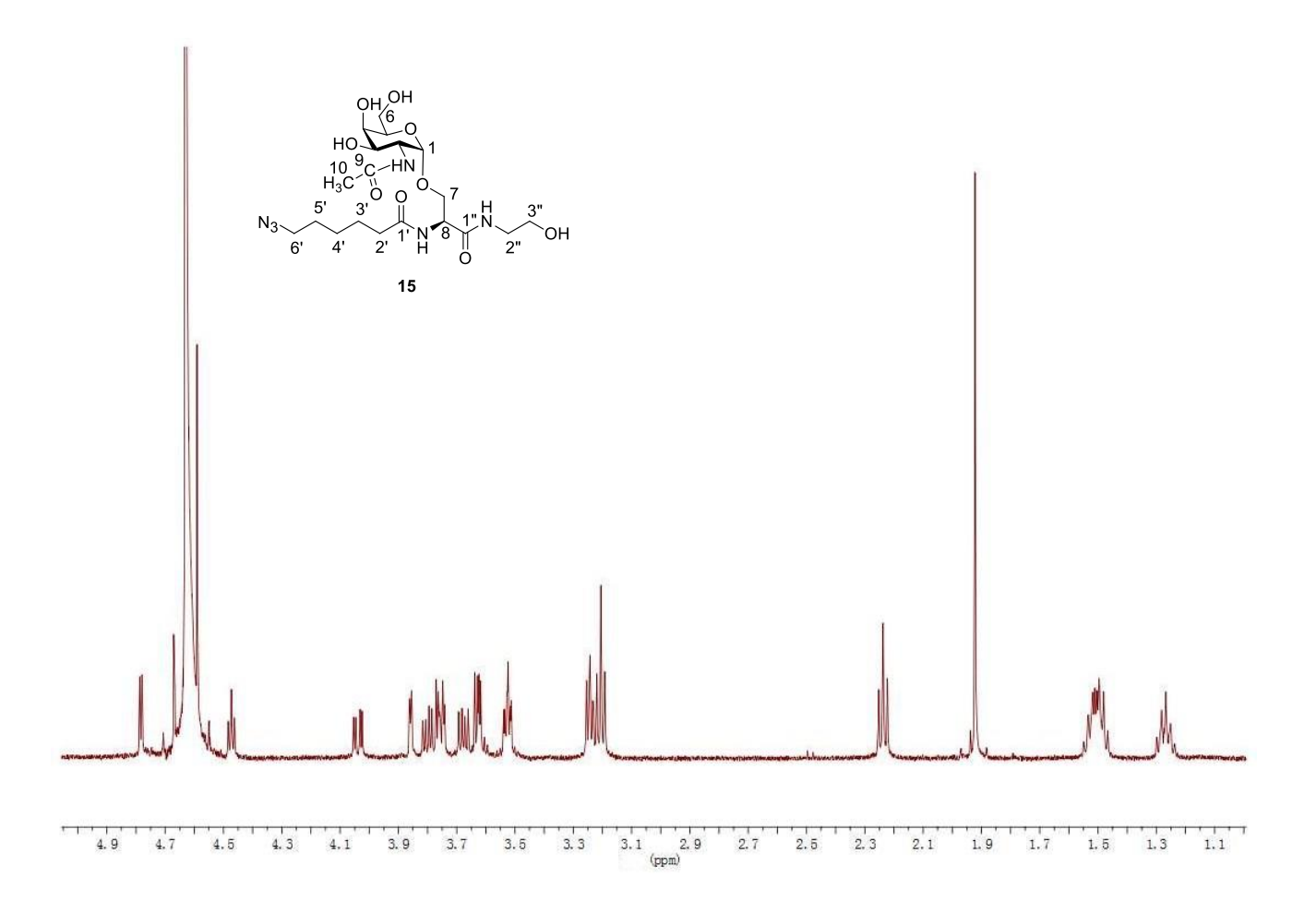


Figure 2.7: 500 MHz (D₂O), ¹H NMR of **15**.

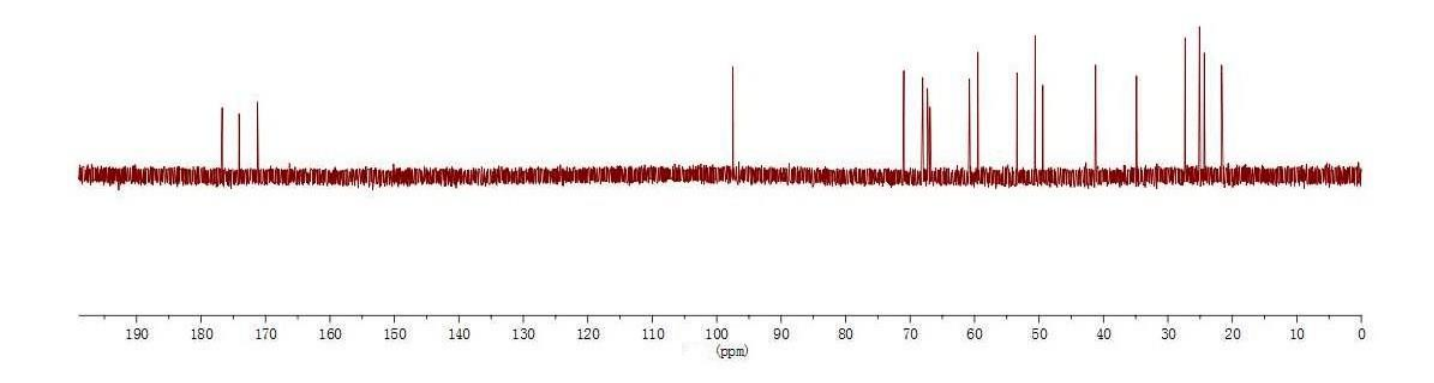


Figure 2.8: 600 MHz (D₂O), ¹³C NMR of **15**.

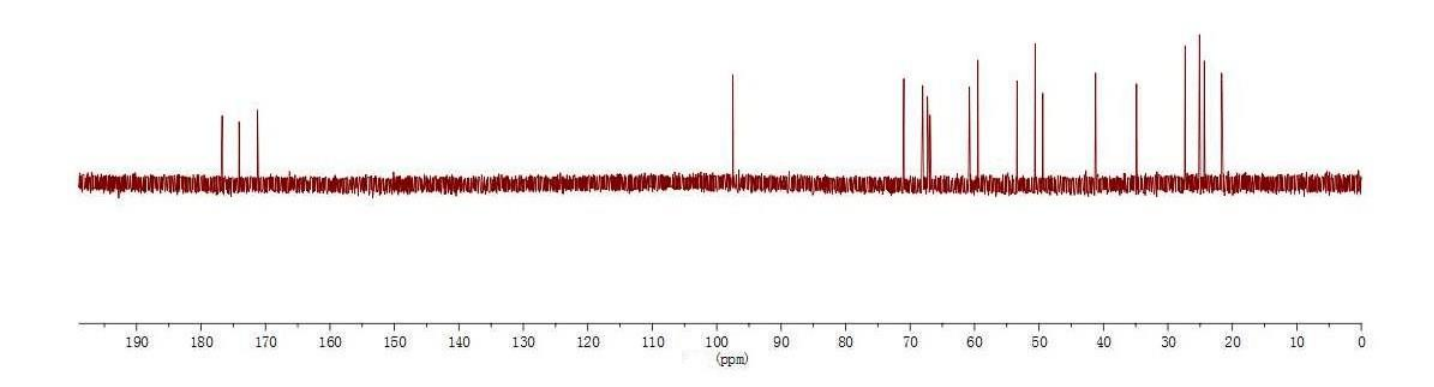


Figure 2.9: 600 MHz (D₂O), ¹³C NMR of **15**.

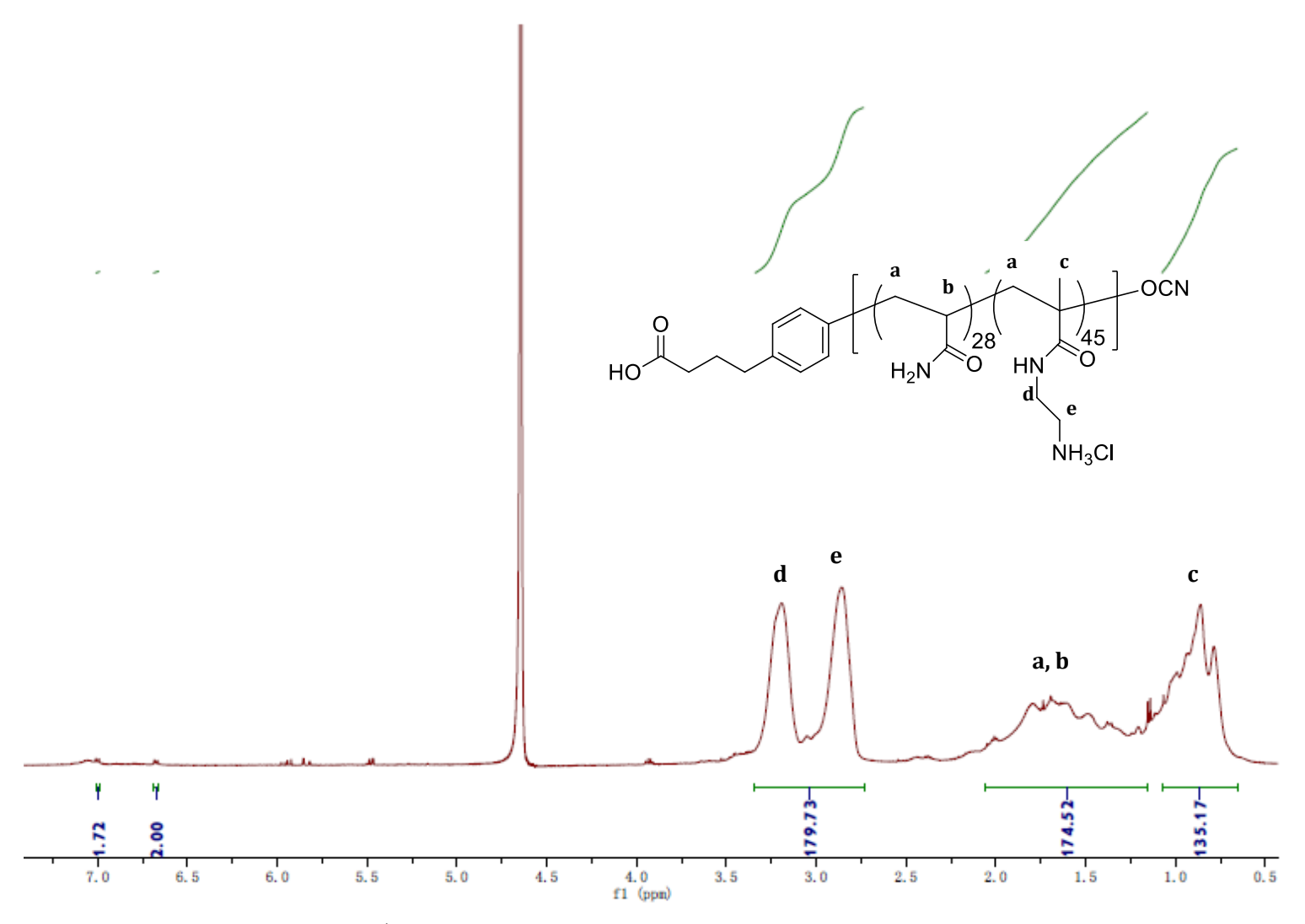


Figure 2.10: 500 MHz (D_2O), ¹H NMR of copolymer 20.

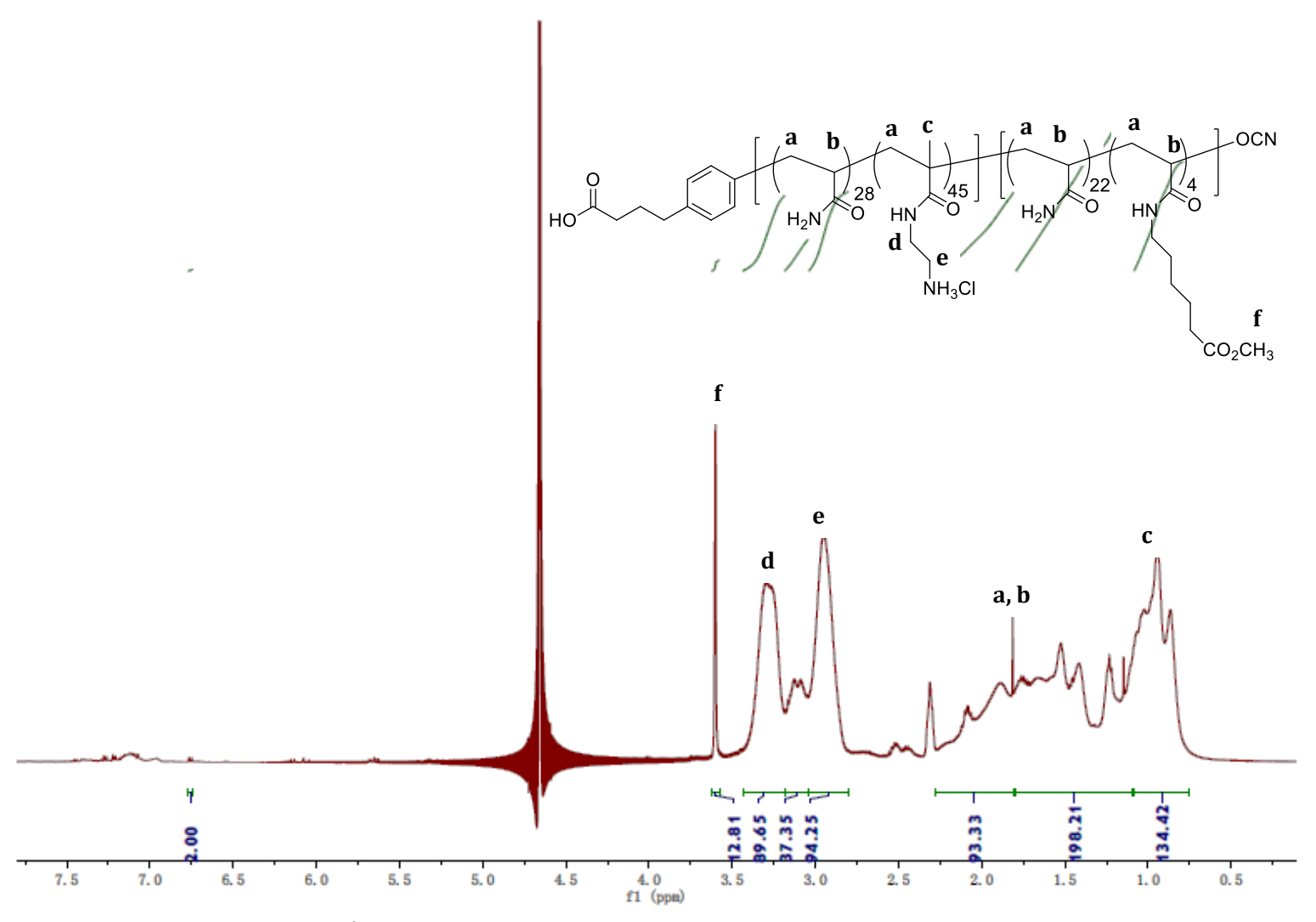


Figure 2.11: 500 MHz (D_2O), ¹H NMR of copolymer 22.

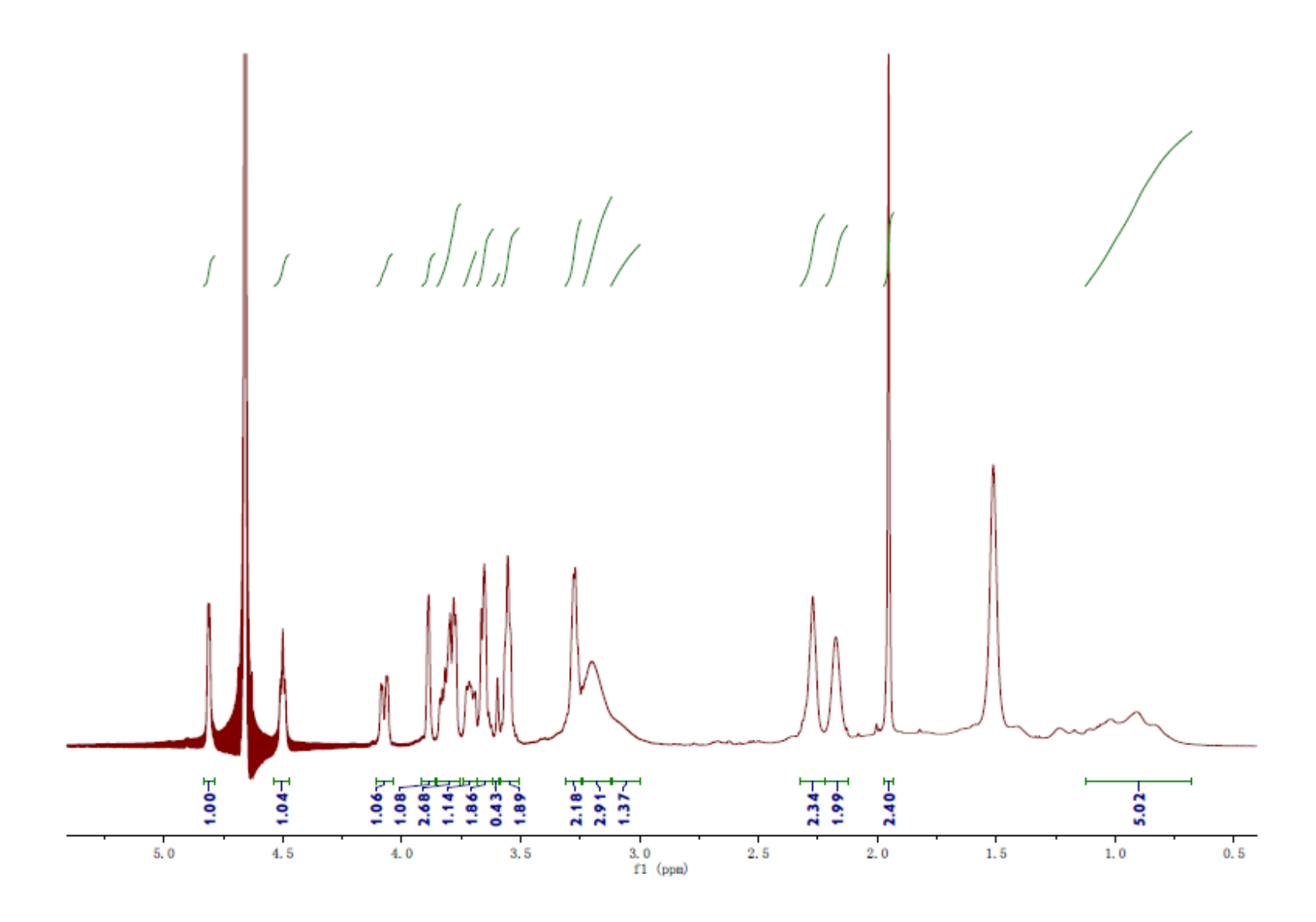


Figure 2.12: 500 MHz (D₂O), ¹H NMR of glycopolymer **24**.

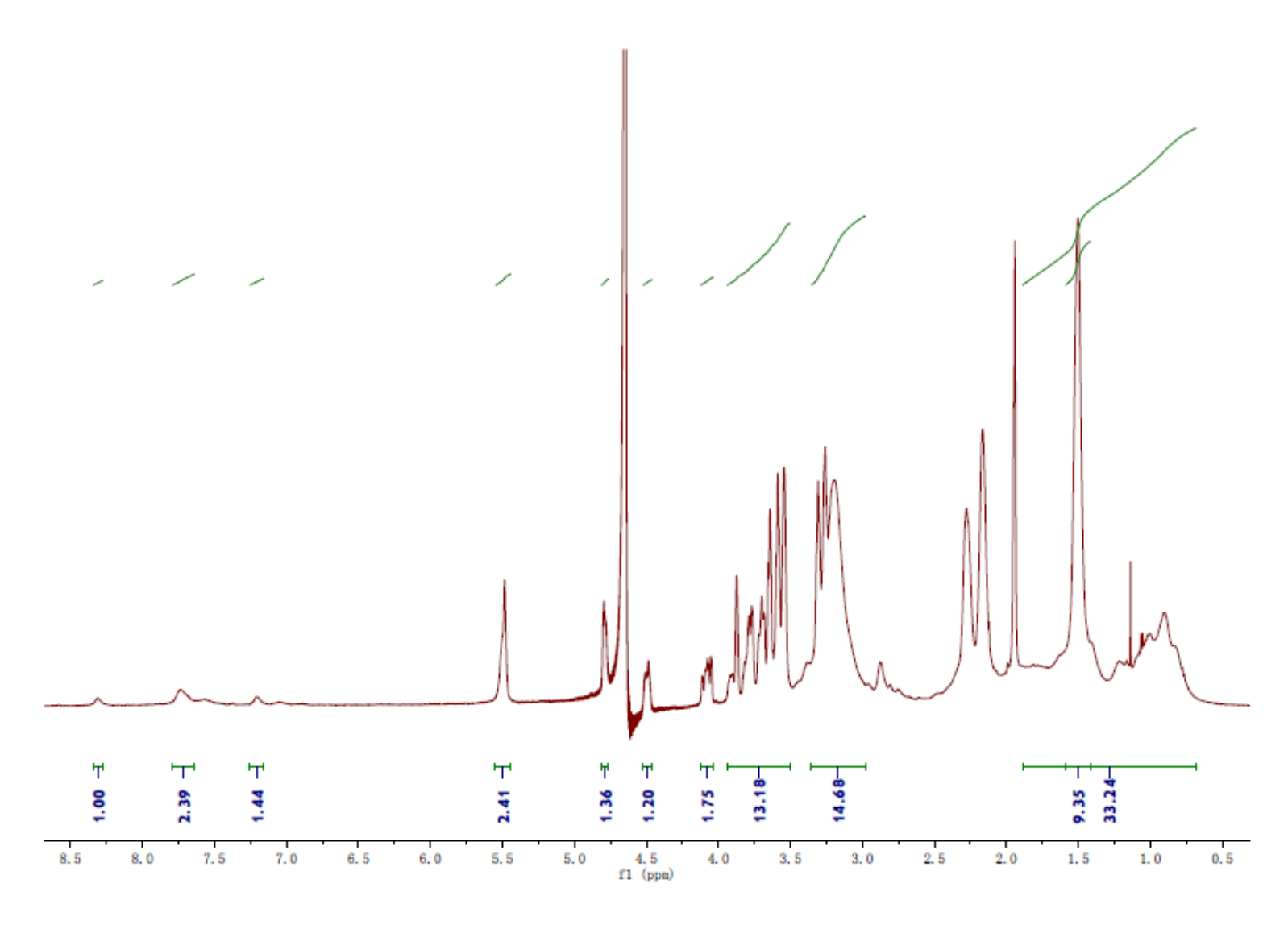


Figure 2.13: 500 MHz (D₂O), ¹H NMR of glycopolymer **26**.

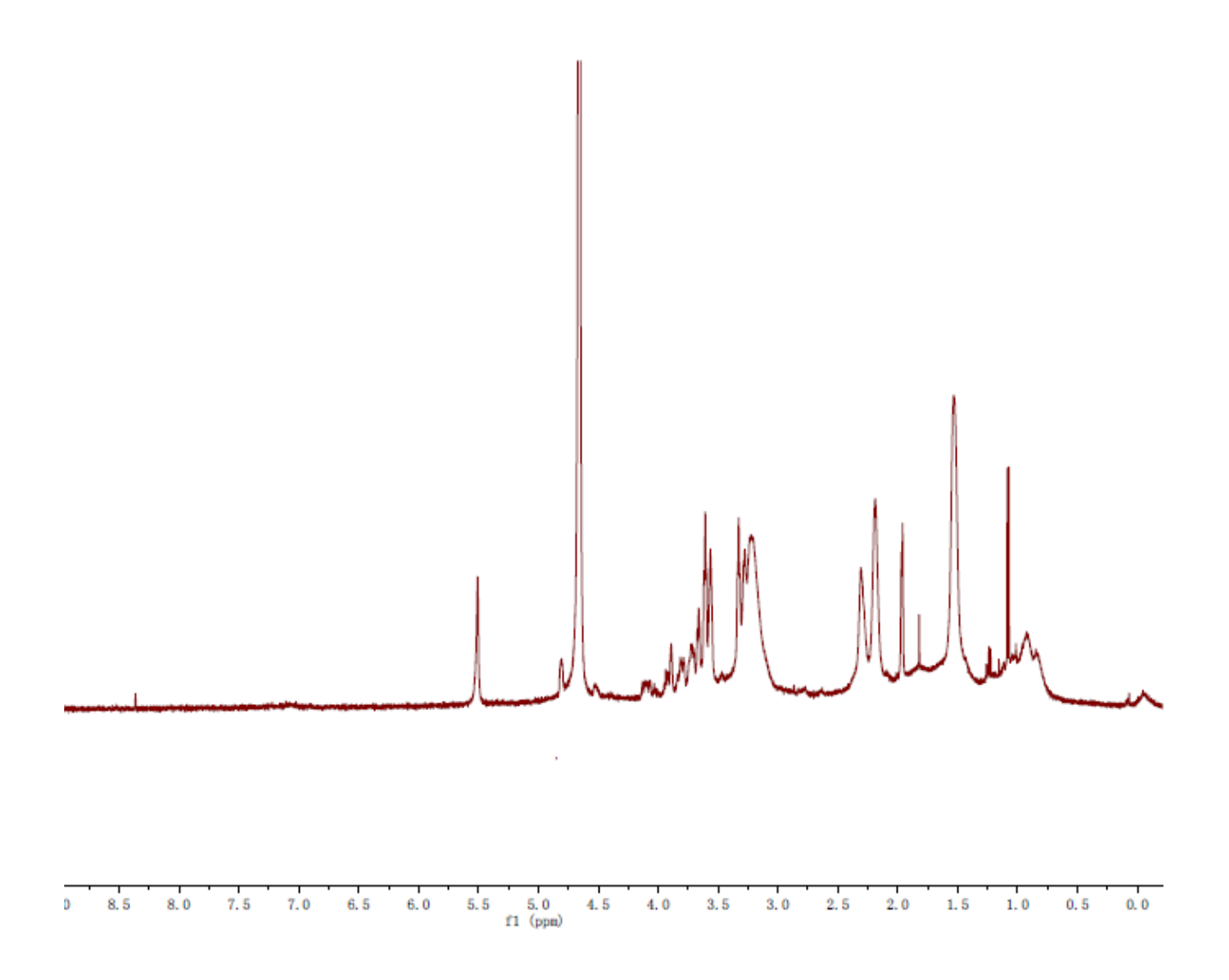


Figure 2.14: 500 MHz (D₂O), ¹H NMR of peptidic glycopolymer 28.

REFERENCES

REFERENCES

- 1. Finn, O. J., Cancer vaccines: between the idea and the reality. *Nat. Rev. Immunol.* 2003, 3, 630-641.
- 2. Hakomori, S., Tumor-associated carbohydrate antigens defining tumor malignancy: basis for development of anti-cancer vaccines. *Adv. Exp. Med. Biol.* 2001, *491*, 369-402.
- 3. Hakomori, S.; Zhang, Y., Glycosphingolipid antigens and cancer therapy. *Chem. Biol.* 1997, 4, 97-104.
- 4. Liu, C.-C.; Ye, X.-S., Carbohydrate-based cancer vaccines: target cancer with sugar bullets. *Glycoconjugate J.* 2012, *29*, 259-271.
- 5. Yin, Z.; Huang, X., Recent development in carbohydrate based anticancer vaccines. *J. Carbohydr. Chem.* 2012, *31*, 143-186 and references cited therein.
- 6. Heimburg-Molinaro, J.; Lum, M.; Vijay, G.; Jain, M.; Almogren, A.; Rittenhouse-Olson, K., Cancer vaccines and carbohydrate epitopes. *Vaccine* 2011, *29*, 8802-8826.
- 7. Morelli, L.; Poletti, L.; Lay, L., Carbohydrates and immunology: synthetic oligosaccharide antigens for vaccine formulation. *Eur. J. Org. Chem.* 2011, 2011, 5723-5777.
- 8. Zhu, J. L.; Warren, J. D.; Danishefsky, S. J., Synthetic carbohydrate-based anticancer vaccines: the Memorial Sloan-Kettering experience. *Expert Rev. Vaccines* 2009, *8*, 1399-1413.
- 9. Guo, Z. W.; Wang, Q. L., Recent development in carbohydrate-based cancer vaccines. *Curr. Opin. Chem. Biol.* 2009, *13*, 608-617.
- 10. Freire, T.; Bay, S.; Vichier-Guerre, S.; Lo-Man, R.; Leclerc, C., Carbohydrate antigens: synthesis aspects and immunological applications in cancer. *Mini-Rev. Med. Chem.* 2006, *6*, 1357-1373.
- 11. Kuberan, B.; Linhardt, R. J., Carbohydrate based vaccines. *Curr. Org. Chem.* 2000, 4, 653-677.
- 12. Galonic, D. P.; Gin, D. Y., Chemical glycosylation in the synthesis of glycoconjugate antitumor vaccines. *Nature* 2007, *446*, 1000-1007.
- 13. Abbas, A. K., Cellular and Molecular Immunology. Seventh ed.; 2011; p 389.
- 14. Gajewski, T. F.; Meng, Y.; Blank, C.; Brown, I.; Kacha, A.; Kline, J.; Harlin, H., Immune resistance orchestrated by the tumor microenvironment. *Immunol. Rev.* 2006, 213, 131-145.

- 15. Acres, B. P., S.; Haegel-Kronenberger, H.; Calmels, B.; Squiban, P., Therapeutic cancer vaccines. *Curr. Opin. Mol. Ther.* 2004, *6*, 40-47.
- 16. Mond, J. J.; Lees, A.; Snapper, C. M., T Cell-independent antigens type 2. *Annu. Rev. Immunol.* 1995, *13*, 655-692.
- 17. Goldsby, R. A.; Kindt, T. J.; Osborne, B. A., Kuby immunology. Freeman: New York, 2000; pp 461-464.
- 18. Holmberg, L. A.; Oparin, D. V.; Gooley, T.; Lilleby, K.; Bensinger, W.; Reddish, M. A.; MacLean, G. D.; Longenecker, B. M.; Sandmaier, B. M., Clinical outcome of breast and ovarian cancer patients treated after high-dose chemotherapy, autologous stem cell rescue and THERATOPE STn-KLH cancer vaccine. *Bone Marrow Transplant.* 2000, 25, 1233-1241.
- 19. Sabbatini, P. J.; Ragupathi, G.; Hood, C.; Aghajanian, C. A.; Juretzka, M.; Iasonos, A.; Hensley, M. L.; Spassova, M. K.; Ouerfelli, O.; Spriggs, D. R.; Tew, W. P.; Konner, J.; Clausen, H.; Abu Rustum, N.; Dansihefsky, S. J.; Livingston, P. O., Pilot study of a heptavalent vaccine-keyhole limpet hemocyanin conjugate plus QS21 in patients with epithelial ovarian, fallopian tube, or peritoneal cancer. *Clin. Cancer Res.* 2007, *13*, 4170-4177.
- 20. Danishefsky, S. J.; Allen, J. R., From the laboratory to the clinic: a retrospective on fully synthetic carbohydrate-based anticancer vaccines. *Angew. Chem. Int. Ed.* 2000, *39*, 836-863.
- 21. Helling, F.; Shang, A.; Calves, M.; Zhang, S.; Ren, S.; Yu, R. K.; Oettgen, H. E.; Livingston, P. O., GD3 vaccines for melanoma: superior immunogenicity of keyhole limpet hemocyanin conjugate vaccines. *Cancer Res.* 1994, *54*, 197-203.
- 22. Hoffmann-Roder, A.; Kaiser, A.; Wagner, S.; Gaidzik, N.; Kowalczyk, D.; Westerlind, U.; Gerlitzki, B.; Schmitt, E.; Kunz, H., Synthetic antitumor vaccines from tetanus toxoid conjugates of MUC1 glycopeptides with the Thomsen-Friedenreich antigen and a fluorine-substituted analogue. *Angew. Chem. Int. Ed.* 2010, *49*, 8498-8503.
- 23. Rich, J. R.; Wakarchuk, W. W.; Bundle, D. R., Chemical and chemoenzymatic synthesis of S-Linked ganglioside analogues and their protein conjugates for use as immunogens. *Chem. Eur. J.* 2006, *12*, 845-858.
- 24. Livingston, P. O.; Wong, G. Y. C.; Adluri, S.; Tao, Y.; Padavan, M.; Parente, R.; Hanlon, C.; Calves, M. J.; Helling, F.; Ritter, G.; Oettgen, H. F.; Old, L. J., Improved survival in stage III melanoma patients with GM2 antibodies: a randomized trial of adjuvant vaccination with GM2 ganglioside. *J. Clin. Oncol.* 1994, *12*, 1036–1044.
- 25. Heegaard, P. M. H.; Boas, U.; Sorensen, N. S., Dendrimers for vaccine and immunostimulatory uses. *Bioconjugate Chem.* 2010, *21*, 405-418.
- 26. Lo-Man, R.; Vichier-Guerre, S.; Perraut, R.; Deriaud, E.; Huteau, V.; BenMohamed,

- L.; Diop, O. M.; Livingston, P. O.; Bay, S.; Leclerc, C., A fully synthetic therapeutic vaccine candidate targeting carcinoma-associated Tn carbohydrate antigen induces tumor-specific antibodies in nonhuman primates. *Cancer Res.* 2004, *64*, 4987-4994.
- 27. Grigalevicius, S.; Chierici, S.; Renaudet, O.; Lo-Man, R.; Deriaud, E.; Leclerc, C.; Dumy, P., Chemoselective assembly and immunological evaluation of multiepitopic glycoconjugates bearing clustered Tn antigen as synthetic anticancer vaccines. *Bioconjugate Chem.* 2005, *16*, 1149-1159.
- 28. Brinas, R. P.; Sundgren, A.; Sahoo, P.; Morey, S.; Rittenhouse-Olson, K.; Wilding, G. E.; Deng, W.; Barchi, J. J., Design and synthesis of multifunctional gold nanoparticles bearing tumor-associated glycopeptide antigens as potential cancer vaccines. *Bioconjugate Chem.* 2012, 23, 1513-1523.
- 29. Ojeda, R.; de Paz, J. L.; Barrientos, A. G.; Martin-Lomas, M.; Penades, S., Preparation of multifunctional glyconanoparticles as a platform for potential carbohydrate-based anticancer vaccines. *Carbohydr. Res.* 2007, *342*, 448-459.
- 30. Lakshminarayanan, V.; Thompson, P.; Wolfert, M. A.; Buskas, T.; Bradley, J. M.; Pathangey, L. B.; Madsen, C. S.; Cohen, P. A.; Gendler, S. J.; Boons, G.-J., Immune recognition of tumor-associated mucin MUC1 is achieved by a fully synthetic aberrantly glycosylated MUC1 triparticle vaccine. *Proc. Natl. Acad. Sci. U.S.A.* 2012, *109*, 261-266.
- 31. Fernandez, L. E.; Alonso, D. F.; Gomez, D. E.; Vazquez, A. M., Ganglioside-based vaccines and anti-idiotype antibodies for active immunotherapy against cancer. *Expert Rev Vaccines* 2003, *2*, 817-823.
- 32. De Silva, R. A.; Wang, Q.; Chidley, T.; Appulage, D. K.; Andreana, P. R., Immunological response from an entirely carbohydrate antigen: design of synthetic vaccines based on Tn-PS A1 conjugates. *J. Am. Chem. Soc.* 2009, *131*, 9622-9623.
- 33. Yin, Z.; Nguyen, H. G.; Chowdhury, S.; Bentley, P.; Bruckman, M. A.; Miermont, A.; Gildersleeve, J. C.; Wang, Q.; Huang, X., Tobacco mosaic virus as a new carrier for tumor associated carbogydrate antigens. *Bioconjugate Chem.* 2012, *23*, 1694-1703.
- 34. Miermont, A.; Barnhill, H.; Strable, E.; Lu, X. W.; Wall, K. A.; Wang, Q.; Finn, M. G.; Huang, X., Cowpea mosaic virus capsid: A promising carrier for the development of carbohydrate based antitumor vaccines. *Chem.-Eur. J.* 2008, *14*, 4939-4947.
- 35. Kagan, E.; Ragupathi, G.; Yi, S. S.; Reis, C. A.; Gildersleeve, J.; Kahne, D.; Clausen, H.; Danishefsky, S. J.; Livingston, P. O., Comparison of antigen constructs and carrier molecules for augmenting the immunogenicity of the monosaccharide epithelial cancer antigen Tn. *Cancer Immunol. Immunother.* 2005, *54*, 424–430.
- 36. Slovin, S. F.; Ragupathi, G.; Musselli, C.; Olkiewicz, K.; Verbel, D.; Kuduk, S. D.; Schwarz, J. B.; Sames, D.; Danishefsky, S.; Livingston, P. O.; Scher, H. I., Fully synthetic carbohydrate-based vaccines in biochemically relapsed prostate cancer: clinical trial results with a-N-acetylgalactosamine-O-serine/threonine conjugate vaccine. *J. Clin.*

- Oncol. 2003, 21, 4292–4298.
- 37. Ragupathi, G.; Coltart, D. M.; Williams, L. J.; Koide, F.; Kagan, E.; Allen, J.; Harris, C.; Glunz, P. W.; Livingston, P. O.; Danishefsky, S. J., On the power of chemical synthesis: immunological evaluation of models for multiantigenic carbohydrate-based cancer vaccines. *Proc. Natl. Acad. Sci. U.S.A.* 2002, *99*, 13699.
- 38. Ragupathi, G.; Koide, F.; Livingston, P. O.; Cho, Y. S.; Endo, A.; Wan, Q.; Spassova, M. K.; Keding, S. J.; Allen, J.; Ouerfelli, O.; Wilson, R. M.; Danishefsky, S. J., Preparation and evaluation of unimolecular pentavalent and hexavalent antigenic constructs targeting prostate and breast cancer: a synthetic route to anticancer vaccine candidates. *J. Am. Chem. Soc.* 2006, *128*, 2715–2725.
- 39. Gendler, S. J.; Lancaster, C. A.; Taylor-Papadimitriou, J.; Duhig, T.; Peat, N.; Burchell, J.; Pemberton, L.; Lalani, E. N.; Wilson, D., Molecular cloning and expression of human tumor-associated polymorphic epithelial mucin. *J. Biol. Chem.* 1990, 265, 15286–15293.
- 40. Becker, T.; Dziadek, S.; Wittrock, S.; Kunz, H., Synthetic glycopeptides from the mucin family as potential tools in cancer immunotherapy. *Curr. Cancer Drug Targets* 2006, *6*, 491-517.
- 41. Hanisch, F. G. N., T., Immunology of O-glycosylated proteins: approaches to the design of a MUC1 glycopeptide-based tumor vaccine. *Curr. Protein Pept. Sci.* 2006, 7, 307–315.
- 42. Gaidzik, N.; Kaiser, A.; Kowalczyk, D.; Westerlind, U.; Gerlitzki, B.; Sinn, H. P.; Schmitt, E.; Kunz, H., Synthetic antitumor vaccines containing MUC1 glycopeptides with two immunodominant domains-induction of a strong immune response against breast tumor tissues. *Angew. Chem. Int. Ed.* 2011, *50*, 9977-9981 and references cited therein.
- 43. Narla, S. N.; Nie, H.; Li, Y.; Sun, X.-L., Recent advances in synthesis and biomedical applications of chain-end functionalized glycopolymers. *J. Carbohydrate Chem.* 2012, 31, 67-92.
- 44. Narain, R., Engineered carbohydrate-based materials for biomedical applications: polymers, surfaces, dendrimers, nanoparticles, and hydrogels. John Wiley & Sons, Inc.: 2011.
- 45. Sun, X.-L.; Faucher, K. M.; Houston, M.; Grande, D.; Chaikof, E. L., Design and synthesis of biotin chain-terminated glycopolymers for surface glycoengineering. *J. Am. Chem. Soc.* 2002, *124*, 7258-7259.
- 46. Suriano, F.; Pratt, R.; Tan, J. P. K.; Wiradharma, N.; Nelson, A.; Yang, Y.-Y.; Dubois, P.; Hedrick, J. L., Synthesis of a family of amphiphilic glycopolymers via controlled ring-opening polymerization of functionalized cyclic carbonates and their application in drug delivery. *Biomaterials* 2010, *31*, 2637-2645.

- 47. Kim, B.; Peppas, N. A., Synthesis and characterization of pH-sensitive glycopolymers for oral drug delivery systems. *J. Biomater. Sci. Polym. Ed.* 2002, *13*, 1271-1281.
- 48. Hudak, J. E.; Canham, S. M.; Bertozzi, C. R., Glycocalyx engineering reveals a Siglec-based mechanism for NK cell immunoevasion. *Nature Chem. Biol.* 2013, *10*, 69-75.
- 49. Wu, L.; Sampson, N. S., Fucose, Mannose, and β-N-Acetylglucosamine Glycopolymers Initiate the Mouse Sperm Acrosome Reaction through Convergent Signaling Pathways. *ACS Chem. Biol.* 2014, *9*, 468-475.
- 50. Parry, A. L.; Clemson, N. A.; Ellis, J.; Bernhard, S. S. R.; Davis, B. G.; Cameron, N. R., 'Mulicopy multivalent' glycopolymer-stabilized gold nanoparticles as potential synthetic cancer vaccines. *J. Am. Chem. Soc.* 2013, *135*, 9362-9365.
- 51. Nuhn, L.; Hartmann, S.; Palitzsch, B.; Gerlitzki, B.; Schmitt, E.; Zentel, R.; Kunz, H., Water-soluble polymers coupled with glycopeptide antigens and T-cell epitopes as potential antitumor vaccines. *Angew. Chem. Int. Ed.* 2013, *52*, 10652-10656.
- 52. Sun, X.-L.; Grande, D.; Baskaran, C.; Hanson, S. R.; Chaikof, E. L., Glycosaminoglycan-mimetic biomaterials. 4. synthesis of sulfated lactose-based glycopolymers that exhibit anticoagulant activity. *Biomacromolecules* 2002, *3*, 1065-1070.
- 53. Baskaran, S.; Grande, D.; Sun, X.-L.; Yayon, A.; Chaikof, E. L., Glycosaminoglycan-mimetic biomaterials. 3. glycopolymers prepared from alkene-derivatized mono- and disaccharide-based glycomonomers. *Bioconjugate Chem.* 2002, *13*, 1309-1313.
- 54. Grande, D.; Baskaran, S.; Chaikof, E. L., Glycosaminoglycan-mimetic biomaterials. 2. alkene- and acrylate-derivatized glycopolymers via cyanoxyl-mediated free-radical polymerization. *Macromolecules* 2001, *34*, 1640-1646.
- 55. Grande, D.; Baskaran, S.; Baskaran, C.; Gnanou, Y.; Chaikof, E. L., Glycosaminoglycan-mimetic biomaterials. 1. nonsulfated and sulfated glycopolymers by cyanoxyl-mediated free-radical polymerization. *Macromolecules* 2000, *33*, 1123-1125.
- 56. Cazet, A.; Julien, S.; Bobowski, M.; Burchell, J.; Delannoy, P., Tumour-associated carbohydrate antigens in breast cancer. *Breast Cancer Res.* 2010, *12*, 204.
- 57. Li, Q.; Anver, M. R.; Butcher, D. O.; Gildersleeve, J. C., Resolving conflicting data on expression of the Tn antigen and implications for clinical trials with cancer vaccines. *Mol. Cancer Ther.* 2009, *8*, 971-979.
- 58. Springer, G. F., T and Tn, general carcinoma autoantigens. *Science* 1984, 224, 1198-1206.
- 59. Buskas, T.; Li, Y.; Boons, G.-J., The immunogenicity of the tumor-associated antigen Lewis^y may be suppressed by a bifunctional cross-linker required for coupling to a carrier

- protein. Chem. Eur. J. 2004, 10, 3517-3524.
- 60. Yin, Z.; Comellas-Aragones, M.; Chowdhury, S.; Bentley, P.; Kaczanowska, K.; BenMohamed, L.; Gildersleeve, J. C.; Finn, M. G.; Huang, X., Boosting immunity to small tumor-associated carbohydrates with bacteriophage Qb capsids. *ACS Chem. Biol.* 2013, 8, 1253-1262.
- 61. Leclerc, C.; Deriaud, E.; Mimic, V.; van der Werf, S., Identification of a T-cell epitope adjacent to neutralization antigenic site 1 of poliovirus type 1. *J. Virol.* 1991, 65, 711-718.
- 62. Deng, K.; Adams, M. M.; Damani, P.; Livingston, P. O.; Ragupathi, G.; Gin, D. Y., Synthesis of QS-21-xylose: establishment of the immunopotentiating activity of synthetic QS-21 adjuvant with a melanoma vaccine. *Angew. Chem. Int. Ed.* 2008, 47, 6395-6398.
- 63. Sad, S.; Gupta, H. M.; Talwar, G. P.; Raghupathy, R., Carrier-induced suppression of the antibody response to a 'self' hapten. *Immunology* 1991, 74, 223-227.
- 64. Di John, D.; Wasserman, S. S.; Torres, J. R.; Cortesia, M. J.; Murillo, J.; Losonsky, G. A.; Herrington, D. A.; Stürcher, D.; Levine, M. M., Effect of priming with carrier on response to conjugate vaccine. *Lancet* 1989, *334*, 1415-1418.
- 65. Herzenberg, L. A.; Tokuhisa, T., Epitope-specific regulation. I. Carrier-specific induction of suppression for IgG antihapten antibody responses. *J. Exp. Med.* 1982, *155*, 1730-1740.
- 66. Nakada, H.; Inoue, M.; Tanaka, N.; Numata, Y.; Kitagawa, H.; Fukui, S.; Yamashina, I., Expression of the Tn antigen on T-lymphoid cell line Jurkat. *Biochem. Biophys. Res. Commun.* 1991, *179*, 762-767.
- 67. Goddard-Borger, E. D.; Stick, R. V., An efficient, inexpensive, and shelf-stable diazotransfer reagent: imidazole-1-sulfonyl azide hydrochloride. *Org. Lett.* 2007, *9*, 3797-3800.
- 68. Koeller, K. M.; Smith, M. E. B.; Wong, C.-H., Chemoenzymatic synthesis of PSGL-1 glycopeptides: sulfation on tyrosine affects glycosyltransferase-catalyzed synthesis of the O-glycan. *Bioorg. Med. Chem.* 2000, *8*, 1017-1025.
- 69. Huang, Y.; Dey, S.; Zhang, X.; Sonnichsen, F.; Garner, P., The α-Helical peptide nucleic acid concept: merger of peptide secondary structure and codified nucleic acid recognition. *J. Am. Chem. Soc.* 2004, *126*, 4626-4640.
- 70. David, O.; Meester, W. J. N.; Bieräugel, H.; Schoemaker, H. E.; Hiemstra, H.; van Maarseveen, J. H., Intramolecular Staudinger ligation: a powerful method to ringclose medium-sized lactams. *Angew. Chem. Int. Ed.* 2003, *42*, 4373-4375.
- 71. Moon, J.-M.; Kim, B.-S.; Choi, Y.-S.; Lee, J.-O.; Nakahara, T.; Yoshinaga, K., Preparation of polymer-coated magnetite fine particles for immunoassay magnetic

marker. Macromol. Res. 2010, 18, 793-799.

CHAPTER 3: Valency and density matter: deciphering impacts of immunogen structures on immune responses against a tumor associated carbohydrate antigen using synthetic glycopolymers

3.1: Introduction

TACAs such as glycolipids and glycoproteins are over-expressed on a wide range of cancers. ¹⁻⁴ Clinical studies have shown that patients with higher levels of naturally generated anti-TACA antibodies are associated with better prognosis. ⁵⁻⁸ Moreover, a monoclonal antibody targeting the glycan structure of ganglioside GD2 has been approved by Food and Drug Administration (FDA) as a first line therapy for pediatric patients with high-risk neuroblastoma validating TACAs as targets for vaccine development. ⁹⁻¹¹ With the increasing appreciation of roles of TACAs, intensive efforts have been dedicated towards TACA based vaccine design. ¹⁻⁴ To facilitate these efforts, a better understanding of how structures of TACA constructs influence antibody generation is much needed.

TACAs elicit humoral responses characteristic of T cell independent (TI) antigens, ¹² which primarily bind to antibody secreting B cells through BCRs. BCRs initiate signaling across the cell membrane leading to either B cell activation or tolerance. ¹³ Antigen requirements for B cell activation and differentiation are complex. ^{12,14-16} Some monovalent antigens such as an ovalbumin peptide and hen egg lysozyme have been shown to be able to activate B cells. ¹⁷⁻¹⁹ For other antigens, multivalent constructs are needed to crosslink multiple BCRs with the number of antigens per construct (valency) needed varying significantly. Using nitro-iodophenol (NIP) as the hapten and polypeptide as the carrier, the Schamel group showed that constructs containing two to three NIPs per peptide could activate NIP specific B cells. ²⁰ The spacing between the antigen (density) was not critical as dimers with NIP on adjacent amino acid residues activated B cells as well as a dimer containing NIPs separated by 24 amino acids. In contrast, Dintzis and coworkers showed

with fluorescein or dinitrophenyl haptens, the constructs must exceed molecular mass of 100 kDa and 20 haptens per chain for induction of antibody secretion. Above these threshold values, higher valency (126 antigens per chain) led to continual increase of B cell responses. Using dinitrophenyl bearing ring-opening metathesis polymers, the Kiessling group showed that low valency polymer (10 mer) could activate B cells, although the high valency (500 mer) construct was much more effective in antibody induction. These meticulous studies suggest the valency needed for B cell activation and antibody production is highly antigen dependent.

Compared to foreign TI antigens such as NIP and dinitrophenyl, the generation of TACA-specific antibody responses poses additional challenges. As they are self-antigens, most high affinity TACA specific B cells undergo cell death during conventional B cell development, resulting in limited frequency and functionality of these cells. Therefore, it is desirable to increase TACA specific B cell numbers and titers of anti-TACA antibodies through interactions with vaccine constructs.

Herein, to better understand how structures of TACA constructs impact B cell functions, we prepared a set of systematically varied synthetic glycopolymers. The antigen valency and density of the constructs were found to significantly influence antibody generation. Decoding the key parameters eliciting TACA specific B cell activation vs non-responsiveness can have important implications for the establishment of effective TACA based anti-cancer vaccines.

3.2: Results and discussion

3.2.1: Design, synthesis and characterization of glycopolymers

Our studies commenced from the synthesis of glycopolymers bearing the TACA Tn antigen, which has been found over-expressed on breast and prostate cancer cells and is an attractive target for vaccine development. To probe the size requirement of vaccine constructs, PAAs with various molecular weights were prepared. PAA 4 was synthesized via CMFRP (Scheme 3.1a). The polymerization was initiated by the treatment of *p*-nitro aniline 1 with sodium nitrite and fluoroboric acid, which was followed by the addition of a mixture of sodium cyanate and acrylic acid 3 and heating at 70 °C. GPC analysis showed that polymer 4 has a Mn of 13 kDa with a PDI of 1.22.

a) NaNO₂, 50% HBF₄, H₂O/THF (1:1)
$$O_2N$$
 O_2N $O_$

Scheme 3.1: Synthesis of glycopolymers.

To obtain longer polymer chains, ATRP was utilized. To a mixture of the initiator methyl 2-bromopropionate **6** and monomer ^tbutyl acrylate **7** were added the catalysts CuBr,

CuBr₂ and ligand *N*,*N*,*N'*,*N'*,*N''*,*N''*, Pentamethyldiethylenetriamine (PMDETA).²⁹ The reaction mixture was stirred at 60 °C until the polymerization was complete. After purification through silica gel chromatography and selective precipitation, the polymer was treated with trifluoroacetic acid (TFA) to cleave the 'butyl esters producing polymer 8 in 85% overall yield with an average molecular weight of 46 kDa (PDI: 1.57) (Scheme 3.1b). To obtain longer polymers, high molecular weight PAA was carefully fractionated by size exclusion chromatography (SEC) leading to polymers with average molecular weights of 100 kDa (PDI: 1.62), 250 kDa (PDI: 1.64) and 450 kDa (PDI: 1.64).

To produce the glycopolymers, the amine bearing Tn antigen 5³⁰ was covalently linked with polymer 4 through amide bonds as promoted by TSTU and DIPEA (**Scheme 3.1a**). Glycan analysis showed that this glycopolymer contained on average 4 Tn molecules per chain (designated as 13k-4) (**Table 3.1**). In a similar manner, Tn was introduced into other polymer backbones. By varying the amounts of Tn utilized in the amidation reactions, the number of Tn per polymer chain was controlled leading to a set of glycopolymers (**Table 3.1**). Polymers 450k-4, 450k-6, 450k-10, 450k-40, 450k-60, 450k-80 and 450k-115 have 450 kDa backbones bearing 4, 6, 10, 40, 60, 80 and 115 Tn respectively. Polymers 46k-40, 100k-40 and 250k-40 all contain an average 40 Tn per chain with backbone molecular weights of 46, 100 and 250 kDa. It was difficult to introduce 40 copies of Tn per chain into the 13 kDa polymer presumably due to steric hindrance. Glycopolymers 13k-10 and 100k-10 were also synthesized using the 13 kDa and 100 kDa polymers respectively. The polymer and glycopolymer were biocompatible with little toxicities to cells as determined by cell viability assays (**Figure 3.5**).

Abbreviation	Backbone MW	Average number
	(kDa)	of Tn per chain
13k	13	0
13k-4	13	4
13k-10	13	10
46k	46	0
46k-40	46	40
100k	100	0
100k-10	100	10
100k-40	100	40
250k	250	0
250k-40	250	40
450k	450	0
450k-4	450	4
450k-6	450	6
450k-10	450	10
450k-40	450	40
450k-60	450	60
450k-80	450	80
450k-115	450	115

 Table 3.1: Polymers and glycopolymers synthesized for the current study.

3.2.2: Tn specific B cell detection by enzyme-linked immunospot assay (ELISPOT) and flow cytometry

With the glycopolymers in hand, their abilities to elicit anti-Tn antibodies were first evaluated *in vitro*. The various glycopolymers as well as control polymers lacking the Tn antigen were incubated individually with naïve B cells freshly isolated from mouse spleens at several different concentrations for four days. If the binding of glycopolymers activated the B cells, the anti-Tn B cells would proliferate and/or differentiate to produce Tn-specific antibodies. The increase in the number of Tn specific antibody-secreting B cells (ASC) could be detected through an ELISPOT assay using ELISPOT plates coated with a BSA-Tn conjugate.³¹

Within the series of glycopolymers with 450kDa backbone, an interesting dependence of the number of Tn specific ASCs generated on antigen valency was observed (Figure 3.1). The 450k-4 and 450k-6 glycopolymers were inactive (Figures 3.1a,b) with 450k-10 being the one with the lowest copies of Tn per chain inducing significant antibody production (Figure 3.1c). With 450k-10, a bell-shaped dose dependent response was detected. The number of Tn specific ASCs increased with the dose of the antigen until a maximum of 56 cells per well was observed at 2.1 µM of Tn, which was followed by a decrease at higher dose of Tn. In comparison, wells containing cells treated with the control polymer at all concentrations gave no more than 2 positive spots. This suggested that the PAA polymer itself did not non-specifically stimulate antibody production.

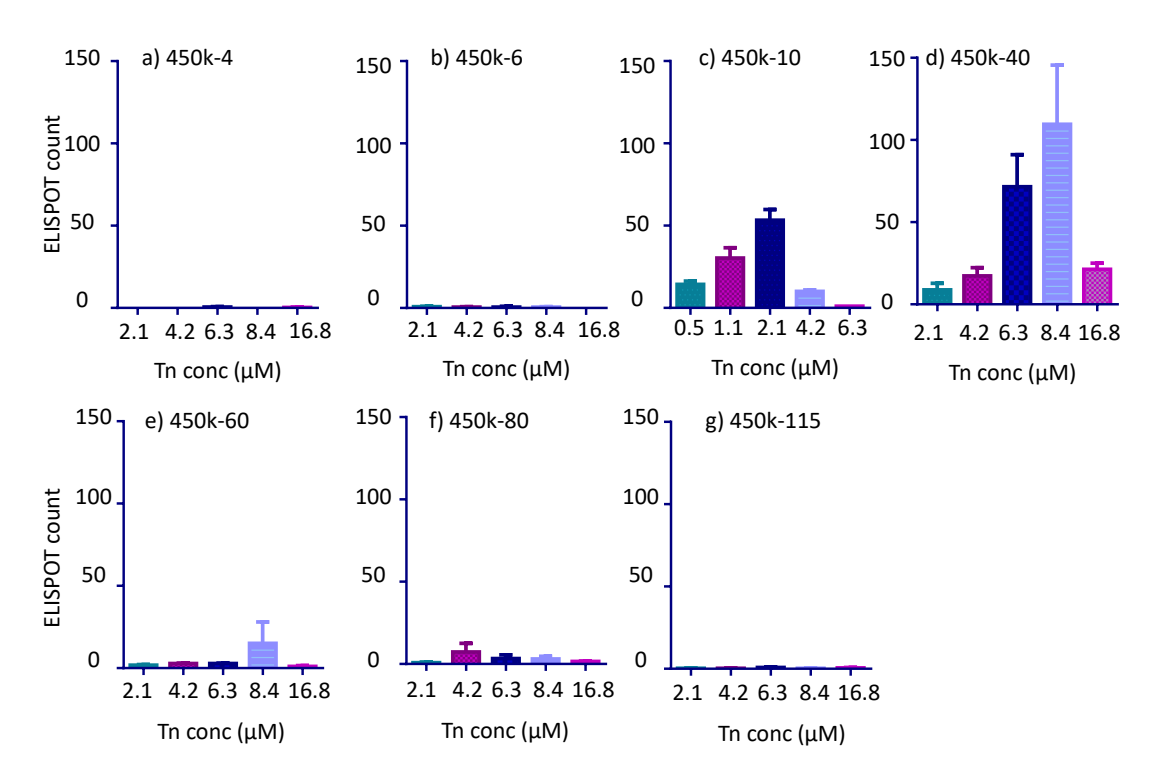


Figure 3.1: ELISPOT results of anti-Tn B cells treated with the following glycopolymers with 450kDa backbones: a) 450k-4; b) 450k-6; c) 450k-10; d) 450k-40; e) 450k-60; f) 450k-80; and g) 450k-115.

Increasing the number of Tn per 450k polymer chain from 10 to 40 led to significant enhancement of the number of spots in ELISPOT. The highest number in ASC (109 per well) was observed with 450k-40 polymer at 8.4 μM of Tn (**Figure 3.1d**), which contained the same number of polymer chain as 450k-10 glycopolymer at Tn concentration of 2.1 μM. Further increases of the valency to 60 or above led to declines in the number of antibody secreting B cells with 450k-115 giving few Tn positive spots (< 3) (**Figures 3.1e-g**).

The percentages of Tn specific cells in the B cell pool were quantified using flow cytometry. Following incubation with various glycopolymers, B cells were labeled with a BSA-Tn conjugate bearing Alexa Fluor 647. Consistent with ELISPOT results, B cells incubated with the 450k-40 glycopolymer at 8.4 µM Tn concentration gave the highest percentage of Tn specific cells, suggesting proliferation had occurred (**Table 3.2**. For

statistical analysis results, see **Figure 3.2**). The flow cytometry results correlated well with the trend observed in ELISPOT, which confirms that for high B cell proliferation and ASC differentiation, it is desirable to have valency of the glycopolymers around 40.

Polymer	Tn concentration (μM)	Percentage of Tn- specific B cells by flow cytometry	ELISPOT count
450k	0	1.0	1
450k-6	2.1	1.2	2
450k-10	1.05	3.2	30
	2.1	3.8	56
450k-40	6.3	4.4	71
	8.4	5.4	109
450k-60	8.4	2.6	15
450k-80	4.2	1.6	7
450k-115	6.3	1.3	1

Table 3.2: Summary of ELISPOT and flow cytometry results of 450kDa glycopolymer treated spleen cells. Flow cytometry data are the average of a minimum of three independent experiments (n≥3). The statistical analysis results are presented in **Figure 3.2**.

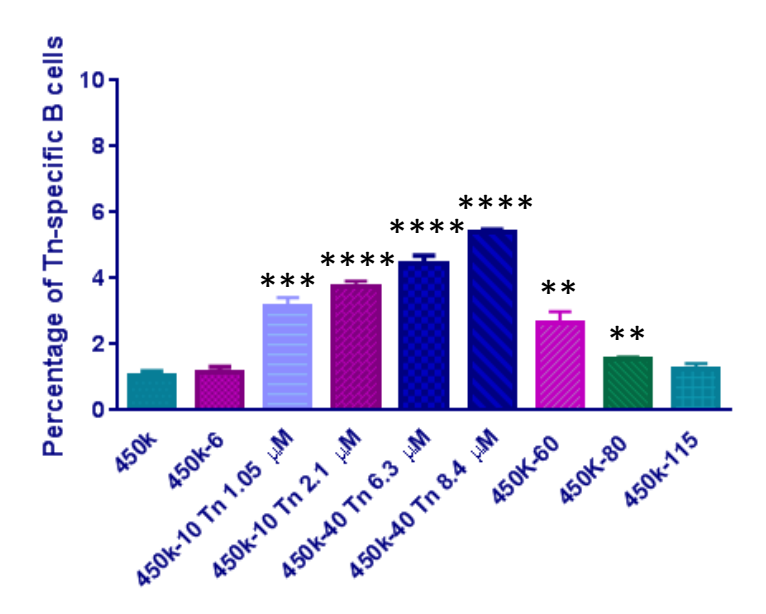


Figure 3.2: Percentage of Tn-specific splenic B cells upon incubation with 450k, 450k-6 (Tn 2.1 μM), 450k-10 (Tn 1.05 μM, 2.1 μM), 450k-40 (Tn 6.3 μM, 8.4 μM), 450k-60 (Tn 8.4 μM), 450k-80 (Tn 4.2 μM), 450k-115 (Tn 6.3 μM) as determined by FACS analysis. Statistical analysis was performed using Student's t test. *** p = 0.0002 450k-10 Tn 1.05 μM vs. 450k; **** p < 0.0001 450k-10 Tn 1.05 μM, 450k-10 Tn 2.1 μM, 450k-40 Tn 6.3 μM, 450k-40 Tn 8.4 μM vs. 450k; *** p < 0.005 450k-60, 450k-80 vs. 450k.

To better understand the origin of differential antibody induction by the glycopolymers, the hydrodynamic radii and zeta potential of the glycopolymers were measured. As shown in **Table 3.3a**, the 450k polymer as well as all glycopolymers bearing the 450 kDa backbone had similar hydrodynamic diameters (~ 34 nm) and zeta potential (~ -2.5 mV) in cell culture media. Furthermore, the glycopolymers with various valency were all readily soluble in water. Similar hydrodynamic diameters of the glycopolymers were observed at multiple concentrations (**Table 3.3b**). This can be explained as the 450 kDa polymer on average contained over 6,000 carboxylic acid moieties, derivatization of a small percentage (<2%) of those with water soluble Tn antigen did not drastically alter the glycopolymers' physical properties such as surface charge, size and aqueous solubility. Thus, changes of the abilities to generate antibody responses by various 450k

glycopolymers could most likely be attributed to the inherent requirements of Tn-BCR interactions.

a

Polymer	Hydrodynamic diameter (nm)	Zeta potential (mV)
450k	34	-2.9
450k-10	34	-2.5
450k-40	33	-2.6
450k-60	32	-2.3
450k-80	35	-2.3
450k-115	31	-2.2

b

Tn concentration	Hydrodynamic diameter (nm)	
(μΜ)	450k-80	450k-115
16.8	35	31
8.4	35	32
4.2	34	32

Table 3.3: a) Summary of hydrodynamic diameters and zeta potential of glycopolymers bearing 450kDa backbones in cell culture media as measured by dynamic light scattering (DLS). b) Hydrodynamic diameters of 450k-80 and 450k-115 glycopolymers at various concentrations. These similar hydrodynamic diameter and zeta potential values suggested that these glycopolymers had similar physical properties and there were no aggregations under the experimental conditions.

The antibody generation abilities of 450k glycopolymers decreased with valency higher than 40. It is known that hypercrosslinking of BCRs can result in B cell tolerance and apoptosis. To test this possibility, the percentages of apoptotic splenic Tn-specific B cells following incubation with 450k-40, 450k-80 and 450k-115 respectively were analyzed. There were significantly higher proportions of cells undergoing apoptosis following incubations with 450k-80 and 450k-115 glycopolymers compared to those with the 450k-40 glycopolymer (**Figure 3.3a**). In comparison, the percentages of apoptotic cells in overall B cell pool were similar upon treatments of the three glycopolymers (**Figure 3.3b**). Therefore, the super high valency of glycopolymers leads to BCR hypercrosslinking resulting in selective apoptosis of Tn specific B cells. This trend is in contrast to polymers bearing dinitrophenyl haptens, where high valency polymers (100-500 mer) have equal or higher activities in B cell activation. This dichotomy is possibly due to the different antigen structures.

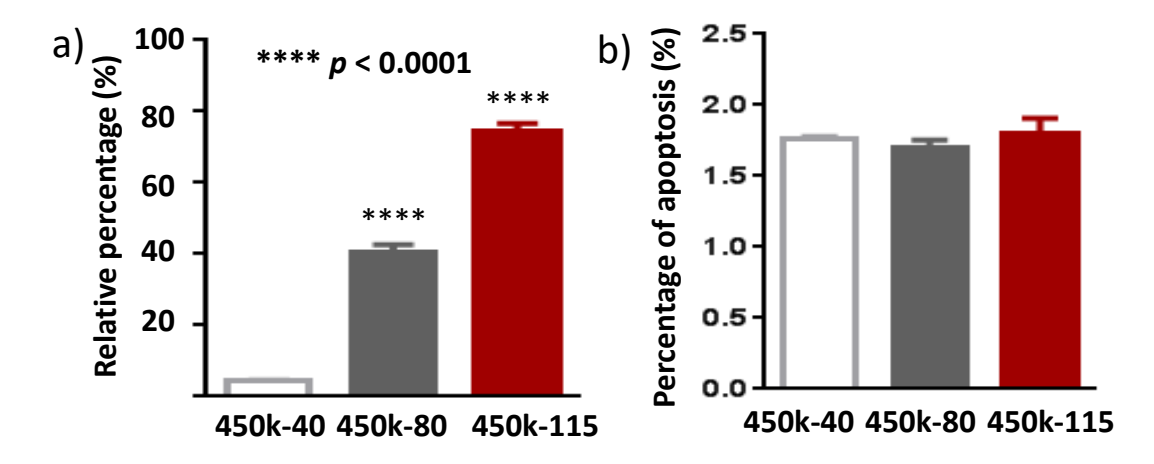


Figure 3.3: a) Percentages of Tn specific apoptotic B cells upon incubation with 450k-40, 450k-80 or 450k-115 glycopolymers. The percentages were calculated by dividing the numbers of Tn-specific apoptotic B cells by the total number of Tn specific B cells as determined by flow cytometry. Statistical analysis was performed using Student's t test with *p* values obtained by comparing with cells incubated with the 450k-40 glycopolymer. Glycopolymers with valency higher than 40 induced more apoptosis of Tn specific B cells. b) Percentages of apoptotic cells in the overall B cell pools upon incubation with 450k-40, 450k-80 or 450k-115 glycopolymers showing no significant differences in overall B cell apoptosis. This suggests the apoptosis induction by higher valency glycopolymers was specific to Tn.

With the ability of 450k-40 glycopolymer to elicit B cell activation established, we examined the effects of antigen density of glycopolymer on cellular activation. The role of antigen density has been investigated using scaffolds such as proteins or virus like particles by varying the average number of epitopes attached. The prior approaches, however, simultaneously alter antigen valency, which complicates analysis. The polymer platform enables us to probe the density effect while maintaining the same valency. The abilities of glycopolymers 450k-40, 250k-40, 100k-40 and 46k-40 to activate B cells were compared. As the molecular weight of the glycopolymer backbone decreased, the number of Tn specific ASCs also decreased as determined by ELISPOT (Figures 3.1d and 3.4a-c). While 46k-40 could induce anti-Tn antibodies (Figure 3.4c), the highest average number of ASCs

per ELISPOT well was ~20% of those induced by the 450k-40 glycopolymer.

With the lower molecular weight polymers such as 46k-40, the Tn would be more densely packed with smaller inter-residue distances as compared to 450k-40. In a completely extended conformation of the 46k-40 polymer, the average spacing between the Tn antigen is around 3 nm assuming ideal sp³ hybridization of polymer backbone carbon atoms and C-C bond length of 0.15 nm. The Y shaped BCR is approximately 10 nm wide.³6 Thus, the Tn molecules in the 46k-40 glycopolymer are presumably too close together for effective clustering of BCRs for potent B cell activation. A similar conclusion could be drawn from the comparison of the ELISPOT results from 13k-10 glycopolymer with those from 100k-10 glycopolymer (**Figures 3.4e** vs **3.4f**). These steric crowding effects have been observed in study of self-assembled monolayer of glycans where enzymes and lectins actually bound more weakly to surfaces with higher glycan densities.³7-38

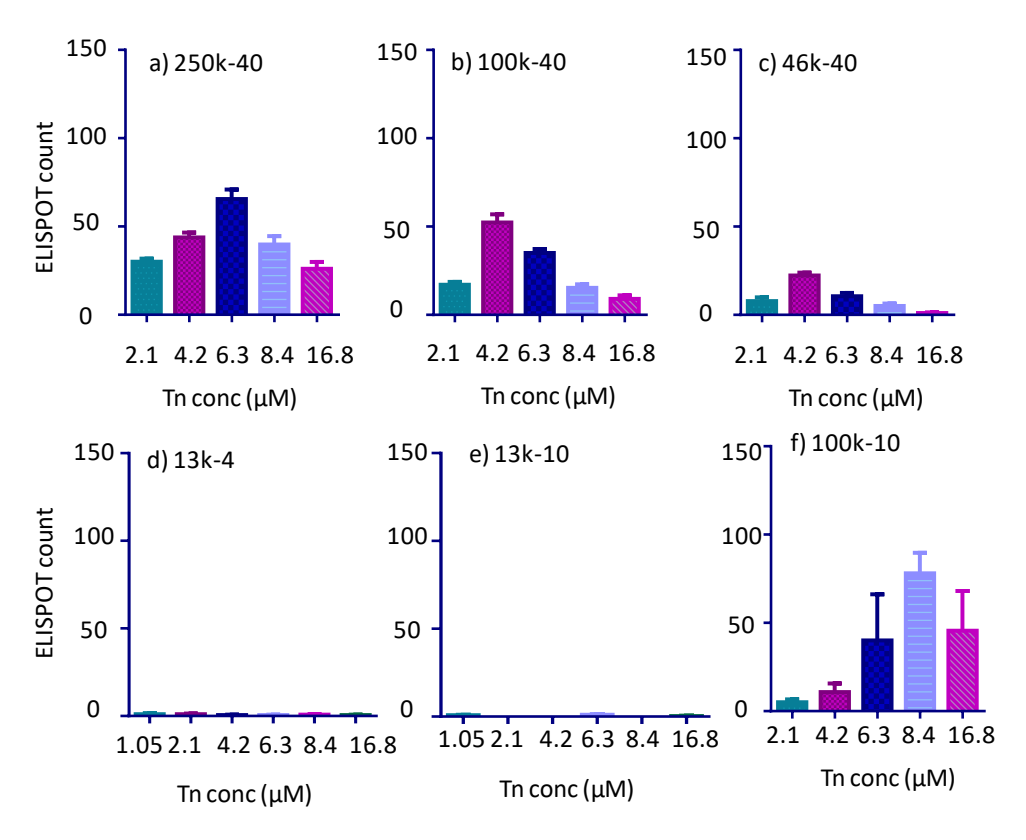


Figure 3.4: ELISPOT of B cells incubated with a) 250k-40, b) 100k-40, c) 46k-40; d) 13k-4; e) 13k-10; and f) 100k-10 at varying Tn concentrations.

Besides antigen density, valency is also crucial in B cell activation and antibody induction. The 100k-40 and 13k-4 glycopolymers have similar Tn spacing. Yet the longer 100k-40 polymer was able to activate B cells with medium activities, while cells incubated with the 13k-4 glycopolymer did not produce antibodies at all (Figures 3.4b vs 3.4d). This indicates despite the suitable Tn density in 13k-4, its valency may be too low and presumably could not cluster sufficient number of BCRs to activate B cells for antibody production. The 100k-10 polymer, which elicited ASCs, has similar Tn density as 450k-40 (Figures 3.4f vs 3.1d). Coupled with the observations that 450k-10 glycopolymer but not 450k-4 and 450k-6 could induce antibodies (Figures 3.1a-c), these results suggest the threshold valency would be more than 6 glycans per chain. The optimum antigen spacing is

around 24 nm in an extended conformation (calculated based on 100k-10 and 450k-40 polymers).

The glycopolymer representatives 450k and 450k-40 were picked to test their cell cytotoxicity. After incubation with different concentration of polymers, cell viability was pretty high indicating little cytotoxicity of the glycopolymers to cells in vitro (**Figure 3.5**).

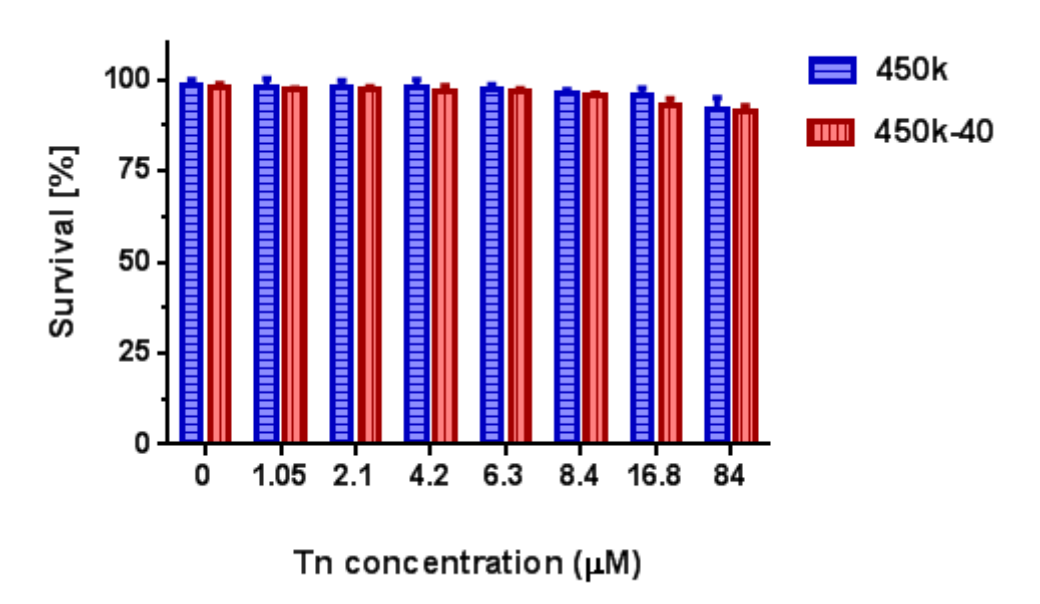


Figure 3.5: Viability of EA.hy 926 cells upon incubation with various concentrations of 450k-40 polymer and 450k polymer (the same polymer concentration as 450k-40) for 48 hours. The cell viability was determined by the CytoTox 96 Non-radioactive cytotoxicity assay.

3.2.3: Early B cell activation events induced by different glycopolymers

To better understand B cell activation by glycopolymers, confocal microscopy studies were performed. Splenic B cells were treated with 450k-40, 450k-80 or 450k with no Tn. Rhodamine-anti-IgM μ chain specific F(ab') and FITC-cholera toxin B subunit were used to label BCR and GM1 (a marker for lipid microdomains) respectively. Both untreated

cells and 450k polymer treated cells showed evenly distributed BCRs and GM1 across the cell surface indicating the lack of BCR clustering (**Figure 3.6a,b**). In contrast, cells incubated with 450k-40 and 450k-80 had a polarized distribution of BCR, which colocalized well with GM1 (**Figure 3.6c,d**). This suggests that glycopolymers could induce aggregation of BCRs, resulting in BCR patches enriched in GM1 rich lipid microdomains.^{24,39-41} These events contribute to the initial signals for B cell activation. The reduced responses at high doses of the glycopolymers observed in ELISPOT assay (**Figures 3.1c-e**) could be explained by the need to cluster multiple BCRs for B cell activation. Too much glycopolymer could compete for BCR binding and decrease the number of BCRs clustered in each complex.

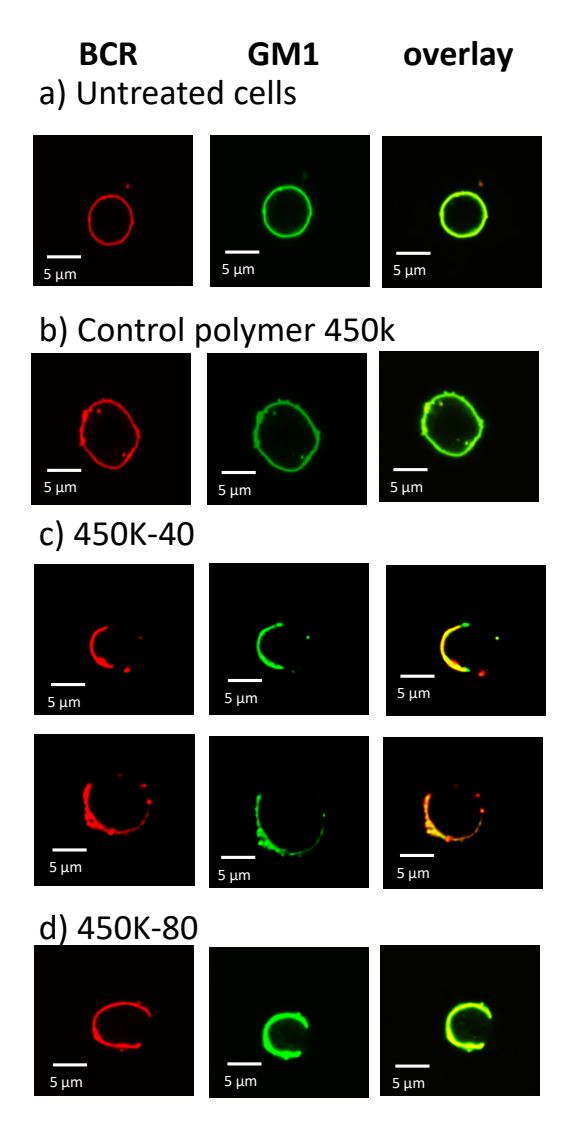


Figure 3.6: Confocal microscopy images of (a) untreated B cells; B cells incubated with (b) the control polymer 450k; (c) 450k-40 (Tn 8.4 μ M); and (d) 450k-80 (Tn 4.2 μ M). BCRs were stained red with rhodamine-anti-IgM μ chain specific F (ab') and GM1 was stained green with FITC-cholera toxin B subunit. Yellow color in the overlay images suggests the colocalization of BCR with GM1.

Ca²⁺ flux is another early event in B cell activation.¹³ The binding of antigens to BCRs triggers phosphorylation of tyrosine kinases, ultimately resulting in production of the second messenger 1,4,5-inositol triphosphate (IP₃) and the release of Ca²⁺ to cytosol from the endoplasmic reticulum.⁴²⁻⁴³ Subsequent activation of store-operated calcium entry supports sustained increases of intracellular calcium necessary for optimal B cell activation. Fluo-4 NW calcium assay was performed to compare the abilities of glycopolymers 450k-40 and the control polymer 450k to elicit calcium flux to the cytosol. Incubation with the control polymer was not able to induce much Ca²⁺ response while strong Ca²⁺ flux was observed in cells incubated with 450k-40 (**Figure 3.7**). When B cells were incubated with 450k-40 for 30 hours and subsequently stimulated again with the same glycopolymer, a more pronounced Ca²⁺ flux was observed suggesting prior exposure of B cells to the glycopolymers could lead to stronger activation of the cells.

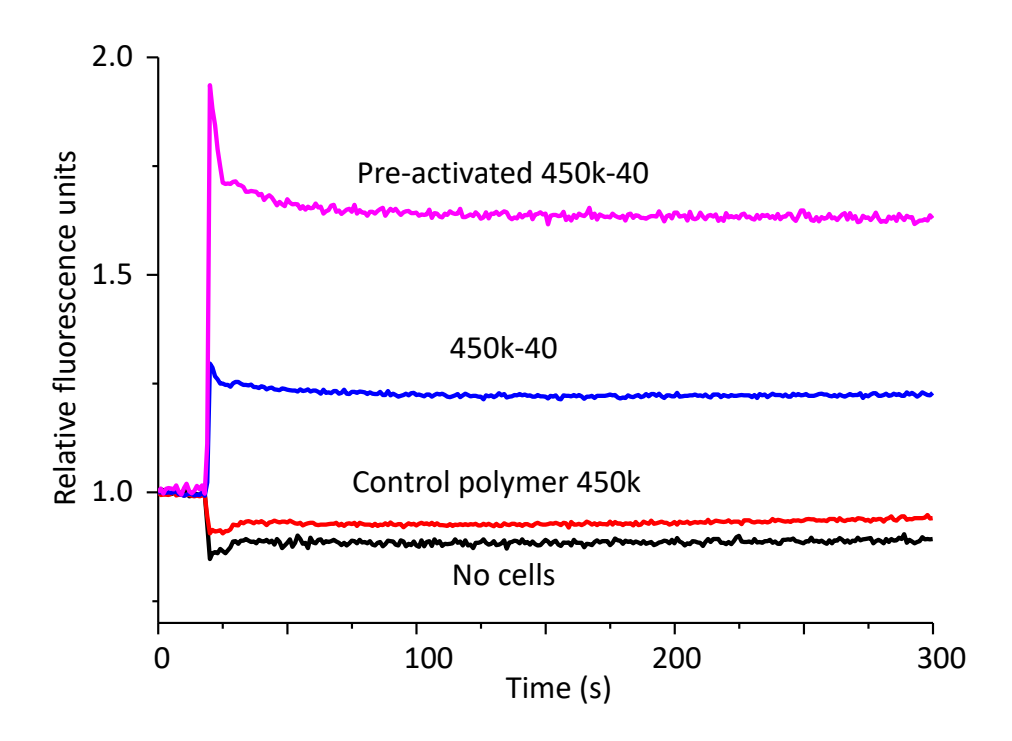


Figure 3.7: Calcium flux of no cells; naïve B cells incubated with 450k polymer; naïve B cells incubated with 450k-40 glycopolymer, and B cells pre-activated with 450k-40 (Tn 8.4 μ M) glycopolymer incubated subsequently with 450k-40 as detected by the fluo-4 NW dye.

CD69 is known as an activation inducer molecule,⁴⁴ whose expression is an indicator of leukocyte activation.⁴⁵ CD86 is another cell surface marker for activated B cells that play important signaling roles.⁴⁶ Naïve mouse B cells were treated with either control polymer or 450k-40 and the levels of CD69 and CD86 expression were analyzed by flow cytometry (**Figure 3.8**). The 450k-40 group showed much enhanced expression of CD69 and CD86 as compared with the control group. The combined results on induction of BCR aggregation, increase of Ca²⁺ flux and upregulation of CD69/CD86 confirm the abilities of 450k-40 glycopolymer to activate B cells.

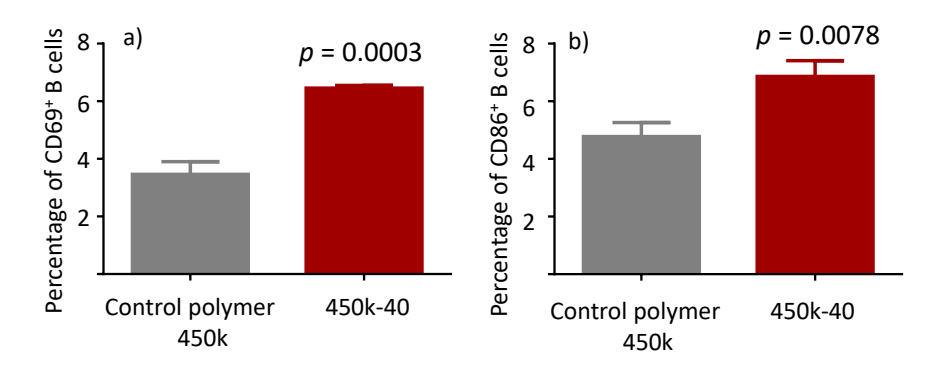


Figure 3.8: Percentages of (a) CD69⁺ or (b) CD86⁺ B cells incubated with either control polymer 450k or 450k-40 as determined by flow cytometry. Higher percentages of cells treated with 450k-40 are CD69 and CD86 positive. Statistical analysis was performed using Student's t test.

3.2.4: *In vivo* studies

With B cell activation by 450k-40 glycopolymer established *in vitro*, abilities of this glycopolymer to induce antibodies were evaluated *in vivo*. The kinetics of IgM antibody generation and optimum dose were investigated first. Mice were immunized with glycopolymer 450k-40 at 4 µg Tn level and sera were obtained from mice 2, 4 and 8 days post inoculation. The amounts of anti-Tn IgM antibodies were determined via ELISA with day 4 sera giving highest average antibody titers (**Figure 3.9a**). Mice were then inoculated with 450k-40 at 1, 4 and 7 µg of Tn dose respectively. The highest IgM titers were obtained at the 4 µg of Tn (**Figure 3.9b**).

The abilities of 450k polymer and various glycopolymers (all at 4 µg of Tn doses) to induce anti-Tn antibodies were compared next *in vivo*. Consistent with *in vitro* results (**Figure 3.1**), 450k-40 was able to generate significantly more anti-Tn IgM antibodies than all other glycopolymers as well as the control polymer, and the 100k-40 glycopolymer was more potent than 13k-4 (**Figure 3.9c**). Spleen cells were harvested from 450k-40

immunized mice and analyzed by ELISPOT. Higher numbers of ASCs were detected in immunized mice further confirming the ability of glycopolymer 450k-40 in inducing the activation of Tn-specific B cells *in vivo* (**Figure 3.9d**).

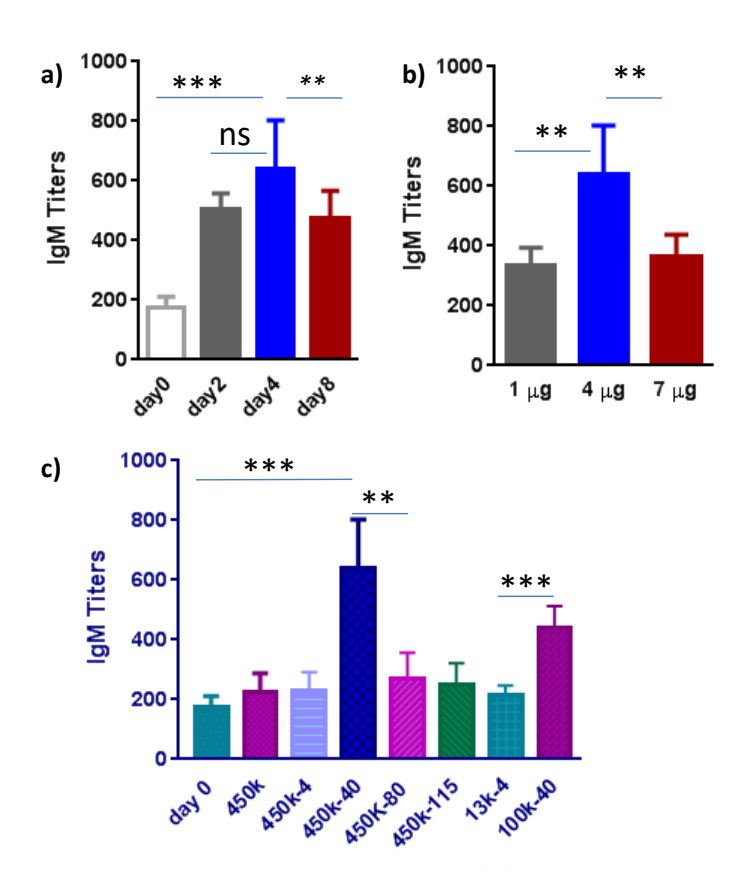
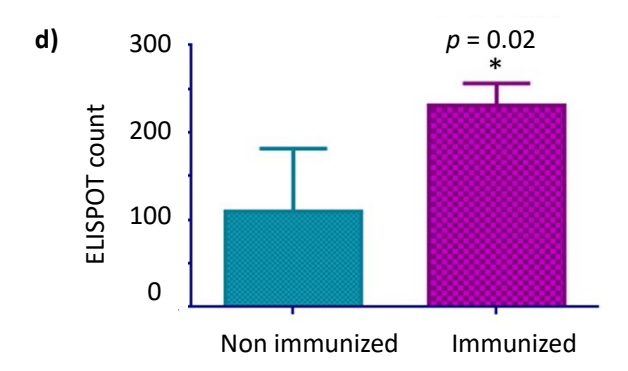


Figure 3.9: (a) Anti-Tn IgM titers of mice vaccinated with 450k-40 glycopolymer (Tn 4 μg), prior to immunization (day 0), 2, 4 and 8 days post immunization (Statistical analysis was performed using Student's t test. ns = nonsignificant; ** p < 0.01). The average IgM titers were highest at day 4; (b) Anti-Tn IgM titers of mice vaccinated with 450k-40 glycopolymer at doses of 1, 4 and 7 μg of Tn (Statistical analysis was performed using Student's t test. ** < 0.01). Blood was collected on day 4 after immunization. 4 μg Tn dose gave the highest average IgM titers; (c) Anti-Tn IgM titers of mice vaccinated with 450k polymer and various glycopolymers (Tn 4 μg) at day 4 after immunization. Consistent with *in vitro* results, 100k-40 and 450k-40 gave the highest average titers (Statistical analysis was performed using Student's t test. The p value for 450k-40 vs day 0 is *** p = 0.0002, vs 450k-80 is ** 0.002; The p value for 100k-40 vs 13k-4 is *** p = 0.0002). (d) ELISPOT of spleen cells (8 x 10⁵ cells per well) from non-immunized and 450k-40 immunized mice upon incubation with 450k-40 (Tn 8.4 μM) glycopolymer. Statistical analysis was performed using Student's t test (* p = 0.02).

Figure 3.9 (cont'd)



3.2.5: B cell tolerance

It is known that ligand binding to B cells can induce either activation or tolerance. 13,47 While 13k-4 could not activate ASCs (**Figures 3.4d and 3.9c**), its impact on ASC activation and antibody generation by 450k-40 glycopolymer was examined *in vitro* and *in vivo*. Spleen B cells were incubated with 450k-40 polymer at 8.4 μM Tn concentration in the presence of vary concentrations of 13k-4 glycopolymers for 4 days and subjected to ELISPOT assay. 13k-4 at 2.1 μM Tn reduced the number of ASCs by more than 60% (**Figure 3.10a**). With increasing concentrations of 13k-4 polymer, the number of Tn specific ASCs decreased further. In comparison, 13k-4 glycopolymer did not have any effects on ASC generation against another antigen, wheat germ agglutinin (**Figure 3.10b**). This suggests the 13k-4 glycopolymer selectively induced non-responsiveness of Tn specific B cells. The suppressive effect of 13k-4 was confirmed *in vivo*. Co-administration of 13-4 with 450-40 glycopolymer into mice reduced the titers of anti-Tn IgM antibodies at both 4 and 8 days post immunization despite the increase in total amounts of Tn

administered (Figure 3.10c).

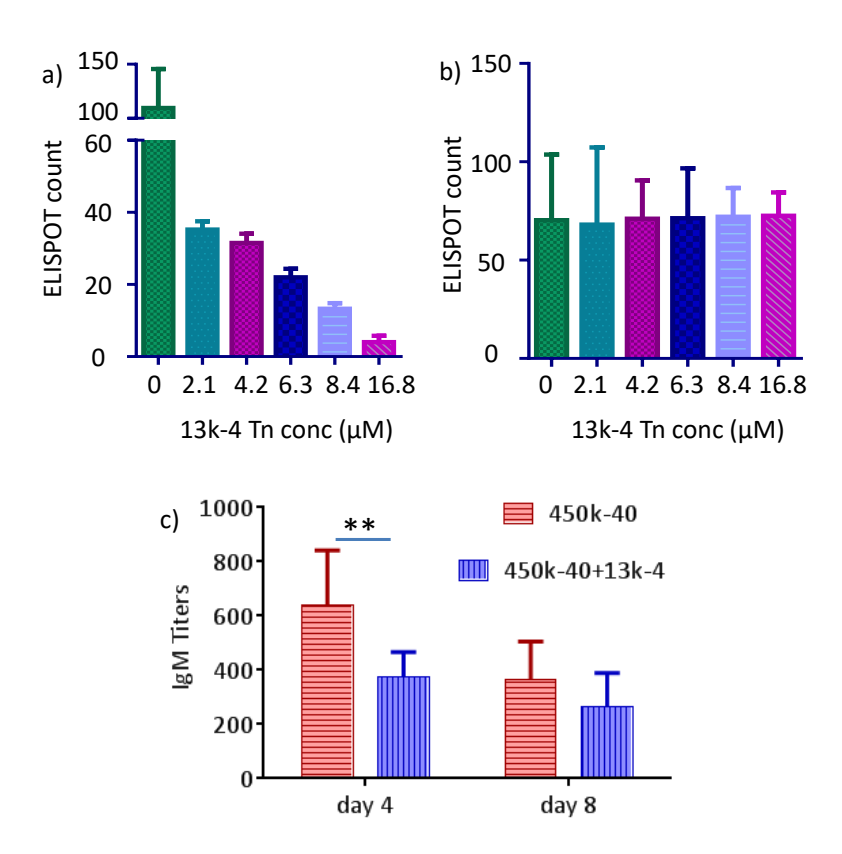


Figure 3.10: (a) Addition of increasing concentrations of 13k-4 to B cells incubated with 450k-40 glycopolymer (8.4 μ M Tn concentration) suppressed the generation of Tn specific ASCs; (b) Addition of 13k-4 to B cells incubated with wheat germ agglutinin (1 μ g/mL) did not have any significant effects on wheat germ agglutinin specific ASCs. (c) Co-administration of 450k-40 (Tn 4 μ g) and 13k-4 (Tn 1 μ g) to mice significantly reduced IgM titers compared to mice receiving 450k-40 (Tn 4 μ g) only. Blood was collected on day 4 and day 8 following immunization. Statistical analysis was performed using Student's t test (** p < 0.01). These results suggest 13k-4 glycopolymer selectively induced non-responsiveness of Tn specific ASCs.

B cells can become non-responsive and/or tolerant towards an antigen through a variety of mechanisms including hypercrosslinking of BCRs,³²⁻³³ clonal anergy or deletion,⁴⁸⁻⁴⁹ suppressive activities of regulatory T cells⁵⁰⁻⁵¹ and anti-idiotypic antibodies.⁵²⁻⁵³ In the case of 13k-4 glycopolymer, it probably competitively bound with BCRs of Tn specific B cells and disrupted the formation of multivalent BCR complexes with the 450k-40 glycopolymer. As Tn is a self-antigen, there are potential concerns that too strong an

immune response elicited by vaccination could lead to auto-immune complications. Suitably designed glycopolymers could provide a new tool to modulate activation and tolerance of Tn specific B cells.

3.3: Conclusions

In summary, while glycopolymers have been applied in immunization studies, ⁵⁴⁻⁵⁷ this is the first time a series of synthetic glycopolymers with defined length and number of carbohydrate antigen Tn have been utilized to decipher the codes of antigen valency and density on T cell independent B cell activation. With the 450 kDa polymer, bell shaped ASC responses were found depending on the number of antigen per chain. The glycopolymer containing 40 copies of Tn per chain resulted in highest Tn specific ASC proliferation. When the Tn valency was maintained at 40, increasing the antigen density by shortening the polymer length led to significant reduction of antibody responses. This suggests overcrowding of antigens is detrimental to B cell activation. The valency of the polymer is another critical parameter with a threshold value above 6 to induce Tn specific antibodies. In addition, our results show that fine-tuning of the glycopolymer structures can also lead to Tn specific B cell non-responsiveness, which could be an intriguing approach to modulate anti-glycan immune responses.

The abilities of suitable glycopolymers to activate B cells were confirmed by B cell activation events including BCR clustering, Ca²⁺ flux into cytoplasm and upregulation of CD69/CD86 on B cell surface. Furthermore, their *in vitro* activities were extended *in vivo* by inducing Tn specific antibodies in mice. The *in vitro* B cell assays could be a useful

approach to triage vaccine constructs prior to the time consuming *in vivo* studies. The current study focused on the production of IgM antibodies, which are generally the first type of antibodies secreted upon vaccination. The expansion of IgM secreting ASCs as a result of glycopolymer inoculation could increase the frequency of Tn specific B cells to better prime the immune system towards IgG responses.

Besides anti-cancer vaccines, glycoconjugate antigens are important in the development of anti-HIV and anti-bacterium vaccines.⁵⁸⁻⁶⁰ While the current study only focused on Tn, the principles established here could have implications in guiding the design of effective glycan based vaccine constructs targeting a variety of important diseases.

3.4: Experimental section

3.4.1: General experimental procedures and methods for synthesis

All reactions were carried out under nitrogen with anhydrous solvents in flame-dried glassware, unless otherwise noted. Chemicals used were reagent grade as supplied except where noted. Compounds were visualized by UV light (254 nm) and by staining with a yellow solution containing Ce(NH₄)₂(NO₃)₆ (0.5 g) and (NH₄)₆Mo₇O₂₄4H₂O (24.0 g) in 6% H₂SO₄ (500mL). Flash column chromatography was performed on silica gel 60 (230-400 Mesh). NMR spectra were referenced using residual CHCl₃ (δ ¹H-NMR 7.26 ppm), D₂O (δ ¹H-NMR 4.79 ppm). The Mn and PDIs of the polymers were determined by GPC at 35 °C using two PLgel 10-μm mixed-B columns with DMF as the eluting solvent.

3.4.2: Synthesis of glycopolymers

Synthesis of polymer 4. A solution of p-nitro aniline 1 (13.8 mg, 0.1 mmol), sodium nitrite (8.3 mg, 0.12 mmol), and a 50% aqueous fluoroboric acid solution (18.7 μL, 0.15 mmol) in water was cooled to 0 °C for 30 minutes. At this time, sodium cyanate (6.5 mg, 0.1 mmol), monomer acrylic acid 3 (2 mL, 0.029 mol) dissolved in water (2 mL) were added. The reaction mixture was heated to 70 °C overnight. The polymer was dialyzed against water and then lyophilized (90% yield). ¹H-NMR: δ 1.25-2.00 (br m, aliphatic H, from CH₂ of polymer backbone), 2.00-2.50 (br s, aliphatic H, from CH of polymer backbone), 7.30 (br s, aromatic H), 8.10 (br s, aromatic H). Peak integration was normalized to the small aromatic peaks at ~7.30 ppm (2 protons) and ~8.10 ppm (2 protons). Based on the integration ratio, there were an average of 180 acrylic acid units per chain (Mn ~ 12.9 kDa). To analyze the polymer by GPC, polymer 4 was converted to its methyl ester form by the following process. Polymer 4 (10 mg) was dissolved in MeOH: toluene (1:1, 1 mL) followed by drop wise addition of TMSCHN₂ (0.1 mL). The reaction mixture was stirred overnight and all the solvent was evaporated. The methylated polymer 4 was analyzed by GPC, which gave PDI of 1.22. Based on the molecular weight determined from GPC of the methylated polymer, the Mn of polymer 4 was determined to be 13.4 kDa.

Synthesis of polymer 8. All solutions used for synthesis of polymer **8** were deoxygenated with three freeze-pump-thaw cycles and the reaction was performed under nitrogen atmosphere. Monomer ^tbutyl acrylate **6** (10 g), initiator methyl 2-bromopropionate **5** (0.016 mL), catalysts CuBr (0.0201 g) and CuBr₂ (0.78 mg) and ligand PMDETA (0.03 mL) in THF (3 mL) were mixed in 500:1:1:0.05:1.05 ratio.

Catalysts were measured into a dry round bottom flask, and the system was purged of O2 by pumping N₂ for 20 min. Distilled monomer was added by syringe and needle, and purged with N₂ for 10 min followed by addition of the ligand and the initiator. The reaction mixture was stirred at 60 °C for 24 h. The reaction was quenched by THF, and catalysts were removed by silica gel column using THF as solvent. ^tBu protected polymer 8 was purified by precipitating with a CH₃OH:H₂O (50:50) solution. The purification process was repeated three times and the final polymer was dried under vacuum. ¹H-NMR: δ 1.30-1.80 (br m, aliphatic **H** from CH₂ of polymer backbone and CH(CH₃)₃), 2.10-2.25 (br m, aliphatic **H**, from CH of polymer backbone). ^tBu protected polymer 8 was dissolved in DCM and treated for 4 h with trifluoroacetic acid (TFA) at 3:1 molar ratio of TFA: monomer. The solid was separated and washed multiple times with diethyl ether. The hydrolysis was repeated three times. The final product polymer 8 was dried under vacuum (85% yield). ¹H-NMR: δ 1.45-1.80 (br m, aliphatic **H** from C**H**₂ of polymer backbone), 2.20-2.30 (br s, aliphatic **H**, from C**H** of polymer backbone). GPC analysis gave Mn of 46 kDa with a PDI value of 1.57.

Synthesis of glycopolymer. For **450k-10**, polymer **450k** (10 mg) was dissolved in 1 mL anhydrous DMF. Tn-NH₂ (0.1 mg, 10 eq), DIPEA (48 μL, 2eq), TSTU (50 mg, 1.2 eq) were added. The reaction mixture was stirred overnight, and the final glycopolymer was purified by a LH-20 column using water as the solvent. The number of Tn/chain was determined by anthrone-sulfuric acid assay⁶¹ using GalNAc as standards. All the other glycopolymers were synthesized and characterized in a similar way.

3.4.3: Cell viability

CytoTox 96 Non-Radioactive Cytotoxicity Assay of Promega (Madison, WI) was used for cell viability assay. EA.hy 926 cells were incubated with 450k-40 polymers at Tn concentrations ranging from 0 to 84 μM. 450k polymers were also tested with the same polymer concentration as the 450k-40. After incubation for 48 h, 50 μL of cell culture medium from each well was transferred to a fresh 96-well flat clear bottom plate, followed by addition of 50 μL of the Cyto Tox 96 Reagent to each well. The plate was incubated for 30 min at room temperature. Next, 50 μL of Stop Solution was added, and absorbance at 490 nm was measured. Each experiment was performed in triplicate. The average values of the culture medium background were subtracted from all values of experimental wells. For maximum lactate dehydrogenase (LDH) release control, 20 μL of 10X Lysis Solution was added 45 min before adding the CytoTox 96 Reagent.

Percentage of survival=[1-OD490(experimental)/OD490(control)]*100%

3.4.4: Cell isolation and culture

Splenic cells were harvested from C57BL/6 mice. Red blood cells were depleted by ACK lysing buffer (Life Technologies). Splenic B cells were isolated by negative selection (Easysep Mouse B cell Isolation Kit, StemCell Technologies) following the manufacturer's protocol. Both nucleated splenic cells and isolated B cells were cultured in RPMI 1640 supplemented with 10% FBS, 10 mM HEPES, 50 μM mercaptoethanol, 2 mM L-glutamine, 100 μg/mL penicillin G and 100 U/mL streptomycin.

3.4.5: ELISOPT assays

Mouse splenic cells were isolated and serially diluted across the plate, which was followed by adding the corresponding glycopolymer, control polymer or cell culture medium and incubated at 37 °C on day 1. On day 4, a 96 well MultiScreen ELISPOT plate (Millipore) was coated overnight at 4 °C with a solution of bovine serum albumin-Tn conjugate (BSA-Tn)³⁰ in PBS buffer (10 μg mL⁻¹) and then incubated at 4 °C overnight. On day 5, the ELISPOT plate was washed three times with PBST (0.1%) and blocked with 300 μL/well 5% BSA-PBST at room temperature for 1 hour. The plate was washed again three times with PBST 0.1% and three times with fresh 1640 culture medium. The splenic cells were transferred to the ELISPOT plate and incubated at 37 °C overnight. On day 6 the plate was washed nine times with PBST (0.1%) and three times with PBS followed by adding a 1:1000 dilution of HRP-conjugated goat anti-mouse IgM (Jackson ImmunoResearch Laboratory) in 1% BSA-PBST to each well. The plate was incubated for one hour at 37 °C, washed three times with 0.1% PBST and three times with PBS. Spots were developed at room temperature for about 15 min by the addition of AEC Staining kit (Sigma-Aldrich). After optimal spot development, plates were washed with water and dried. Data were collected and analyzed using the CTL ImmunoSpot system (Cellular Technology Ltd., Shaker Heights, OH).

For tolerization experiments, on day 1, 13k-4 polymers at Tn concentrations at 0, 2.1, 4.2, 6.3, 8.4 and 16.8 μ M respectively were added to wells containing fresh isolated spleen cells (8 x 10⁵ cells/well) incubated with polymer 450k-40 (at 8.4 μ M Tn) or wheat germ agglutinin (1 μ g/mL). The numbers of Tn specific ASCs were determined using ELISPOT as described above.

3.4.6: Flow cytometry for Tn specific B cells

After incubation with glycopolymers for 4 days, mouse spleen cells (5 x 10⁵ cells) were washed twice with FACS buffer (1% BSA + 0.1% NaN₃/PBS) and incubated with 2 μL of BSA-Tn-Alex Fluor 647 solution (0.5 mg/mL), which was prepared by reacting BSA-Tn³⁰ with Alexa Fluor 647 NHS ester (Thermo Fisher Scientific A-20006). After incubation for 1 h on ice, cells were incubated with 2 μL mouse Fc block (0.5 mg/mL, BD 55142) for 10 min on ice followed by staining with 2 μL PE rat anti-mouse CD19 (0.2 mg/mL, BD 553786) for 30 min on ice. The cells were washed twice and resuspended in FACS buffer, and then analyzed by LSR II (BD Biosciences). 2 μL 7-AAD (0.05 mg/mL, BD 559925) was added to the samples to exclude dead cells before analysis. Data was processed by FlowJo software.

3.4.7: Measurement of apoptosis

Isolated mouse spleen cells were incubated with 450k-40 (Tn 8.4 μM), 450k-80 (Tn 4.2 μM) and 450k-115 (Tn 6.3 μM) respectively for 4 days (the Tn concentrations were chosen based on **Figure 3.1** where maximum responses were observed with 450k-40, 450k-80 and 450k-115 respectively), and then cells (5 x 10⁵ cells) were washed twice with FACS buffer (1% BSA + 0.1% NaN₃/PBS) and incubated with 2 μL of BSA-Tn-Alexa Fluor 647 (0.5 mg/mL) on ice. After 1 h, cells were incubated with 2 μL mouse Fc block (0.5 mg/mL, BD 55142) for 10 min on ice followed by staining with 2 μL PE rat anti-mouse CD19 (0.2 mg/mL, BD 553786) for 30 min on ice. Next, cells were stained with 5 μL Annexin V-FITC (eBioscience) for 15 min at RT. The cells were washed twice

and re-suspended in FACS buffer, and then analyzed by LSR II (BD Biosciences). 2 μ L 7-AAD (0.05 mg/mL, BD 559925) was added to the samples to exclude dead cells before analysis. Data was processed by FlowJo software.

3.4.8: BCR clustering and colocalization with GM1

Isolated B cells were washed three times with binding buffer (PBS supplemented with 1% BSA). Cells (5 x 10⁶ cells/mL) were stained with 16 μg/mL Rhodamine Red-X-conjugated Affinipure Fab fragment goat anti-mouse IgM, μ chain specific (Jackson ImmunoResearch) for 30 min on ice and washed followed by staining with 50μg/mL Cholera toxin B subunit from Vibrio cholera FITC conjugate (Sigma) for 30 min on ice. After extensive washing by binding buffer, cells were incubated with buffer or different polymers for 10 min on ice. After washing, cells were fixed with 4% paraformaldehyde for 30 min on ice. After washing with binding buffer, cells were mounted on polylysine-coated slides. Confocal laser microscopy images were collected on an Olympus FluoView 1000 LSM confocal microscope. For cells incubated with 450k-40 (Tn 8.4 μM) and 450k-80 (Tn 4.2 μM) glycopolymers, from confocal images, it was estimated that 4.3% and 2.7% of cells appeared with punctate staining as shown in **Figures 3c** and **3d** respectively. These percentages were consistent with the percent of Tn specific B cells determined by FACS (**Table 3.2**).

3.4.9: Calcium flux assay

Fluo-4 NW calcium assay kit (Thermo Fisher Scientific) was used for detecting intracellular calcium. Briefly, B cells were washed and resuspended in Hank's balanced salt solution (HBSS), 20 mM 4-(2-hydroxyethyl)-1-piperazineethanesulfonic acid (HEPES) buffer to a density of ~2.5 \times 10⁶ cells/mL, and added to 96-well microplates. Plates were incubated at 37 °C and 5% of CO₂ for 60 minutes. Fluo-4 NW dye was mixed with 100 μ L probenecid stock solution and 5 mL assay buffer, and added to the plates. Plates were then incubated at 37 °C for 30 minutes and at room temperature for an additional 30 minutes. Fluorescence was measured by FDSS/ μ CELL functional drug screening system. After collection of baseline emission for 20 seconds, control polymer 450k or glycopolymer 450k-40 (Tn 8.4 μ M) were added to the cells and the cellular fluorescence was continuously monitored.

3.4.10: Flow cytometry for cell surface markers

After incubation with the glycopolymers, mouse B cells (5 x 10⁵ cells) were washed twice with FACS buffer (1% BSA + 0.1% NaN₃/PBS), and incubated with 2 μL mouse Fc block (0.5 mg/mL, BD 55142) for 10 min on ice followed by staining with 2 μL PE rat anti-mouse CD19 (0.2 mg/mL, BD 553786), 2 μL FITC anti-mouse CD69 (0.5 mg/mL, Biolegend 104505) or 2 μL FITC anti-mouse CD86 (0.5 mg/mL, Biolegend 105109) for 30 min on ice. The cells were washed twice and re-suspended in FACS buffer. Prior to analysis by LSR II (BD Biosciences), 2 μL 7-AAD (0.05 mg/mL, BD

559925) was added to the samples to exclude dead cells. Data was processed by FlowJo software.

3.4.11: Mouse immunization

Pathogen-free female C57BL/6 mice age 6–10 weeks were obtained from Charles River and maintained in the University Laboratory Animal Resources facility of Michigan State University. All animal care procedures and experimental protocols have been approved by IACUC of Michigan State University. Groups of five mice were injected intravenously on day 0 with 0.1 mL of the polymer (glycopolymer concentration was 4 µg Tn) in PBS. Serum samples were collected on days 0 (before immunization), 4 and 8.

To study the effect of 13k-4 polymer on antibody responses to 450k-40, a group of five mice were injected intravenously on day 0 with 0.1 mL of the mixture of 450k-40 (4 μ g Tn) and 13k-4 (1 μ g Tn) in PBS. Serum samples were collected on days 0 (before immunization), 4, and 8.

3.4.12: ELISA assays

A 96-well microtiter plate was coated with a solution of BSA-Tn³⁰ in PBS buffer (10 μg mL⁻¹) and then incubated at 4 °C overnight. The plate was washed four times with PBST, followed by addition of 1% (w/v) BSA in PBS to each well and incubation at RT for one hour. The plate was washed again with PBST and mice sera were added in 0.1%

(w/v) BSA/PBS. The plate was incubated for two hours at 37 °C and washed. A 1:2000 dilution of HRP-conjugated goat antimouse IgM (Jackson ImmunoResearch Laboratory) in 0.1% BSA/PBS was added to each well. The plate was incubated for one hour at 37 °C, washed and a solution of TMB was added. Color was allowed to develop for 15 min, and then a solution of 0.5 M H_2SO_4 was added to quench the reaction. The optical density (OD) was then measured at 450 nm.

APPENDIX

APPENDIX

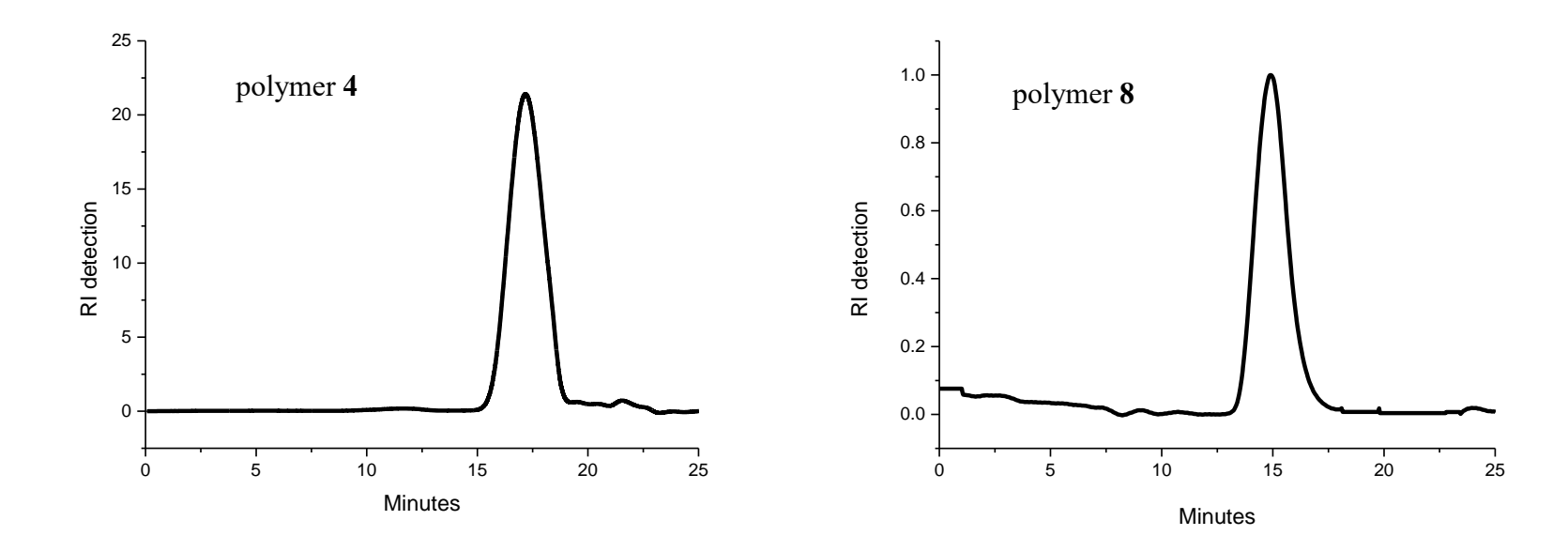
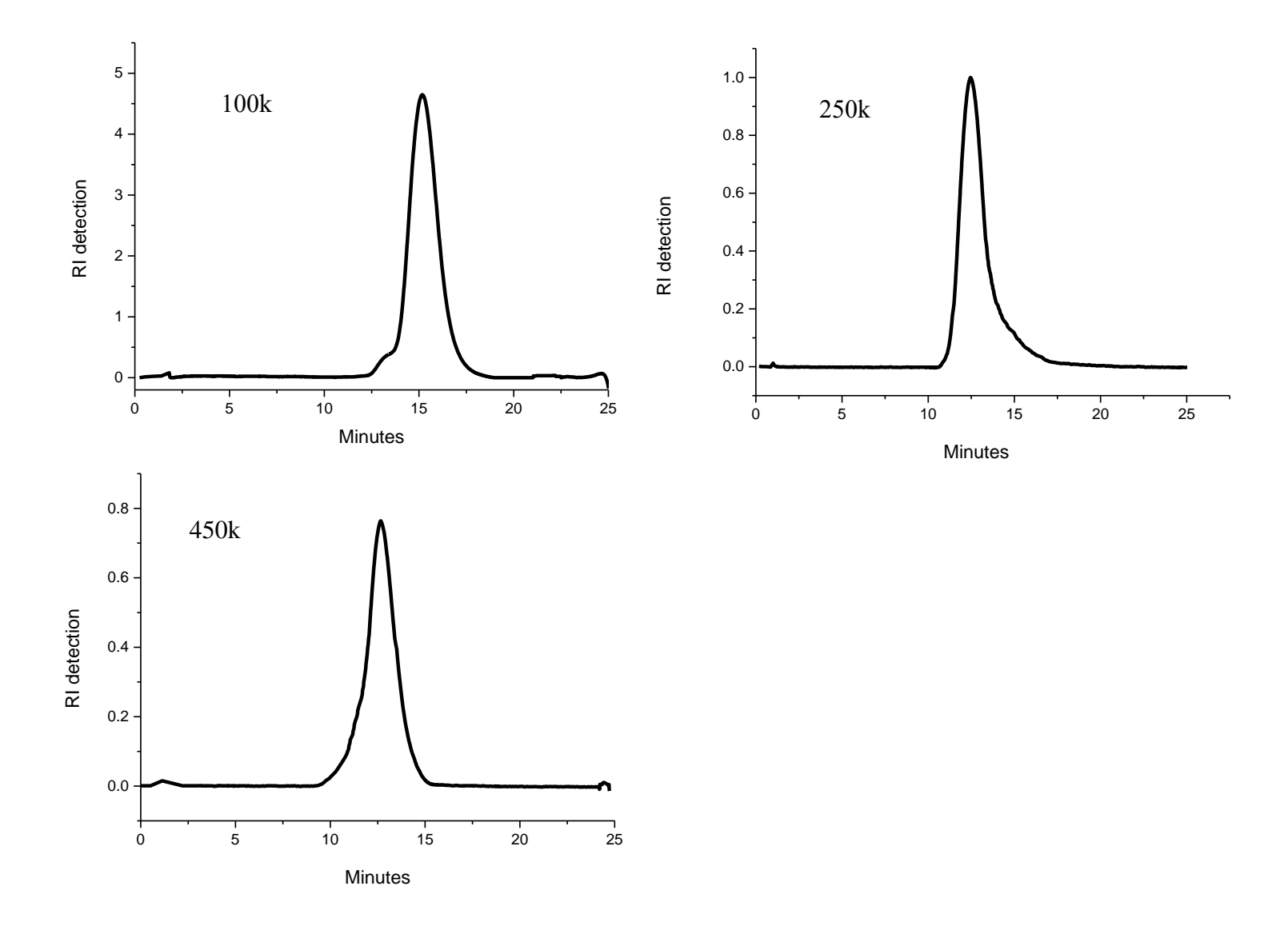


Figure 3.11: GPC traces of methylated polymer 4, 8, 100k, 250k and 450k. (eluent : DMF).

Figure 3.11 (cont'd)



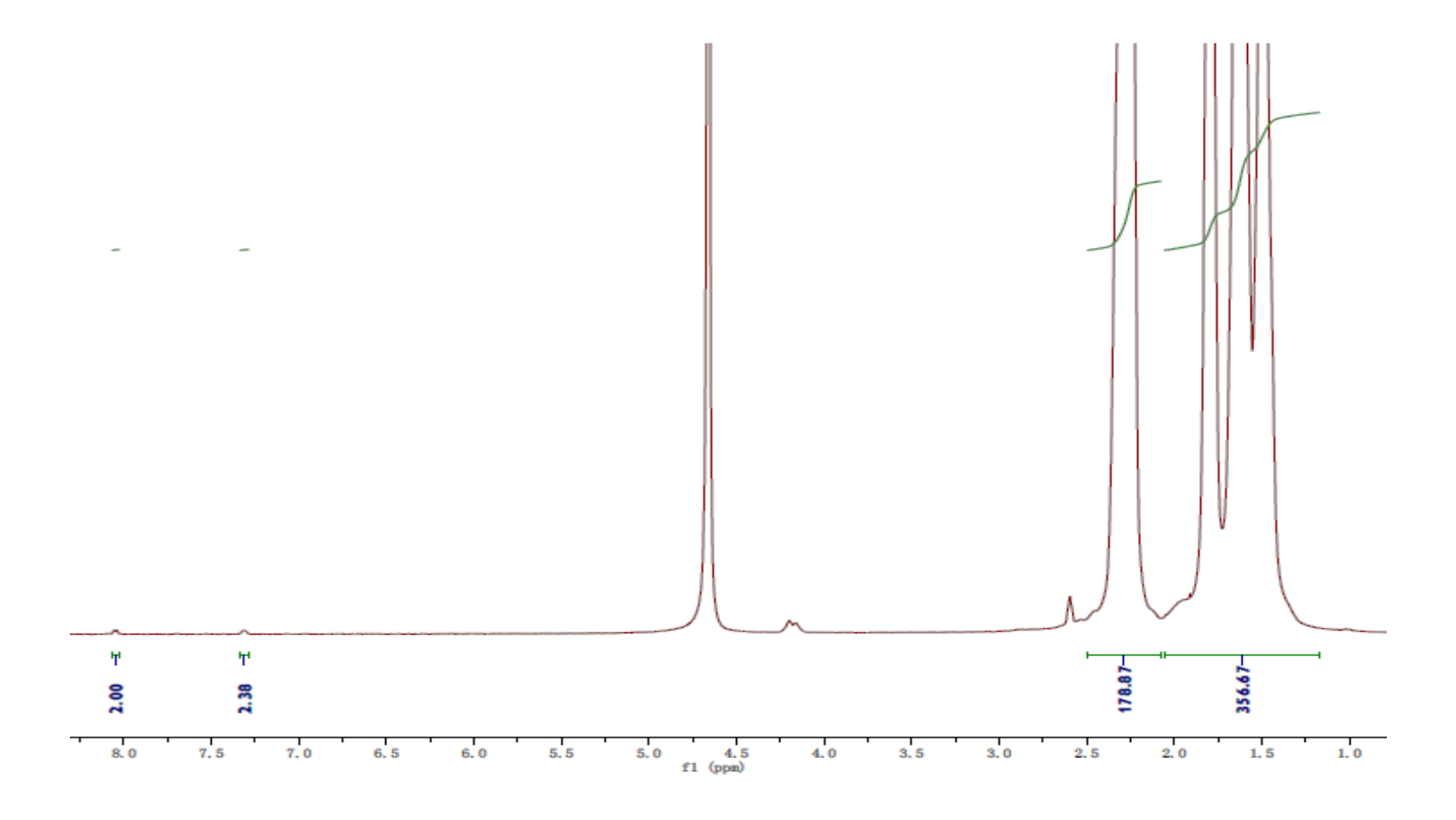


Figure 3.12: 500 MHz (D_2O), ¹H-NMR of polymer 4.

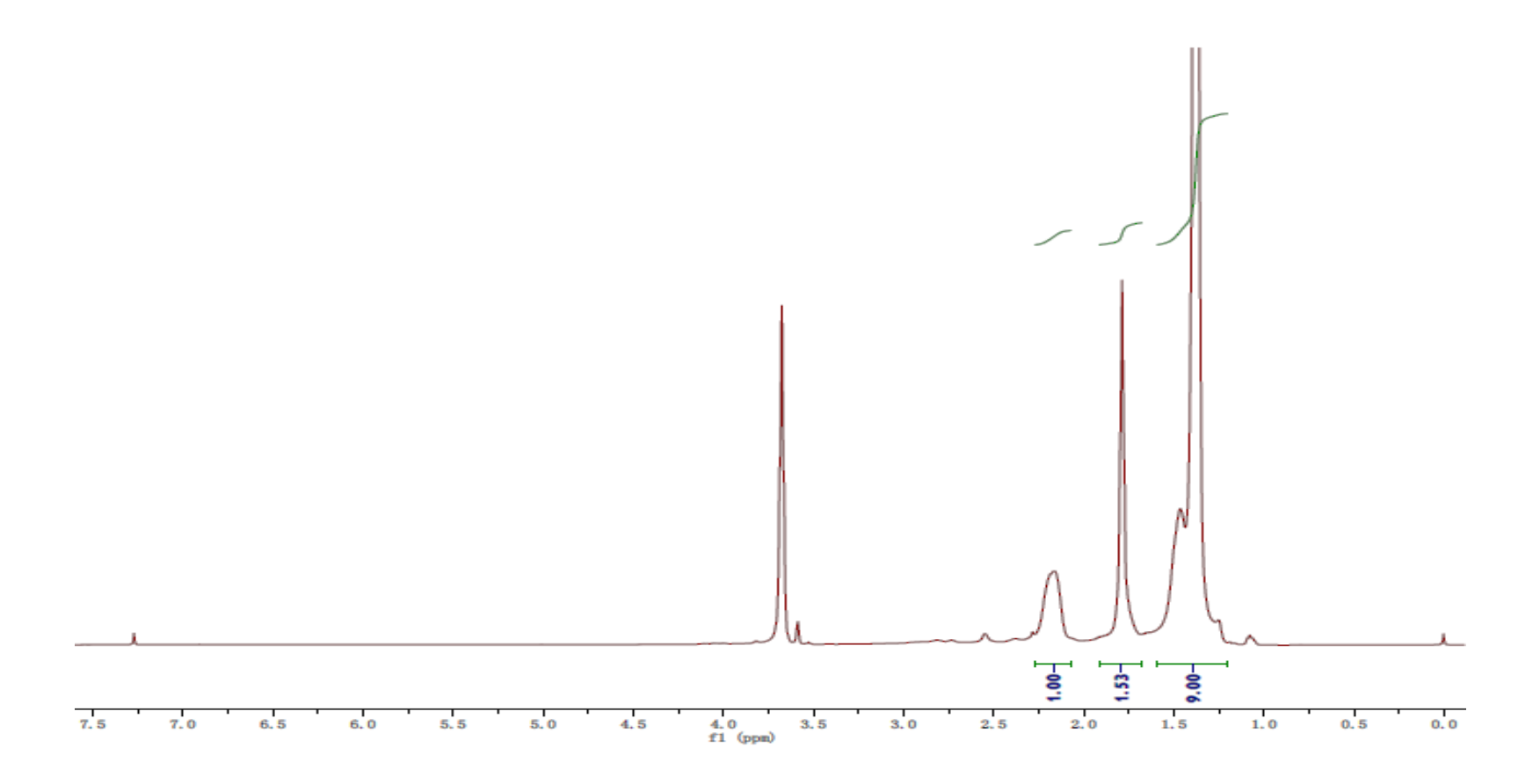


Figure 3.13: 500 MHz (CDCl₃), ¹H-NMR of ^tBu protected polymer **8**.

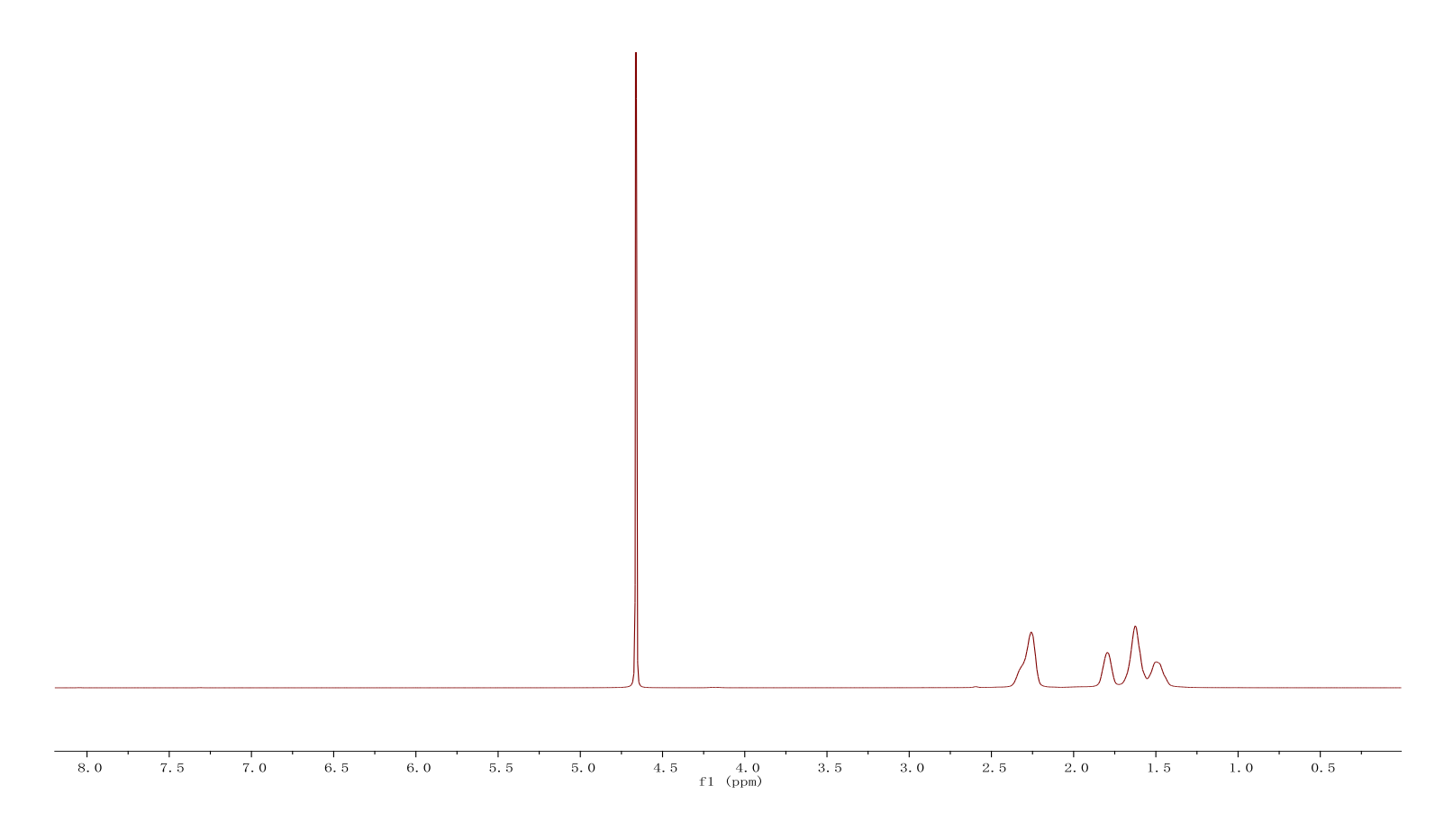


Figure 3.14: 500 MHz (D_2O), ¹H-NMR of polymer 8.

REFERENCES

REFERENCES

- 1. Danishefsky, S. J.; Allen, J. R., From the laboratory to the clinic: A retrospective on fully synthetic carbohydrate-based anticancer vaccines *Angew. Chem. Int. Ed.* **2000**, *39*, 836-863.
- 2. Guo, Z. W.; Wang, Q. L., Recent development in carbohydrate-based cancer vaccines. *Curr. Opin. Chem. Biol.* **2009**, *13*, 608-617.
- 3. Buskas, T.; Thompson, P.; Boon, G.-J., Immunotherapy for cancer: synthetic carbohydrate-based vaccines. *Chem. Commun.* **2009**, 5335-5349.
- 4. Yin, Z.; Huang, X., Recent development in carbohydrate based anti-cancer vaccines. *J. Carbohydr. Chem.* **2012**, *31*, 143-186.
- 5. Livingston, P. O.; Wong, G. Y.; Adluri, S.; Tao, Y.; Padavan, M.; Parente, R.; Hanlon, C.; Calves, M. J.; Helling, F.; Ritter, G.; Oettgen, H. F.; Old, L. J., Improved survival in stage III melanoma patients with GM2 antibodies: a randomized trial of adjuvant vaccination with GM2 ganglioside. *J. Clin. Oncol.* **1994**, *12*, 1036-1044.
- 6. Jones, P. C.; Sze, L. L.; Liu, P. Y.; Morton, D. L.; Irie, R. F., Prolonged survival for melanoma patients with elevated igm antibody to oncofetal antigen. *J. Nat. Cancer Inst.* **1981**, *66*, 249-254.
- 7. Hirasawa, Y.; Kohno, N.; A., Y.; Kondo, K.; Hiwada, K.; Miyake, M., Natural autoantibody to MUC1 is a prognostic indicator for non-small cell lung cancer. *Am. J. Respir. Crit. Care Med.* **2000**, *161*, 589-594.
- 8. Hamanaka, Y.; Suehiro, Y.; Fukui, M.; Shikichi, K.; Imai, K.; Hindoda, Y., Circulating anti-MUC1 IgG antibodies as a favorable prognostic factor for pancreatic cancer. *Int. J. Cancer* **2003**, *103*, 97-100.
- 9. Cheung, N. K.; Kushner, B. H.; Yeh, S. D.; Larson, S. M., 3F8 monoclonal antibody treatment of patients with stage 4 neuroblastoma: a phase II study. *Int. J. Oncol.* **1998**, *12*, 1299-1306.
- 10. Cheung, N. K.; Cheung, I. Y.; Kramer, K.; Modak, S.; Kuk, D.; Pandit-Taskar, N.; Chamberlain, E.; Ostrovnaya, I.; Kushner, B. H., Key role for myeloid cells: phase II results of anti-G(D2) antibody 3F8 plus granulocyte-macrophage colony-stimulating factor for chemoresistant osteomedullary neuroblastoma. *Int. J. Cancer* **2014**, *135*, 2199-2205.
- 11. Yu, A. L.; Gilman, A. L.; Ozkaynak, M. F.; London, W. B.; Kreissman, S. G.; Chen, H. X.; Smith, M.; Anderson, B.; Villablanca, J. G.; Matthay, K. K.; Shimada, H.; Grupp, S. A.; Seeger, R.; Reynolds, C. P.; Buxton, A.; Reisfeld, R. A.; Gillies, S. D.; Cohn, S. L.; Maris, J. M.; Sondel, P. M., Anti-GD2 antibody with GM-CSF, interleukin-2, and

- isotretinoin for neuroblastoma. N. Engl. J. Med. 2010, 363, 1324-1334.
- 12. Mond, J. J.; Lees, A.; Snapper, C. M., T Cell-independent Antigens Type 2. *Annu. Rev. Immunol.* **1995**, *13*, 655-692.
- 13. Harwood, N. E.; Batista, F. D., Early events in B cell activation. *Annu. Rev. Immunol.* **2010**, *28*, 185-210.
- 14. Bachmann, M. F.; Hengartner, H.; Zinkernagel, R. M., T helper cell-independent neutralizing B cell response against vesicular stomatitis virus: role of antigen patterns in B cell induction? *Eur. J. Immunol.* **1995**, *25*, 3445-3451.
- 15. Bachmann, M. F.; Rohrer, U. H.; Kundig, T. M.; Burki, K.; Hengartner, H.; Zinkernagel, R. M., The influence of antigen organization on B cell responsiveness. *Science* **1993**, *262*, 1448-1451.
- 16. Vos, Q.; Lees, A.; Wu, Z. Q.; Snapper, C. M.; Mond, J. J., B-cell activation by T-cell-independent type 2 antigens as an integral part of the humoral immune response to pathogenic microorganisms. *Immunol. Rev.* **2000**, *176*, 154.
- 17. Avalos, A. M.; Ploegh, H. L., earlyBCR events and antigencapture, processing, and loading on MHC class II on B cells. *Front. Immunol.* **2014,** *5*, 92.
- 18. Avalos, A. M.; Bilate, A. M.; Witte, M. D.; Tai, A. K.; He, J.; Frushicheva, M. P.; Thill, P. D.; Meyer-Wentrup, F.; Theile, C. S.; Chakraborty, A. K.; Zhuang, X.; Ploegh, H. L., Monovalent engagement of the BCR activates ovalbumin-specific transnuclear B cells. *J. Exp. Med.* **2014**, *211*, 365-379.
- 19. Kim, Y. M.; Pan, J. Y.; Korbel, G. A.; Peperzak, V.; Boes, M.; Ploegh, H. L., Monovalent ligation of the B cell receptor induces receptor activation but fails to promote antigen presentation. *Proc. Natl. Acad. Sci. USA* **2006**, *103*, 3327-3210.
- 20. Minguet, S.; Dopfer, E.; Schamel, W. W. A., Low-valency, but not monovalent, antigens trigger the B-cell antigen receptor (BCR). *Int. Immunol.* **2010**, *22*, 205-212.
- 21. Dintzis, R. Z.; Middleton, M. H.; Dintzis, H. M., Studies on the immunogenicity and tolerogenicity of T-independent antigens. *J. Immunol.* **1983**, *131*, 2196-2203.
- 22. Dintzis, R. Z.; Okajima, M.; Middleton, M. H.; Greene, G.; Dintzis, H. M., The immunogenicity of soluble haptenated polymers is determined by molecular masss and hapten valency. *J. Immunol.* **1989**, *143*, 1239-1244.
- 23. Dintzis, H. M.; Dintzis, R. Z.; Vogelstein, B., Molecular determinants of immunogenicity: the immuno model of immune response. *Proc. Natl. Acad. Sci. USA* **1976,** *73*, 3671-3675.
- 24. Puffer, E. B.; Pontrello, J. K.; Hollenbeck, J. J.; Kink, J. A.; Kiessling, L. L., Activating B cell signaling with defined multivalent ligands. *ACS Chem. Biol.* **2007**, *2*,

- 25. Lunn, M. P.; Johnson, L. A.; Fromholt, S. E.; Itonori, S.; Huang, J.; Vyas, A. A.; Hildreth, J. E.; Griffin, J. W.; Schnaar, R. L.; Sheikh, K. A., High-affinity anti-ganglioside IgG antibodies raised in complex ganglioside knockout mice: reexamination of GD1a immunolocalization. *J. Neurochem.* **2000**, *75*, 404-412.
- 26. Springer, G. F., T and Tn, general carcinoma autoantigens. *Science* **1984**, *224*, 1198-1206.
- 27. Springer, G. F., Immunoreactive T and Tn epitopes in cancer diagnosis, prognosis, and immunotherapy. *J. Mol. Med.* **1997**, *75*, 594-602.
- 28. Hou, S.; Sun, X.-L.; Dong, C.-M.; Chaikof, E. L., Facile synthesis of chain-end functionalized glycopolymers for site-specific bioconjugation. *Bioconjuate Chem.* **2004**, *15*, 954-959.
- 29. Treat, N. D.; Ayres, N. A.; Boyes, S. G.; Brittain, W. J., A facile route to poly(acrylic acid) brushes using atom transfer radical polymerization. *Macromolecules* **2006**, *39*, 26-29.
- 30. Yin, Z.; Nguyen, H. G.; Chowdhury, S.; Bentley, P.; Bruckman, M. A.; Miermont, A.; Gildersleeve, J. C.; Wang, Q.; Huang, X., Tobacco mosaic virus as a new carrier for tumor associated carbogydrate antigens. *Bioconjugate Chem.* **2012**, *23*, 1694-1703.
- 31. Yin, Z.; Wright, W. S.; McKay, C.; Baniel, C.; Kaczanowska, K.; Bentley, P.; Gildersleeve, J. C.; Finn, M. G.; BenMohamed, L.; Huang, X., Significant impact of immunogen design on the diversity of antibodies generated by carbohydrate-based anticancer vaccine. *ACS Chem. Biol.* **2015**, *10*, 2364-2372.
- 32. Parry, S. L.; Hasbold, J.; Holman, M.; Klaus, G. G., Hypercross-linking surface IgM or IgD receptors on mature B cells induces apoptosis that is reversed by costimulation with 11-4 and anti-CD40. *J. Immunol.* **1994**, *152*, 2821-2829.
- 33. Mayumi, M.; Ohshima, Y.; Hata, D.; Kim, K. M.; Heike, T.; Katamura, K.; Furusho, K., IgM-mediated B cell apoptosis. *Crit. Rev. Immunol.* **1995,** *15*, 255-269.
- 34. Cherukuri, A.; Cheng, P. C.; Sohn, H. W.; Pierce, S. K., The CD19/CD21 complex functions to prolong B cell antigen receptor signaling from lipid rafts. *Immunity* **2001**, *14*, 169-179.
- 35. Yin, Z.; Comellas-Aragones, M.; Chowdhury, S.; Bentley, P.; Kaczanowska, K.; BenMohamed, L.; Gildersleeve, J. C.; Finn, M. G.; Huang, X., Boosting immunity to small tumor-associated carbohydrates with bacteriophage Qb capsids. *ACS Chem. Biol.* **2013**, *8*, 1253-1262.
- 36. Reth, M., Matching cellular dimensions with molecular sizes. *Nature Immunol.* **2013**, *14*, 765-767.

- 37. Houseman, B. T.; Mrksich, M., The role of ligand density in the enzymatic glycosylation of carbohydrates presented on self-assembled monolayers of alkanethiolates on gold. *Angew. Chem. Int. Ed.* **1999**, *38*, 782-785.
- 38. Grant, C. F.; Kanda, V.; Yu, H.; Bundle, D. R.; McDermott, M. T., Optimization of immobilized bacterial disaccharides for surface plasmon resonance imaging measurements of antibody binding. *Langmuir* **2008**, *24*, 14125-14132.
- 39. Batista, F. D.; Iber, D.; Neuberger, M. S., B cells acquire antigen from target cells after synapse formation. *Nature* **2001**, *411*, 489-494.
- 40. Thyagarajan, R.; Arunkumar, N.; Song, W., Polyvalent antigens stabilize B cell antigen receptor surface signaling microdomains. *J. Immunol.* **2003**, *170*, 6099-6106.
- 41. Unanue, E. R.; Perkins, W. D.; Karnovsky, M. J., Ligand-induced movement of lymphocyte membrane macromolecules. *J. Exp. Med.* **1972**, *136*, 885-897.
- 42. Lewis, R. S., Calcium signaling mechanisms in T lymphocytes. *Annu. Rev. Immunol.* **2001**, *19*, 497-521.
- 43. Scharenberg, A. M.; Humphires, L. A.; Rawlings, D. J., Calcium signaling and cell-fate choice in B cells. *Nat. Rev. Immunol.* **2007,** *7*, 778-789.
- 44. Cebrián, M.; Yague, E.; Rincón, M.; López-Botet, M.; de Landázuri, M.; Sánchez-Madrid, F., Triggering of T cell proliferation through AIM, an activation inducer molecule expressed on activated human lymphocytes. *J. Exp. Med.* **1988**, *168*, 1621-1637.
- 45. Vazquez, B. N.; Laguna, T.; Carabana, J.; Krangel, M. S.; Lauzurica, P., CD69 gene is differentially regulated in T and B cells by evolutionarily conserved promoter-distal elements. *J. Immunol.* **2009**, *183*, 6513-6521.
- 46. Jeannin, P.; Delneste, Y.; Lecoanet-Henchoz, S.; Gauchat, J. F.; Ellis, J.; Bonnefoy, J. Y., CD86 (B7-2) on human B cells. A functional role in proliferation and selective differentiation into IgE- and IgG4-producing cells. *J. Biol. Chem.* **1997**, *272*, 15613-15619.
- 47. Basten, A.; Silveira, P. A., B-cell tolerance: mechanisms and implications. *Curr. Opin. Immunol.* **2010**, *22*, 566-574.
- 48. Haniuda, K.; Nojima, T.; Ohyama, K.; Kitamura, D., Tolerance induction of IgG+memory B cells by T cell-independent type II antigens. *J. Immunol.* **2011**, *186*, 5620-5628.
- 49. Coleman, A. S.; Akkoyunlu, M., Bacterial polysaccharide-mediated downregulation of TACI and B-cell apoptosis contribute to the hyporesponsiveness against bacterial polysaccharides vaccines. *J. Infect Dis.* **2013**, *207*, 872-873.

- 50. Baker, P. J.; Amsbaugh, D. F.; Stashak, P. W.; Caldes, G.; Prescott, B., Direct evidence for the involvement of T suppressor cells in the expression of low-dose paralysis to type III pneumococcal polysaccharide. *J. Immunol.* **1982**, *128*, 1059-1062.
- 51. Jandinski, J. J.; Scott, D. W., Role of self carriers in the immune response and tolerance. IV. Active T cell suppression in the maintenance of B cell tolerance to a "T-independent" antigen. *J. Immunol.* **1979**, *123*, 2447-2450.
- 52. Fernandez, C.; Möller, G., Antigen-induced strain-specific autoantiidiotypic antibodies modulate the immune response to dextran B 512. *Proc. Natl. Acad. Sci. USA* **1979,** *76*, 5944-5947.
- 53. Lehle, G.; Weiler, E., Thymus-independent induction of idiotype suppression in newborn mice by syngeneic anti-idiotype antisera. *Eur. J. Immunol.* **1985**, *15*, 580-586.
- 54. Lipinski, T.; Kitov, P. I.; Szpacenko, A.; Paszkiewicz, E.; Bundle, D. R., Synthesis and immunogenicity of a glycopolymer conjugate. *Bioconjugate Chem.* **2011**, *22*, 274-281.
- 55. Nuhn, L.; Hartmann, S.; Palitzsch, B.; Gerlitzki, B.; Schmitt, E.; Zentel, R.; Kunz, H., Water-soluble polymers coupled with glycopeptide antigens and T-cell epitopes as potential antitumor vaccines. *Angew. Chem. Int. Ed.* **2013**, *52*, 10652-10656.
- 56. Parry, A. L.; Clemson, N. A.; Ellis, J.; Bernhard, S. S. R.; Davis, B. G.; Cameron, N. R., 'Mulicopy multivalent' glycopolymer-stabilized gold nanoparticles as potential synthetic cancer vaccines. *J. Am. Chem. Soc.* **2013**, *135*, 9362-9365.
- 57. Qin, Q.; Yin, Z.; Bentley, P.; Huang, X., Carbohydrate antigen delivery by water soluble copolymers as potential anti-cancer vaccines. *Med. Chem. Commun.* **2014**, *5*, 1126-1129.
- 58. Horiya, S.; MacPherson, I. S.; Krauss, I. J., Recent strategies targeting HIV glycans in vaccine design. *Nat. Chem. Biol.* **2014**, *10*, 990-999.
- 59. Astronomo, R. D.; Burton, D. R., Carbohydrate vaccines: developing sweet solutions to sticky situations? *Nat. Rev. Drug Disc.* **2010**, *9*, 309-324.
- 60. Wang, L. X., Synthetic carbohydrate antigens for HIV vaccine design. *Curr. Opin. Chem. Biol.* **2013**, *17*, 997-1005.
- 61. Leyva, A.; Quintana, A.; Sánchez, M.; Rodríguez, E. N.; Cremata, J.; Sánchez, J. C., Rapid and sensitive anthrone-sulfuric acid assay in microplate format to quantify carbohydrate in biopharmaceutical products: method development and validation. *Biologicals* **2008**, *36*, 134-141.